Supporting Information

Electronically and Sterically Varied Tungsten Carbonyls Applied to the Selective Dearomatization of *N*-Heteroarenes

Pengtao Bai,[1] Yuzan Liu,[1] Li Fang,[1] Ying Li,[1] Jiahao Wang,[1] Yougen Cai,[1] Lei Chen,[1] Jia-Jia Zhao,[1] Heng Song*,[1] Luyi Zong*,[2] Chen Xu,*,[1]

[1]School of Environmental and Chemical Engineering, Jiangsu University of Science and Technology, Zhenjiang 212003, Jiangsu, P. R. China.

[2]College of Chemistry and Pharmaceutical Engineering, Nanyang Normal University, Nan yang 473061, P. R. China.

Table of content

1 Experimental Section

General Considerations. All manipulations were conducted under a N_2 atmosphere on Schlenk techniques or in a glovebox, unless otherwise stated. In addition to borane purchased from Bide Pharmaceuticals, other pharmaceuticals were purchased from Energy Chemical Company, Baika Chemistry and used without further purification unless otherwise noted. Dichloromethane, *n*-hexane, tetrahydrofuran, toluene were dried and degassed by Solvent Purification Systems (Innovative Technology). ^{1}H, ^{13}C and ^{19}F NMR spectra were recorded on a JEOL 400M spectrometer. The chemical shifts are reported on ppm relative to either the residual solvent peak or TMS as an internal standard. Coupling constants (*J*) was reported on Hz. Attribution of peaks was performed by using the multiplicity and integrals of the peaks. Coupling patterns are indicated as s (singlet), d (doublet), t (triplet), dd (doublet of doublet), td (triplet of doublet), or m (multiplet). Crystal of **W-1** and **W-3** suitable for X-ray diffraction was obtained by slowly diffusing pentane into the concentrated CH_2Cl_2 solution of **W-1**. The solid structures are shown in **Figure S7-S8**. Freezing the acetonitrile solution of **W-2** yielded **W-2** crystals suitable for X-ray diffraction analysis. The solid structures are shown in **Figure S9**. Single crystals with appropriate dimensions were selected under an optical microscope and quickly coated with high vacuum grease (Dow Corning Corporation) to prevent decomposition. Crystallographic data were collected using a Bruker D8 VENTURE with Mo Kα radiation (λ = 0.71073 Å) or micro-focus Cu Kα radiation (λ = 1.5418 Å) at 297 K. Crystal data collection and refinement parameters are summarized in **Table S5**.

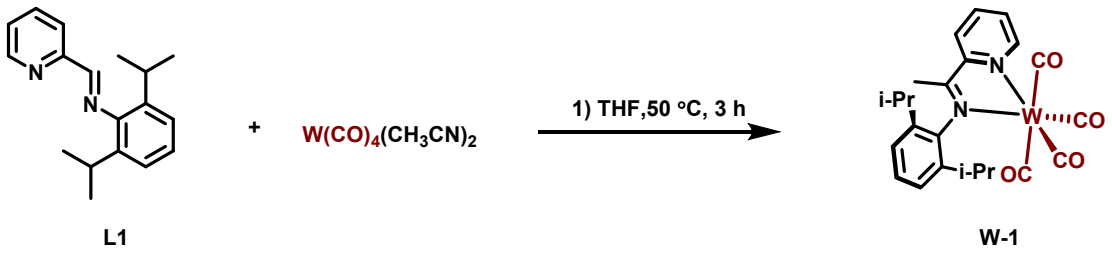

L1 W-1

Synthesis of Complexes. *Synthesis of* ***W-1.*** To a 10 mL Schlenk tube fitted with a stir bar was added $W(CO)_4(NCMe)_2$ (0.2 mmol, 70 mg), (*E*)-N-(2,6-

Diisopropylphenyl)-1-(pyridin-2-yl)methanimine (**L1**, 0.2 mmol, 53 mg) and THF (15 mL). The mixture was conducted in an oil bath at 50 °C for 3 h. After removing of the solvent under vacuum, the resulting residue was separated and purified by recrystallization, affording **W-1** as purplish red solid (yield, 71%, 82 mg). ^{1}H NMR (400 MHz, Chloroform-*d*) δ 9.35 (d, J = 4.3 Hz, 1H), 8.68 (d, J = 2.8 Hz, 1H), 8.00 – 7.91 (m, 2H), 7.50 – 7.42 (m, 1H), 7.27 (t, J = 6.8 Hz, 3H), 2.93 (p, J = 6.5 Hz, 2H), 1.34 (dd, J = 6.7, 2.8 Hz, 6H), 1.15 – 1.10 (m, 6H). ^{13}C{^{1}H}NMR (101 MHz, Chloroform-d) δ 217.9, 214.0, 198.9, 164.4, 155.1, 153.1, 147.2, 139.3, 136.5, 128.7, 127.5, 127.2, 124.3, 28.1, 26.1, 23.6. HRMS [ESI-TOF] m/z: $[M+H]^+$ calcd for $C_{23}H_{24}N_2O_4W$ 577.1324; found, 577.1325.

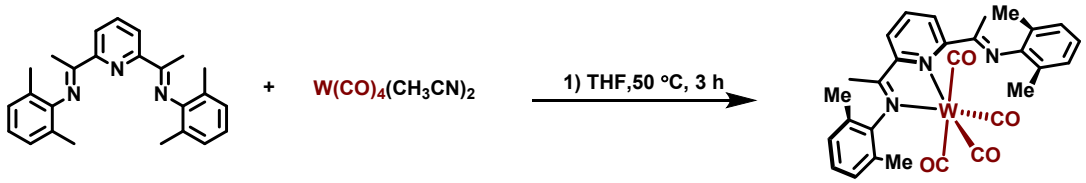

Synthesis of ***W-2.*** To a 10 mL Schlenk tube fitted with a stir bar was added $W(CO)_4(NCMe)_2$ (0.2 mmol, 70 mg), (1E,1'E)-*N*,*N*′-(2,6-diisopropylphenyl)-2,6-pyridinediiminyl (**L2**, 0.2 mmol, 96 mg) and THF (15 mL). The mixture was conducted in an oil bath at 50 °C for 3 h. After removing of the solvent under vacuum, the resulting residue was separated and purified by recrystallization, affording **W-2** as red solid (yield, 70%, 109 mg). ^{1}H NMR (400 MHz, Chloroform-*d*) δ 8.49 (d, *J* = 7.8 Hz, 2H), 7.94 (t, *J* = 7.7 Hz, 1H), 7.18 (d, *J* = 6.8 Hz, 4H), 7.14 – 7.09 (m, 2H), 2.81 – 2.74 (m, 4H), 2.28 (s, 6H), 1.17 (d, *J* = 8.2 Hz, 24H). ^{13}C{^{1}H}NMR (101 MHz, Chloroform-*d*) δ 167.1, 155.2, 146.6, 137.0, 135.9, 123.7, 123.1, 122.3, 28.4, 23.3, 23.0, 17.3. HRMS [ESI-TOF] m/z: $[M+H]^+$ calcd for $C_{37}H_{43}N_3O_4W$ 777.2841; found, 777.2848.

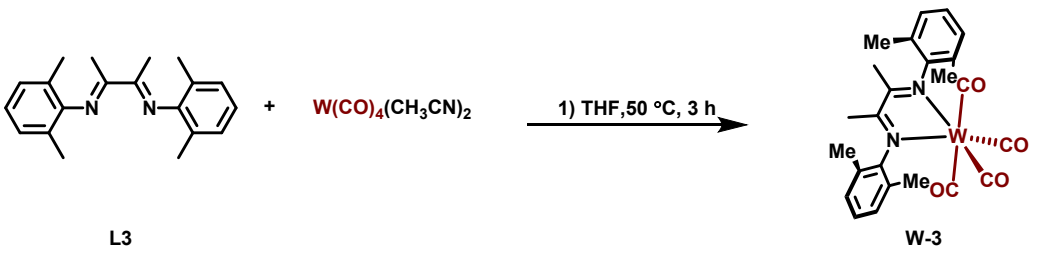

*Synthesis of **W-3**.* To a 10 mL Schlenk tube fitted with a stir bar was added $W(CO)_4(NCMe)_2$ (0.2 mmol, 70 mg), bis(2,6-dimethylphenyl)butane-2,3-diimine (**L3**, 0.2 mmol, 58 mg) and THF (15 mL). The mixture was conducted in an oil bath at 50 °C for 3 h. After removing of the solvent under vacuum, the resulting residue was separated and purified by recrystallization, affording **W-3** as red solid (yield, 75%, 88 mg). ^{1}H NMR (400 MHz, Chloroform-*d*) δ 7.20 (d, *J* = 7.8 Hz, 4H), 7.13 (dd, *J* = 8.5, 6.4 Hz, 2H), 2.16 (s, 12H), 1.98 (s, 6H). ^{13}C{^{1}H}NMR (101 MHz, Chloroform-*d*) δ 209.4, 167.1, 149.4, 129.0, 127.8, 126.1, 19.2, 18.3. HRMS [ESI-TOF] m/z: [M] calcd for $C_{24}H_{24}N_2O_4W$ 588.1245; found, 588.1276.

General Method for dearomatization of pyridines: To a 5 mL Schlenk tube fitted with a stir bar was added pyridine (0.3 mmol), **W-1** (0.015 mmol, 5 mol%), HBpin (0.9 mmol, 3.0 equiv.). The tube was sealed and the mixture was conducted in an oil bath at 50 °C for 24 h. After cooling to room temperature, the solvent was removed under vacuum. Yields were determined by ^{1}H NMR spectroscopy of the crude reaction mixture versus tetraethylsilane as the internal standard.

General Method for dearomatization of quinolines: To a 5 mL Schlenk tube fitted with a stir bar was added quinoline (0.3 mmol), **W-1** (0.015 mmol, 5 mol%), HBpin (0.9 mmol, 3.0 equiv.). The tube was sealed and the mixture was conducted in an oil bath at 50 °C for 16 h. After cooling to room temperature, the solvent was removed under vacuum. Yields were determined by ^{1}H NMR spectroscopy of the crude reaction mixture versus tetraethylsilane as the internal standard.

Catalytic Reactivity for N-Heteroarenes Selective Dearomatization. We initially studied the reaction of pyridine (**1a**, 0.3 mmol) with pinacolborane (HBpin) (0.6 mmol) in the presence of 5 mol % catalyst **W-1**, which produced exclusively N-Bpin-1,2-DHP (**2a**) product with an NMR yield of 56% after 24 h at 50 °C (Entry 1). In the absence of catalyst **W-1,** pyridine did not react with HBpin at 50 °C for 24 h. Subsequently, we evaluated a series of solvents including polar or non-polar solvents at 50 °C (Entries 2–8). The results indicated that the reaction proceeded best under solvent-free conditions. However, when the reaction temperature was increased to 70 °C, the yield decreased (Entry 9). The results likely caused by tungsten complex decomposition at a high

temperature. Notably, increasing the amount of pinacolborane from 2.0 to 3.0 equiv. significantly improved the reaction efficiency (Entry 10). Afterwards, the catalytic reactivity of **W-2**, **W-3** and $W(CO)_6$ were also investigated for this reaction (Entries 12–14).

2 Characterization Data of Complex

2.1 NMR Spectra of Complex W-1

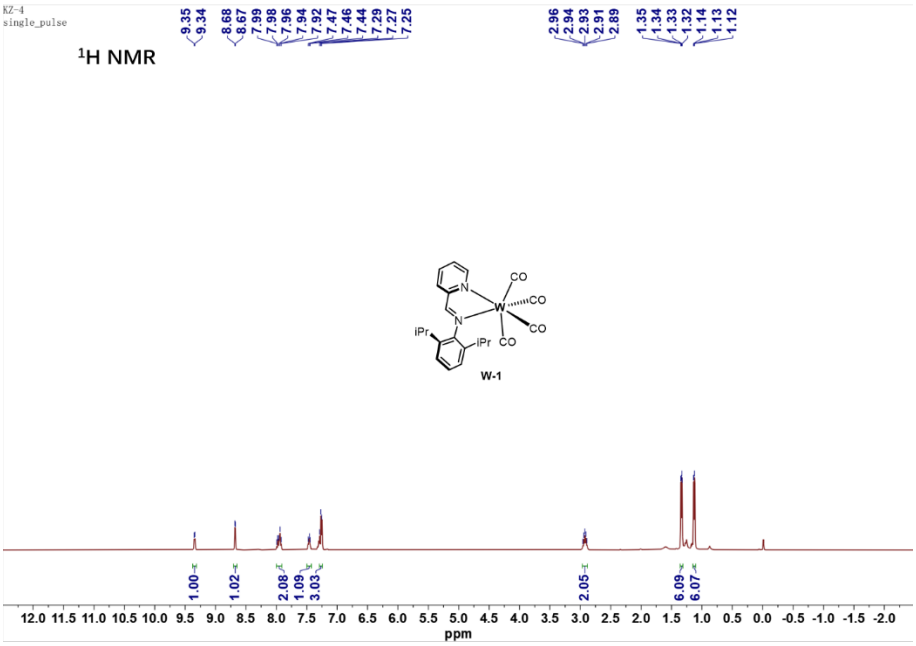

Figure S1. ^{1}H NMR spectrum of **W-1** (400 MHz, Chloroform-*d*).

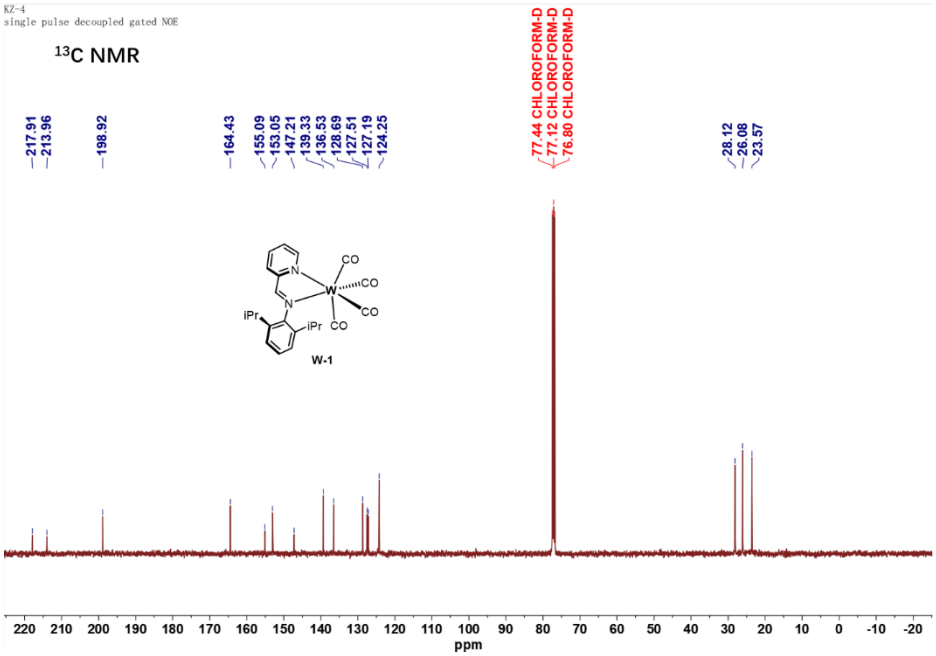

Figure S2. ^{13}C NMR spectrum of **W-1** (101 MHz, Chloroform-*d*).

2.2 NMR Spectra of Complex W-2

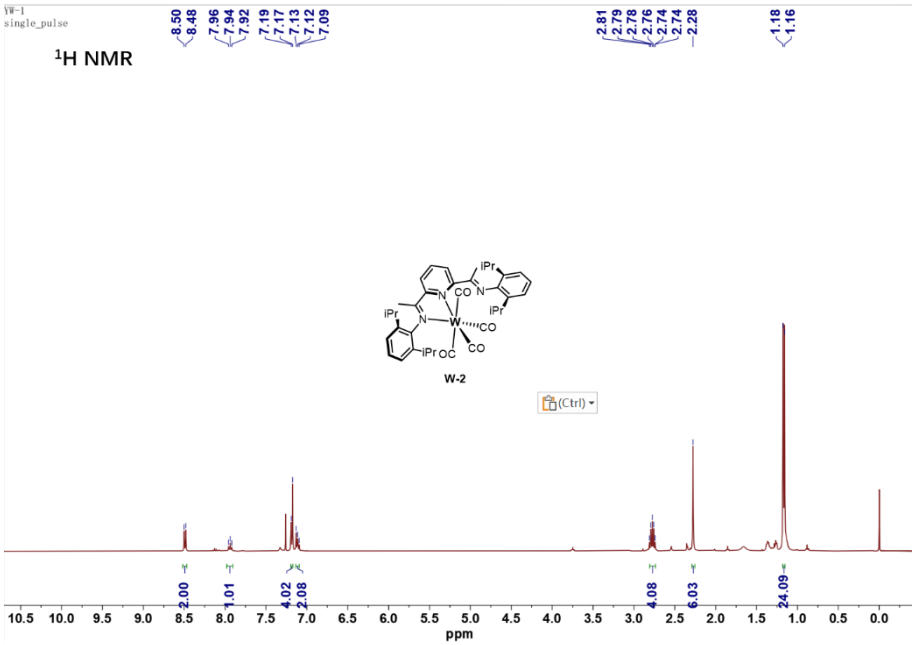

Figure S3. ^{1}H NMR spectrum of **W-2** (400 MHz, Chloroform-*d*).

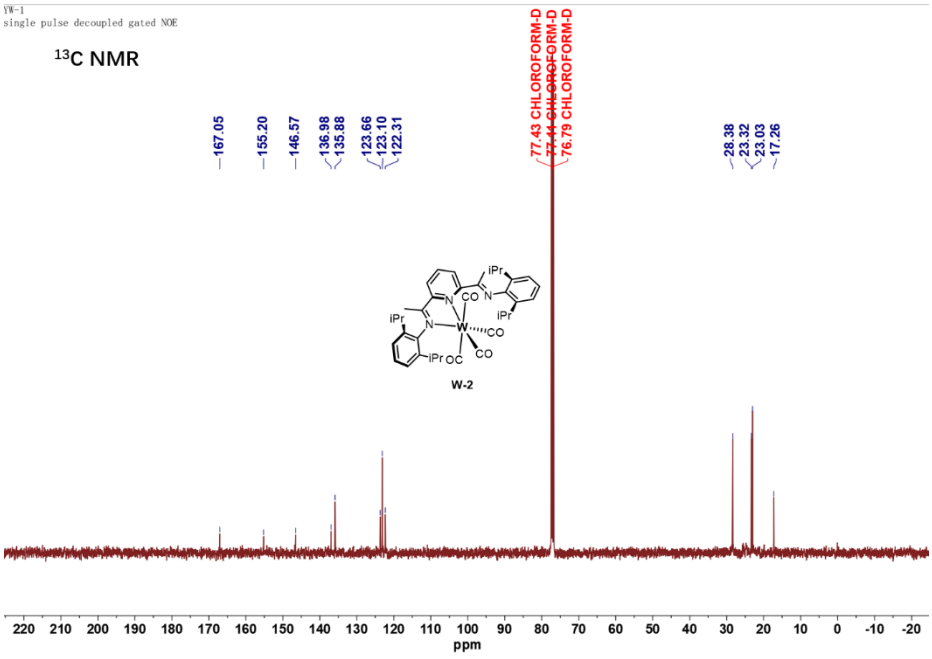

Figure S4. ^{13}C NMR spectrum of **W-2** (101 MHz, Chloroform-*d*).

2.3 NMR Spectra of Complex W-3

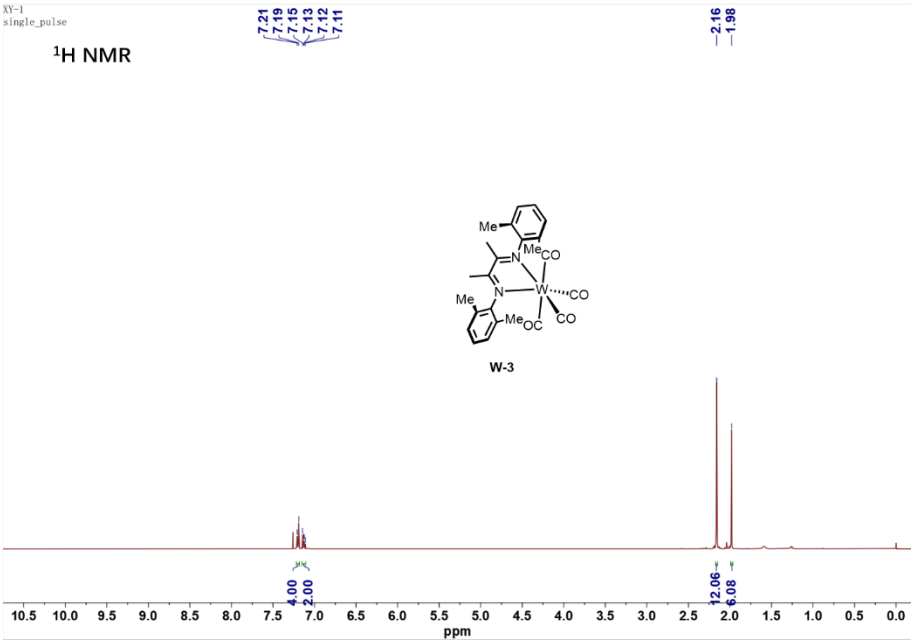

Figure S5. [1]H NMR spectrum of **W-3** (400 MHz, Chloroform-*d*).

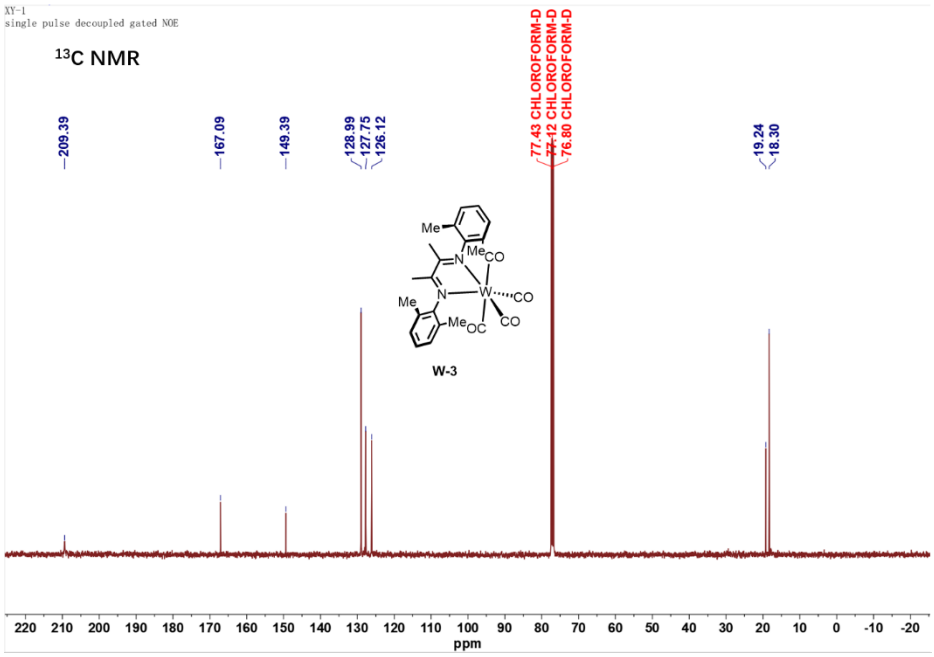

Figure S6. [13]C NMR spectrum of **W-3** (101 MHz, Chloroform-*d*).

2.4 Solid-Sate Structure of W-1 (CCDC Deposition Number 2463721)

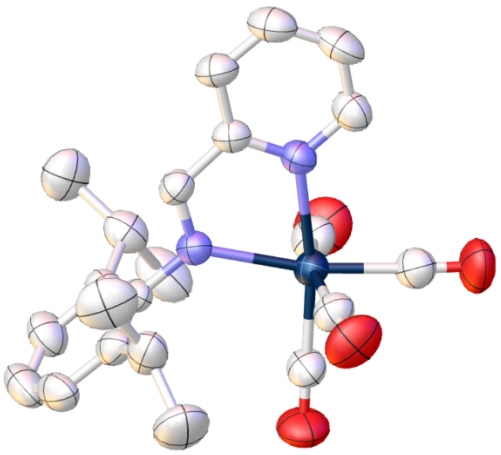

Figure S7. Molecular view of **W-1** with 50% probability thermal ellipsoids. Partial hydrogen atoms are omitted for clarity.

2.5 Solid-Sate Structure of W-2 (CCDC Deposition Number 2463727)

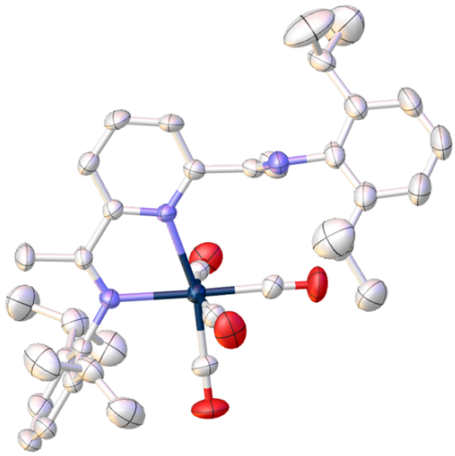

Figure S8. Molecular view of **W-2** with 50% probability thermal ellipsoids. Partial hydrogen atoms are omitted for clarity.

2.6 Solid-Sate Structure of W-3 (CCDC Deposition Number 2463731)

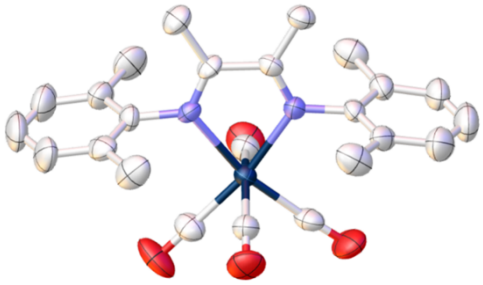

Figure S9. Molecular view of **W-3** with 50% probability thermal ellipsoids. Partial hydrogen atoms are omitted for clarity.

2.7 HRMS analysis of complex W-1

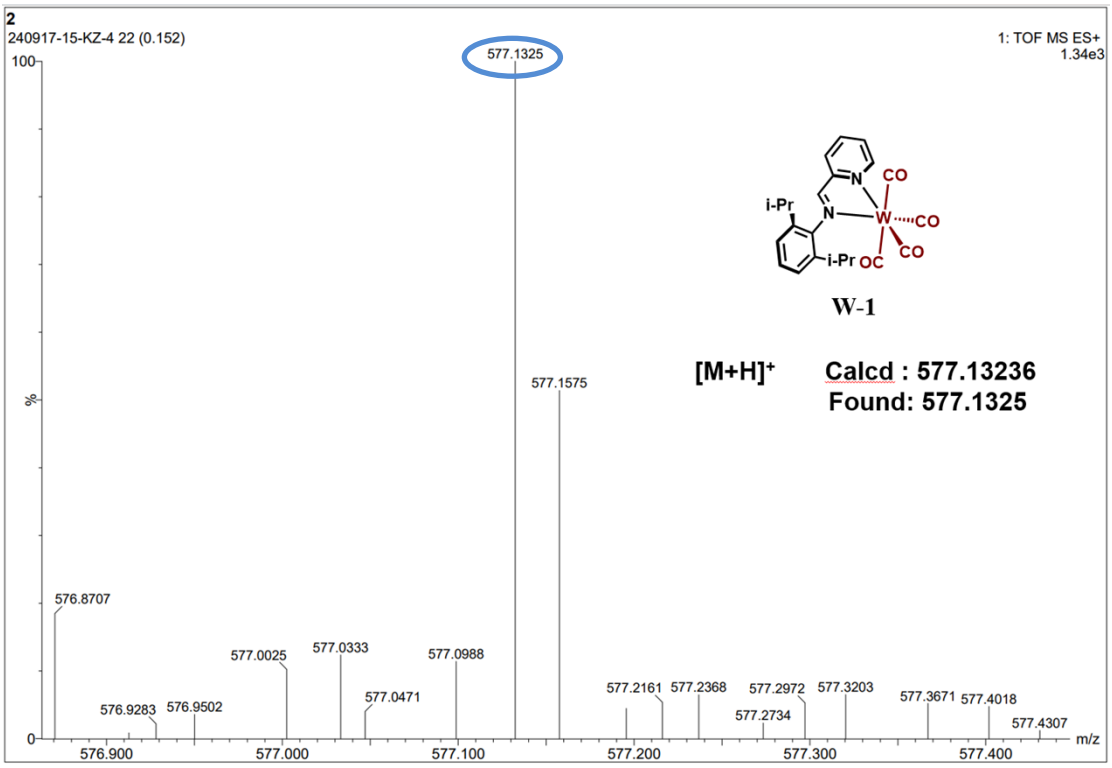

Figure S10. HRMS analysis of complex **W-1**.

2.8 HRMS analysis of complex W-2

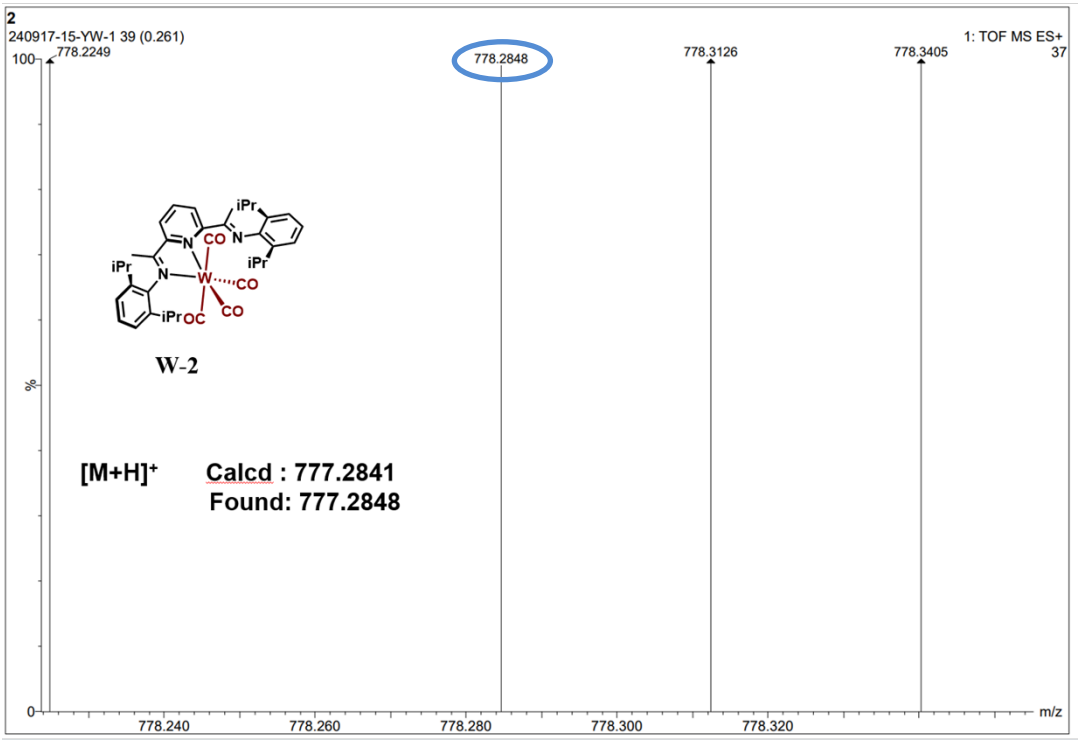

Figure S11. HRMS analysis of complex **W-2**.

2.9 HRMS analysis of complex W-3

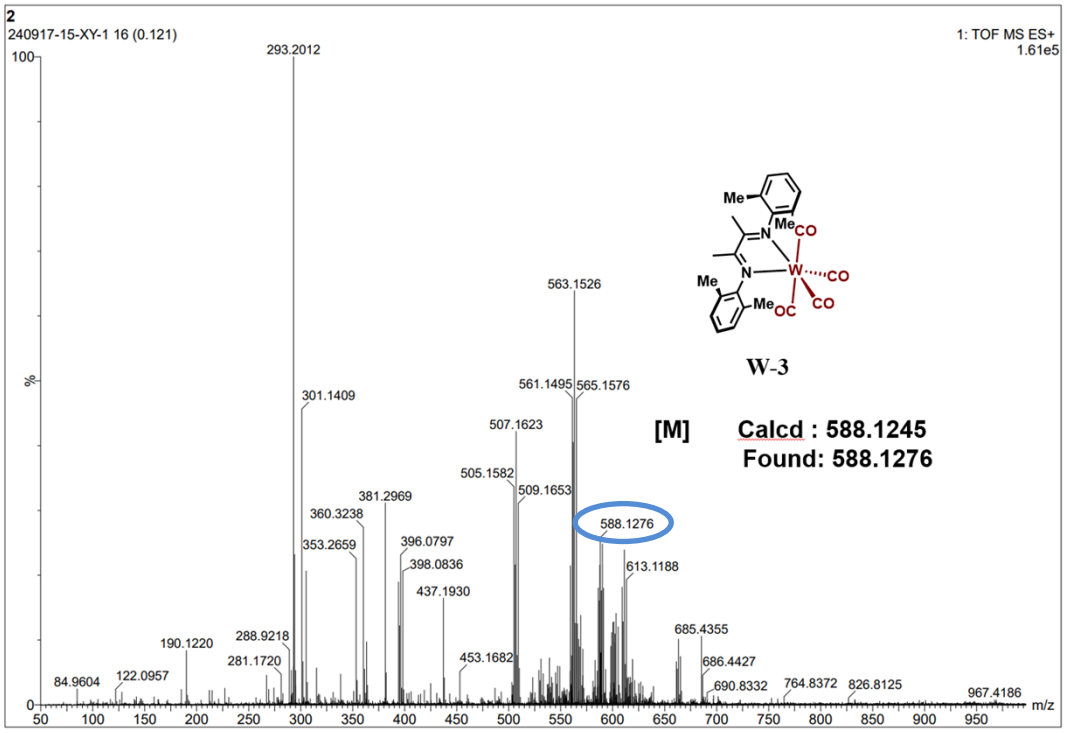

Figure S12. HRMS analysis of complex **W-3**.

2.10 HRMS analysis of complex Int 1

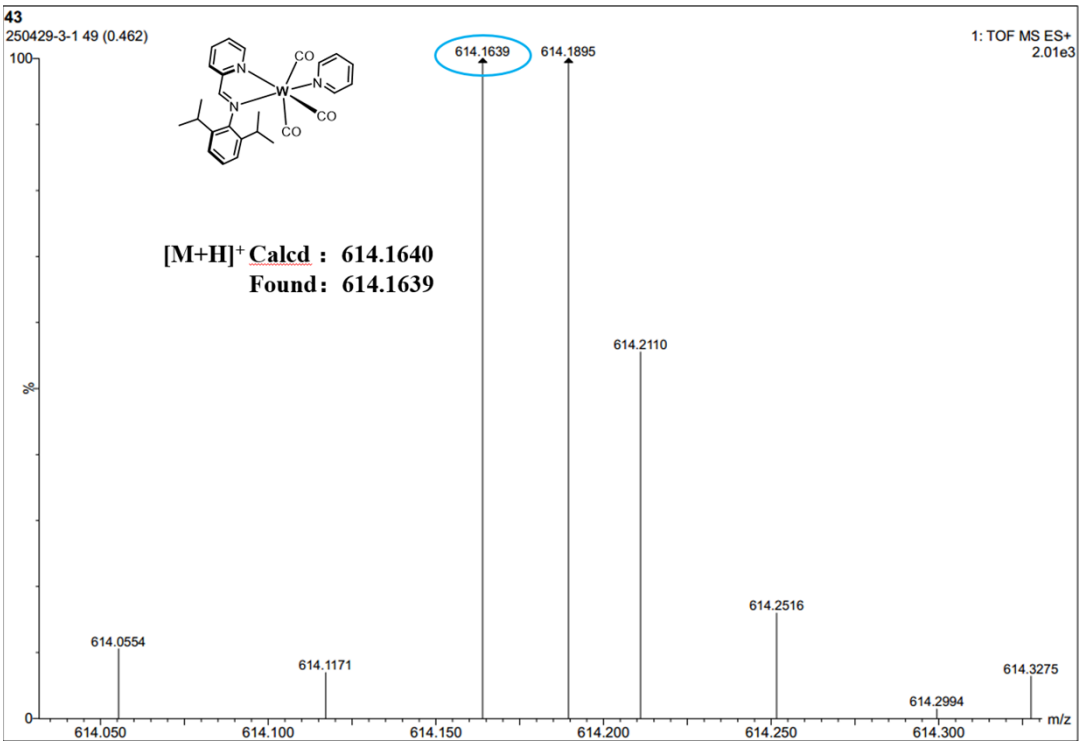

Figure S13. HRMS analysis of complex **Int 1**.

2.11 HRMS analysis of complex Int 2

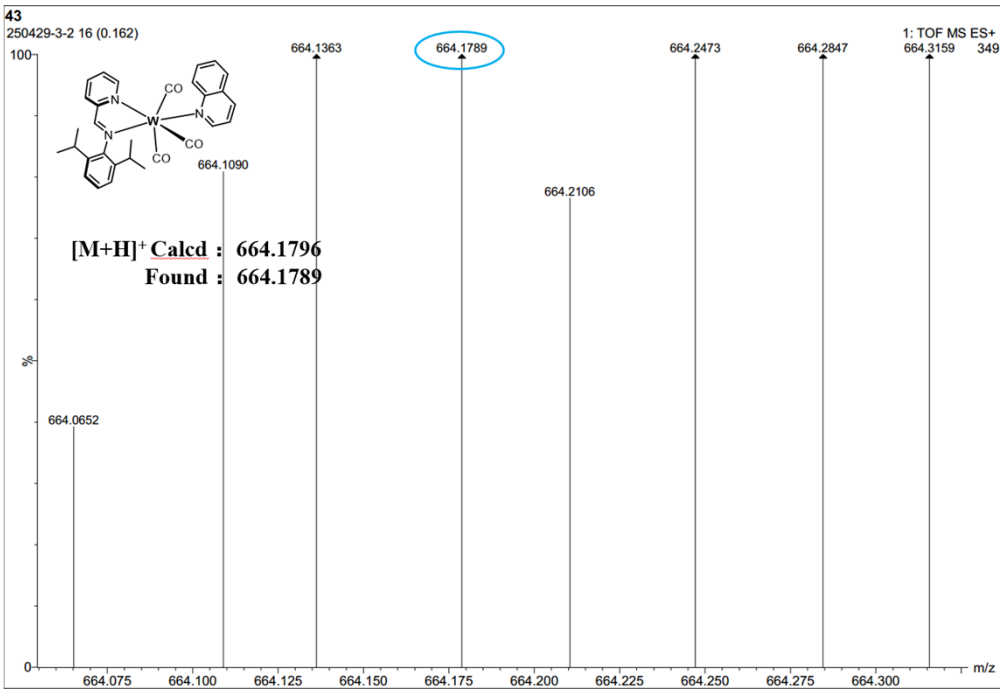

Figure S14. HRMS analysis of complex **Int 2**.

3. Optimization of the dearomatization reaction of quinoline and pyridine

Table S1. Screening of Reaction Conditions[a]

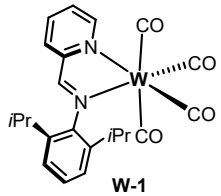

W-1

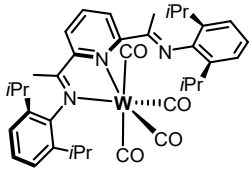

W-2

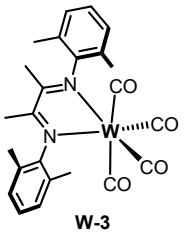

W-3

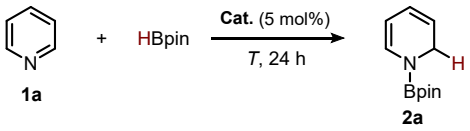

entry	solvent	t [°C]	HBpin [equiv.]	cat.	yield for **6a**[b] [%]
1	Neat	50	2	**W-1**	56
2	Toluene	50	2	**W-1**	23
3	THF	50	2	**W-1**	trace
4	C_6D_6	50	2	**W-1**	32
5	Hexane	50	2	**W-1**	trace
6	CPME	50	2	**W-1**	trace
7	DME	50	2	**W-1**	trace
8	CH_2Cl_2	50	2	**W-1**	trace
9	Neat	70	2	**W-1**	40
10	Neat	50	3	**W-1**	86
12	Neat	50	3	**W-2**	81
13	Neat	50	3	**W-3**	60
14	Neat	50	3	$W(CO)_6$	trace

[a]Reaction conditions: quinoline (0.3 mmol), HBpin (3.0 equiv.), and Cat. (5 mol %); [b]yields were determined by ^{1}H NMR spectroscopy using tetraethylsilane as the internal standard.

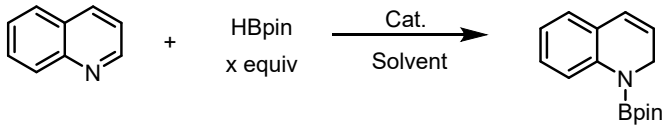

3a **4a**

entry	solvent	t [°C]	time [h]	HBpin [equiv]	catalyst [5 mol%]	yield for **4a**[b] [%]
1	Toluene	70	16	3	$W(CO)_6$	trace
2	Toluene	70	16	3	$W(CO)_4(NCMe)_2$	73
3	Toluene	70	16	3	No catalyst	trace
4	C_6D_6	70	16	3	$W(CO)_4(NCMe)_2$	58
5	CD_3CN	70	16	3	$W(CO)_4(NCMe)_2$	72
6	$CDCl_3$	70	16	3	$W(CO)_4(NCMe)_2$	trace
7	$(CD_3)_2CO$	70	16	3	$W(CO)_4(NCMe)_2$	trace
8	THF	70	16	3	$W(CO)_4(NCMe)_2$	80
9	THF	50	16	3	$W(CO)_4(NCMe)_2$	46
10	THF	30	16	3	$W(CO)_4(NCMe)_2$	35
11	THF	50	16	3	W-1	88
12	THF	50	16	3	W-2	85
13	THF	50	16	3	W-3	96
14	**Neat**	**50**	**16**	**3**	**W-1**	**99**
15	**Neat**	**50**	**16**	**3**	**W-2**	**99**
16	**Neat**	**50**	**16**	**3**	**W-3**	**99**

[a]Reaction conditions: quinoline (0.3 mmol), HBpin (3.0 equiv.), and Cat. (5 mol %); [b]yields were determined by ^{1}H NMR spectroscopy using tetraethylsilane as the internal standard.

4. Kinetic Studies

4.1 Kinetic experiments for the hydroboration of 3m

We started the kinetic experiments to determine the overall order and the rate equation of the hydroboration reaction of 6-fluoroquinoline (**3m**) with HBpin using **W-1** as a catalyst. Yields were determined by ^{19}F NMR integration. We started the investigation one by one: (i) the order of the hydroboration reaction with respect to the catalyst, (ii) the order of the hydroboration reaction with respect to HBpin, and (iii) the order of the hydroboration reaction with respect to **3m**.

4.2 Representative procedure for 3m hydroboration reaction carried out with various concentrations of W-1

The order of dependence of the catalyst **W-1** for hydroboration reaction of 6-fluoroquinoline (**3m**) with HBpin was determined by the methods of initial rates. Initial rate (k_{obs}) were determined using various concentrations of W-1 (0.002 M, 0.006 M, 0.01 M, and 0.014 M) by keeping the concentration of HBpin (0.6 M) and 6-fluoroquinoline (**3m**) (0.2 M) constant. We observed k_{obs} values of the reaction from [product] *vs* time plot, which was equal to the slope of the linear fit lines (**Table S2**). The experimental procedure that has been used is described below.

To a 10 mL Schlenk tube fitted with a stir bar was added **W-1** (in different concentrations, 0.002 M, 0.006 M, 0.01 M, and 0.014 M), 6-fluoroquinoline (**3m**) (0.2M), HBpin (0.6 M) and toluene (1 mL) inside the glove box. The tube was sealed and the mixture was conducted in an oil bath at 50 °C. After that, the ^{19}F NMR spectra were recorded at various time intervals. The varying catalyst concentration and the concentration of HBpin and 6-fluoroquinoline (**3m**) for each set of experiments are given in **Table S2** and represent the data graphically.

Table S2. Initial rates (k_{obs}) for the hydroboration reaction of 6-fluoroquinoline (**3m**) with HBpin carried out under varying concentrations of **W-1**.

3m (M)	**HBpin** (M)	**W-1** (M)	**initial rate** (M/min)	R^2
0.2	0.6	0.002	$(3.49\pm0.052)\times10^{-4}$	0.99
0.2	0.6	0.006	$(3.54\pm0.084)\times10^{-4}$	0.99
0.2	0.6	0.010	$(3.58\pm0.083)\times10^{-4}$	0.99
0.2	0.6	0.014	$(3.81\pm0.06)\times10^{-4}$	0.98

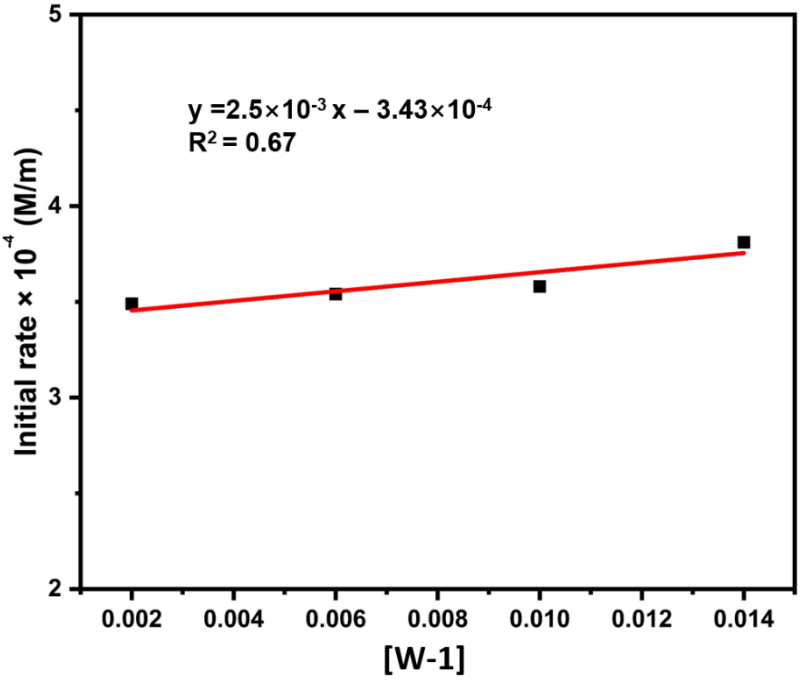

Figure S15. Plot of reaction initial rate (M/min) *vs* **W-1**

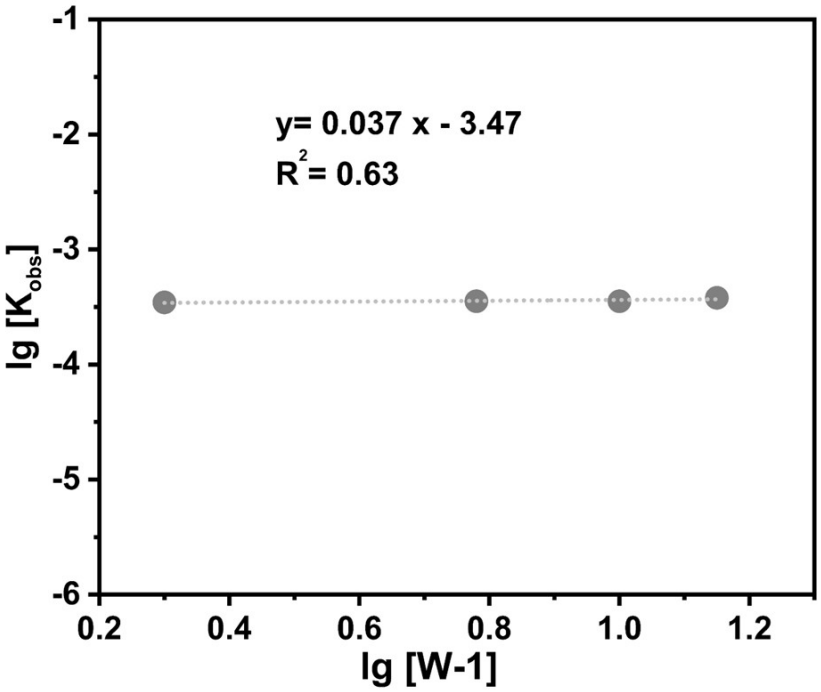

Figure S16. Plot of lg(k_{obs}) *vs* lg(concn of catalyst)

4.3 Representative procedure for the 6-fluoroquinoline (3m) hydroboration reaction carried out with various concentrations of HBpin

Initial rate (k_{obs}) were determined using various concentrations of HBpin (0.2 M, 0.4 M, 0.6 M, and 0.8 M) by keeping the concentration of W-1 (0.01 M) and 6-fluoroquinoline (**3m**) (0.2 M) constant. We observed k_{obs} values of the reaction from [product] *vs* time plot, which was equal to the slope of the linear fit lines (**Table S3**). The experimental procedure that has been used is described below.

To a 10 mL Schlenk tube fitted with a stir bar was added W-1(0.01 M), 6-fluoroquinoline (**3m**) (0.2 M), HBpin (in different concentrations, 0.2 M, 0.4 M, 0.6 M, and 0.8 M) and toluene (1 mL) inside the glove box. The tube was sealed and the mixture was conducted in an oil bath at 50 °C. After that, the ^{19}F NMR spectra were recorded at various time intervals. The varying HBpin concentration and the constant concentration of W-1 and 6-fluoroquinoline (**3m**) for each set of experiments are given in **Table S3** and represent the data graphically.

Table S3. Initial rates (k_{obs}) for the hydroboration reaction of 6-fluoroquinoline (**3m**) were carried out under varying concentrations of HBpin.

3m (M)	**HBpin** (M)	**W-1** (M)	**initial rate** (M/min)	R^2
0.2	0.2	0.01	$(0.343\pm0.067)\times10^{-4}$	0.88
0.2	0.4	0.01	$(1.73\pm0.127)\times10^{-4}$	0.98
0.2	0.6	0.01	$(3.58\pm0.083)\times10^{-4}$	0.99
0.2	0.8	0.01	$(4.48\pm0.770)\times10^{-4}$	0.97

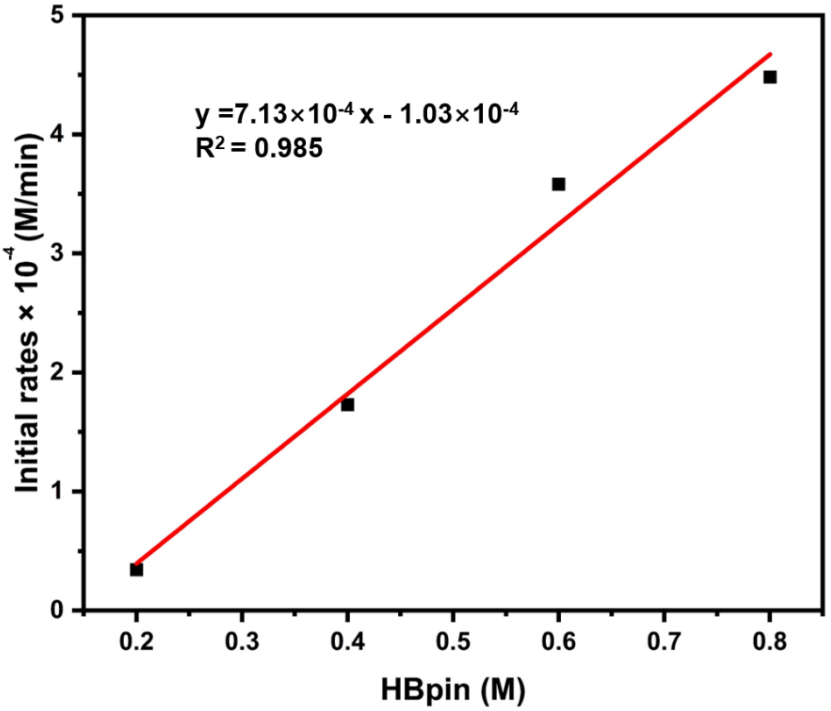

Figure S17. Plot of reaction initial rate (M/min) *vs* HBpin.

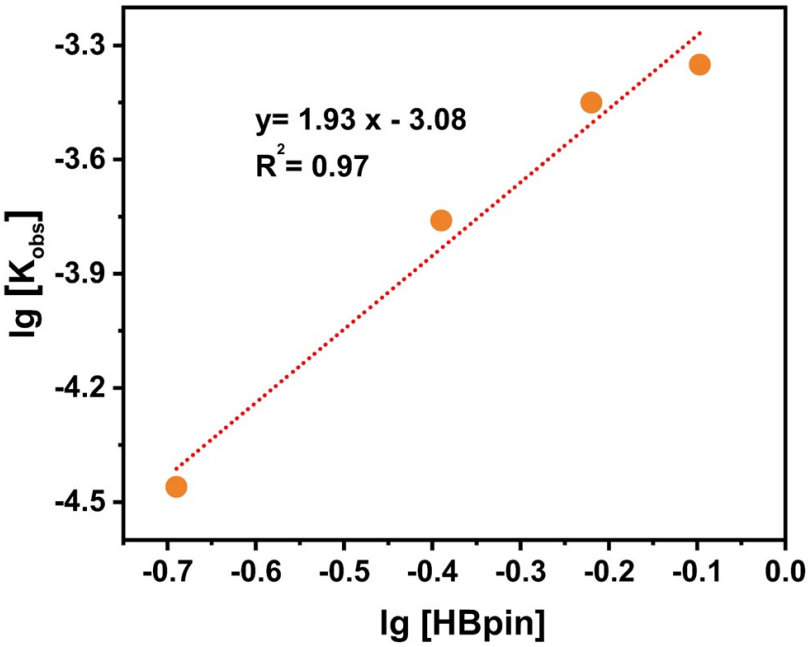

Figure S18. Plot of lg(k_{obs}) *vs* lg(concn of HBpin)

4.4 Representative procedure for the 6-fluoroquinoline (3m) hydroboration reaction carried out with various concentrations of 6-fluoroquinoline (3m)

Initial rate (k_{obs}) were determined using various concentrations of 6-fluoroquinoline (3m) (0.2 M, 0.4 M, 0.6 M, and 0.8 M) by keeping the concentration of **W-1** (0.01 M) and HBpin (0.6 M) constant. We observed k_{obs} values of the reaction from [product] *vs* time plot, which was equal to the slope of the linear fit lines (**Table S4**). The experimental procedure that has been used is described below.

To a 10 mL Schlenk tube fitted with a stir bar was added **W-1** (0.01 M), 6-fluoroquinoline (**3m**) (in different concentrations, 0.2 M, 0.4 M, 0.6 M, and 0.8 M), HBpin (0.6 M) and toluene (1 mL) inside the glove box. The tube was sealed and the mixture was conducted in an oil bath at 50 °C. After that, the ^{19}F NMR spectra were recorded at various time intervals. The varying 6-fluoroquinoline (**3m**) concentration and the constant concentration of **W-1** and HBpin for each set of experiments are given in **Table S4** and represent the data graphically.

Table S4. Initial rates (k_{obs}) for the hydroboration reaction of 6-fluoroquinoline (**3m**) were carried out under varying concentrations of 6-fluoroquinoline (**3m**).

3m (M)	**HBpin** (M)	**$W(CO)_4(NCMe)_2$** (M)	**initial rate** (M/min)	**R^2**
0.2	0.6	0.01	$(3.58\pm0.083)\times10^{-4}$	0.99
0.4	0.6	0.01	$(3.85\pm0.167)\times10^{-4}$	0.99
0.6	0.6	0.01	$(3.75\pm0.202)\times10^{-4}$	0.99
0.8	0.6	0.01	$(3.94\pm0.235)\times10^{-4}$	0.98

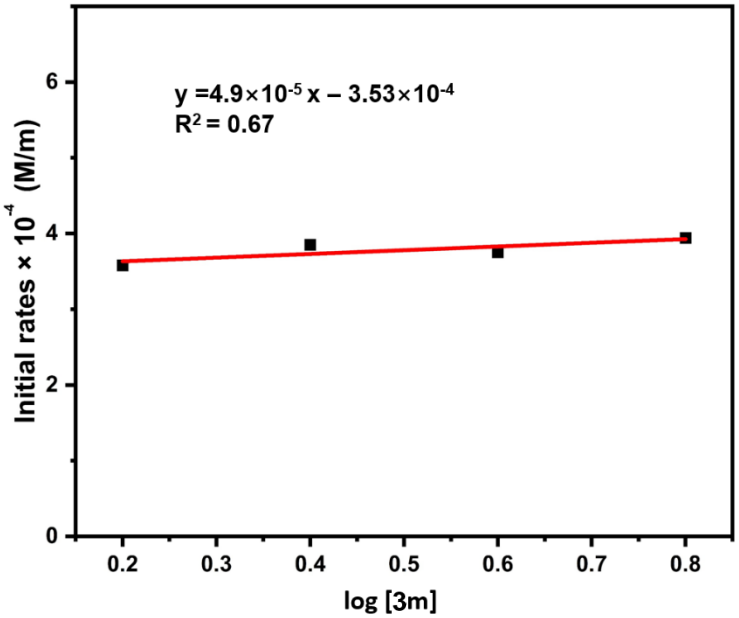

Figure S19. Plot of reaction initial rate (M/min) *vs* **3m**.

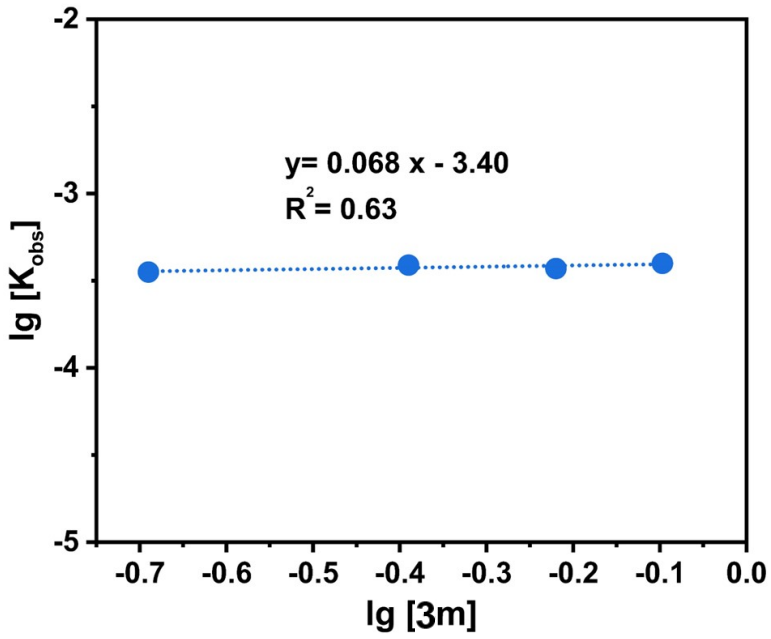

Figure S20. Plot of lg(k_{obs}) *vs* lg(concn of 3m).

5. Characterization Data of Compounds

5.1 Characterization Data of pyridines

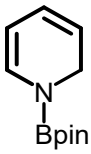

2a

1-(4,4,5,5-tetramethyl-1,3,2-dioxaborolan-2-yl)-1,2-dihydropyridine (2a)[1]**.** ^{1}H NMR (400 MHz, Benzene-d_6) ^{1}H NMR (400 MHz, Benzene-d_6) δ 6.55 (d, J = 7.4 Hz, 1H), 5.73 – 5.67 (m, 1H), 5.06 – 4.94 (m, 2H), 4.03 (dd, J = 4.2, 1.7 Hz, 2H), 0.95 (s, 12H), 0.86 (t, J = 8.0 Hz, 12H), 0.42 (q, J = 8.0 Hz, 8H). ^{13}C{^{1}H}NMR (101 MHz, Benzene-d_6) δ 132.4, 124.0, 114.6, 103.5, 82.6, 42.2, 24.3, 7.4, 3.0.

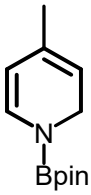

2b

4-methyl-1-(4,4,5,5-tetramethyl-1,3,2-dioxaborolan-2-yl)-1,2-dihydropyridine (2b)[2]**.** ^{1}H NMR (400 MHz, Benzene-d_6) δ 7.28 (d, J = 6.5 Hz, 4H), 7.23 – 7.17 (m, 1H), 3.45 (s, 2H), 2.35 (s, 4H), 1.57 – 1.52 (m, 4H), 1.40 (td, J = 6.5,

3.7 Hz, 2H), 1.24 (s, 24H), 0.90 (t, J = 7.9 Hz, 12H), 0.48 (q, J = 7.9 Hz, 8H). $^{13}C\{^{1}H\}$NMR (101 MHz, Benzene-d_6) δ 138.6, 129.3, 128.2, 126.9, 83.0, 63.9, 54.5, 26.0, 24.6, 7.5, 3.0.

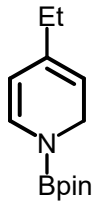

2c

4-ethyl-1-(4,4,5,5-tetramethyl-1,3,2-dioxaborolan-2-yl)-1,2-dihydropyridine (2c)[1]**.** ^{1}H NMR (400 MHz, Benzene-d_6) δ 6.62 (dd, J = 7.5, 1.1 Hz, 1H), 4.92 (d, J = 7.5 Hz, 1H), 4.81 (s, 1H), 4.09 (d, J = 4.1 Hz, 2H), 1.84 (dd, J = 7.5, 1.5 Hz, 2H), 1.05 (s, 3H), 0.96 (s, 12H), 0.86 (d, J = 7.9 Hz, 14H), 0.42 (q, J = 7.9 Hz, 10H). $^{13}C\{^{1}H\}$NMR (101 MHz, Benzene-d_6) δ 137.3, 132.1, 108.5, 105.5, 82.7, 42.6, 27.7, 24.4, 12.5, 7.3, 3.0.

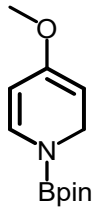

2d

4-methoxy-1-(4,4,5,5-tetramethyl-1,3,2-dioxaborolan-2-yl)-1,2-dihydropyridine (2d)[1]**.** ^{1}H NMR (400 MHz, Benzene-d_6) δ 6.61 (d, J = 7.7 Hz, 1H), 5.07 (dd, J = 7.8, 2.4 Hz, 1H), 4.21 (d, J = 4.1 Hz, 2H), 3.98 (s, 1H), 3.19 (s, 3H), 1.02 (s, 12H), 0.94 – 0.90 (m, 12H), 0.47 (q, J = 8.0 Hz, 9H). $^{13}C\{^{1}H\}$NMR (101 MHz, Benzene-d_6) δ 154.0, 134.4, 101.6, 82.9, 82.5, 53.4, 42.5, 24.3, 7.3, 2.9.

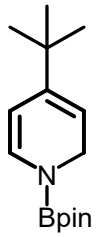

2e

4-(tert-butyl)-1-(4,4,5,5-tetramethyl-1,3,2-dioxaborolan-2-yl)-1,2-dihydropyridine (2e)[3]**.** ^{1}H NMR (400 MHz, Benzene-d_6) δ 6.69 – 6.63 (m, 1H), 5.17

(dd, J = 7.7, 2.0 Hz, 1H), 4.94 (s, 1H), 4.11 (d, J = 4.3 Hz, 2H), 1.03 (s, 12H), 0.99 (s, 9H), 0.92 (t, J = 8.0 Hz, 12H), 0.48 (q, J = 8.0 Hz, 8H). $^{13}C\{^{1}H\}$NMR (101 MHz, Benzene-d_6) δ 143.8, 132.2, 106.4, 103.4, 82.7, 42.6, 33.3, 28.6, 24.4, 7.3, 2.9.

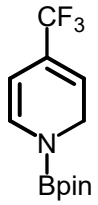

2f

1-(4,4,5,5-tetramethyl-1,3,2-dioxaborolan-2-yl)-4-(trifluoromethyl)-1,2-dihydropyridine (2f)[3]**.** ^{1}H NMR (400 MHz, Benzene-d_6) δ 7.15 (d, J = 7.6 Hz, 1H), 5.93 (d, J = 1.6 Hz, 1H), 5.69 (dd, J = 7.6, 1.9 Hz, 1H), 4.51 (s, 2H), 1.62 (s, 12H), 1.53 (t, J = 8.0 Hz, 14H), 1.09 (q, J = 8.0 Hz, 9H). $^{13}C\{^{1}H\}$NMR (101 MHz, Benzene-d_6) δ 135.2, 125.1, 122.4, 115.7, 97.5, 83.7, 41.8, 24.7, 7.7, 3.3.

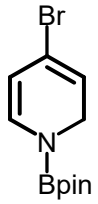

2g

4-bromo-1-(4,4,5,5-tetramethyl-1,3,2-dioxaborolan-2-yl)-1,2-dihydropyridine (2g)[4]**.** ^{1}H NMR (400 MHz, Benzene-d_6) δ 6.35 (d, J = 8.5 Hz, 1H), 5.10 (t, J = 3.9 Hz, 1H), 5.01 (dd, J = 7.6, 2.0 Hz, 1H), 3.85 (d, J = 4.5 Hz, 2H), 0.93 (s, 12H), 0.86 (t, J = 8.0 Hz, 33H), 0.42 (q, J = 7.9 Hz, 21H). $^{13}C\{^{1}H\}$NMR (101 MHz, Benzene-d_6) δ 150.5, 128.4, 119.7, 108.9, 82.6, 42.2, 24.3, 7.4, 3.0.

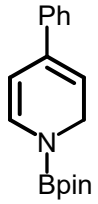

2h

4-phenyl-1-(4,4,5,5-tetramethyl-1,3,2-dioxaborolan-2-yl)-1,2-dihydropyridine (2h)[1]**.** ^{1}H NMR (400 MHz, Benzene-d_6) δ 7.22 (d, J = 8.1 Hz, 2H), 7.06 (t, J = 7.7 Hz, 2H), 7.01 (d, J = 7.5 Hz, 1H), 6.69 (d, J = 7.6 Hz, 1H), 5.39 (d, J =

7.6 Hz, 1H), 5.27 (s, 1H), 4.15 (s, 2H), 0.98 (s, 12H), 0.86 (t, J = 8.0 Hz, 14H), 0.45 – 0.37 (m, 9H). $^{13}C\{^{1}H\}$NMR (101 MHz, Benzene-d_6) δ 139.8, 135.8, 133.3, 128.2, 127.0, 125.5, 110.9, 104.0, 83.0, 42.8, 24.6, 7.3, 2.9.

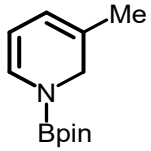

2i

3-methyl-1-(4,4,5,5-tetramethyl-1,3,2-dioxaborolan-2-yl)-1,2-dihydropyridine (2i)[5]**.** ^{1}H NMR (400 MHz, Benzene-d_6) δ 6.62 (d, J = 7.0 Hz, 1H), 5.52 (d, J = 4.7 Hz, 1H), 5.05 (dd, J = 7.4, 5.5 Hz, 1H), 4.09 (s, 2H), 1.42 (s, 3H), 1.03 (s, 12H). $^{13}C\{^{1}H\}$NMR (101 MHz, Benzene-d_6) δ 129.0, 124.4, 118.3, 102.7, 82.8, 47.0, 24.5, 20.5.

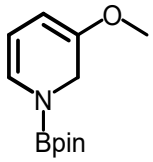

2j

3-methoxy-1-(4,4,5,5-tetramethyl-1,3,2-dioxaborolan-2-yl)-1,2-dihydropyridine (2j)[5]**.** ^{1}H NMR (400 MHz, Benzene-d_6) δ 6.38 (d, J = 7.2 Hz, 1H), 5.06 (t, J = 6.7 Hz, 1H), 4.74 (d, J = 6.2 Hz, 1H), 4.21 (s, 2H), 3.18 (s, 3H), 1.02 (s, 12H), 0.93 (t, J = 8.0 Hz, 15H), 0.48 (q, J = 7.9 Hz, 9H). $^{13}C\{^{1}H\}$NMR (101 MHz, Benzene-d_6) δ 148.9, 124.5, 102.3, 91.2, 82.7, 53.8, 45.0, 24.4, 7.3, 2.9.

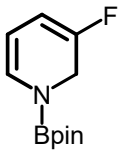

2k

3-fluoro-1-(4,4,5,5-tetramethyl-1,3,2-dioxaborolan-2-yl)-1,2-dihydropyridine (2k)[5]**.** ^{1}H NMR (400 MHz, Benzene-d_6) δ 6.34 (dd, J = 7.3, 1.9 Hz, 1H), 5.30 (dd, J = 12.0, 6.3 Hz, 1H), 4.71 (d, J = 7.4 Hz, 1H), 4.26 (s, 2H), 0.99 (s, 12H), 0.94 (t, J = 8.0 Hz, 19H), 0.49 (q, J = 8.0 Hz, 12H). $^{13}C\{^{1}H\}$NMR (101 MHz, Benzene-d_6) δ 152.7, 150.1, 127.3, 127.2, 99.8, 99.6, 98.8, 98.7, 83.1, 43.3, 42.9, 24.3, 7.3, 3.0.

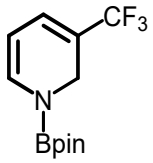

2l

1-(4,4,5,5-tetramethyl-1,3,2-dioxaborolan-2-yl)-3-(trifluoromethyl)-1,2-dihydropyridine (2l). ^{1}H NMR (400 MHz, Benzene-d_6) δ 7.09 (d, J = 1.6 Hz, 1H), 5.86 (dd, J = 9.9, 1.8 Hz, 1H), 4.91 (dtd, J = 9.8, 4.0, 3.4, 2.0 Hz, 1H), 3.89 (dd, J = 4.0, 1.9 Hz, 2H), 1.01 (s, 12H), 0.93 (t, J = 8.0 Hz, 21H), 0.49 (q, J = 7.9 Hz, 14H). ^{13}C NMR (101 MHz, Benzene-d6) δ 134.6, 125.1, 118.9, 115.6, 82.6, 42.2, 24.3, 22.8, 7.4, 3.0.

5.2 Characterization Data of quinolines

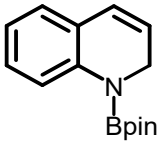

4a

1-(4,4,5,5-tetramethyl-1,3,2-dioxaborolan-2-yl)-1,2-dihydroquinoline (4a)[6]. ^{1}H NMR (400 MHz, Benzene-d_6) δ 7.72 (d, J = 10.9 Hz, 1H), 7.11 – 7.01 (m, 1H), 6.88 – 6.73 (m, 2H), 6.24 (d, J = 7.6 Hz, 1H), 5.62 – 5.53 (m, 1H), 4.11 (d, J = 5.8 Hz, 2H), 1.05 (s, 12H), 0.93 (t, J = 8.0 Hz, 11H), 0.49 (q, J = 7.9 Hz, 7H). ^{13}C{^{1}H}NMR (101 MHz, Benzene-d_6) δ 141.9, 127.8, 126.7, 126.6, 124.3, 124.2, 121.5, 120.9, 82.5, 43.3, 24.4, 7.4, 3.0.

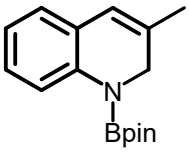

4b

3-methyl-1-(4,4,5,5-tetramethyl-1,3,2-dioxaborolan-2-yl)-1,2-dihydroquinoline(4b)[1]. ^{1}H NMR (400 MHz, Benzene-d_6) δ 7.76 (d, J = 8.1 Hz, 1H), 7.05 – 6.99 (m, 1H), 6.79 (d, J = 14.0 Hz, 2H), 5.94 (d, J = 1.8 Hz, 1H), 4.01 (s, 2H), 1.45 (s, 3H), 1.00 (s, 12H), 0.88 (t, J = 8.0 Hz, 14H), 0.43 (q, J = 8.0 Hz, 8H). ^{13}C{^{1}H}NMR (101 MHz, Benzene-d_6) δ 140.4, 133.7, 127.0, 125.8, 121.7, 121.5, 120.4, 82.6, 48.0, 24.3, 20.2. 7.4. 3.0.

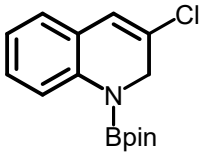

4c

3-chloro-1-(4,4,5,5-tetramethyl-1,3,2-dioxaborolan-2-yl)-1,2-dihydroquinoline (4c)[4]**.** ^{1}H NMR (400 MHz, Benzene-d_6) δ 7.47 (dt, J = 7.8, 1.6 Hz, 1H), 6.80 – 6.63 (m, 3H), 5.57 (d, J = 9.8 Hz, 1H), 3.90 (dt, J = 4.1, 2.1 Hz, 2H), 0.98 (s, 12H), 0.87 (t, J = 7.9 Hz, 12H), 0.43 (q, J = 8.0 Hz, 8H). ^{13}C{^{1}H}NMR (101 MHz, Benzene-d_6) δ 143.6, 131.2, 127.9, 125.7, 124.6, 122.7, 122.2, 119.6, 82.8, 42.7, 24.3, 7.4, 3.0.

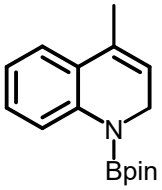

4d

4-methyl-1-(4,4,5,5-tetramethyl-1,3,2-dioxaborolan-2-yl)-1,2-dihydroquinoline (4d)[6]**.** ^{1}H NMR (400 MHz, Benzene-d_6) δ 7.69 (d, J = 8.1 Hz, 1H), 7.03 (dd, J = 20.9, 7.7 Hz, 2H), 6.82 – 6.76 (m, 1H), 5.38 (s, 1H), 4.02 (dd, J = 4.2, 1.9 Hz, 2H), 1.74 (s, 3H), 1.00 (s, 12H), 0.88 (t, J = 8.0 Hz, 10H), 0.43 (q, J = 8.0 Hz, 7H). ^{13}C{^{1}H}NMR (101 MHz, Benzene-d_6) δ 142.0, 131.2, 128.4,127.6. 123.4, 121.4, 121.3, 121.0, 82.5, 43.1, 24.4, 18.4, 7.4, 3.0.

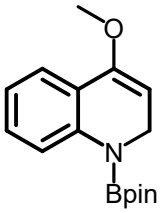

4e

4-methoxy-1-(4,4,5,5-tetramethyl-1,3,2-dioxaborolan-2-yl)-1,2-dihydroquinoline (4e)[4]**.** ^{1}H NMR (400 MHz, Benzene-d_6) δ 18 (d, J = 4.4 Hz, 2H), 3.17 (s, 3H), 1.01 (s, 12H), 0.87 (t, J =7.71 (d, J = 8.1 Hz, 1H), 7.65 (d, J = 9.4 Hz, 1H), 7.06 – 7.02 (m, 1H), 6.82 – 6.77 (m, 1H), 4.45 (t, J = 4.4 Hz, 1H), 4. 7.9 Hz, 15H), 0.42 (q, J = 7.9 Hz, 10H). ^{13}C{^{1}H}NMR (101 MHz, Benzene-d_6) δ 151.8, 142.8, 124.4, 122.3, 122.2, 121.1, 120.7, 120.6, 82.6, 42.7, 24.3, 7.4, 3.0.

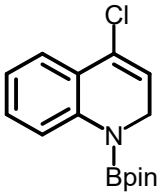

4f

4-chloro-1-(4,4,5,5-tetramethyl-1,3,2-dioxaborolan-2-yl)-1,2-dihydroquinoline (4f)[4]**.** ^{1}H NMR (400 MHz, Benzene-d_6) δ 7.57 (dd, J = 8.1, 1.2 Hz, 1H), 7.48 (d, J = 7.8 Hz, 1H), 7.00 – 6.94 (m, 1H), 6.72 (t, J = 7.6 Hz, 1H), 5.56 (t, J = 4.6 Hz, 1H), 3.90 (d, J = 4.7 Hz, 2H), 0.98 (s, 12H), 0.86 (t, J = 8.0 Hz, 12H), 0.42 (q, J = 8.0 Hz, 8H). ^{13}C{^{1}H}NMR (101 MHz, Benzene-d_6) δ 142.5, 129.3, 129.1, 124.9, 124.6, 121.8, 121.6, 120.8, 82.8, 43.9, 24.6, 7.4, 2.9.

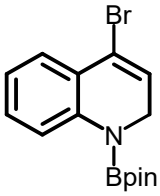

4g

4-bromo-1-(4,4,5,5-tetramethyl-1,3,2-dioxaborolan-2-yl)-1,2-dihydroquinoline (4g)[4]**.** ^{1}H NMR (400 MHz, Benzene-d_6) δ 7.54 (dd, J = 8.1, 1.2 Hz, 1H), 7.48 (dd, J = 7.8, 1.6 Hz, 1H), 6.99 – 6.92 (m, 1H), 6.71 (t, J = 7.6 Hz, 1H), 5.79 (t, J = 4.6 Hz, 1H), 3.83 (d, J = 4.7 Hz, 2H), 0.97 (s, 12H), 0.87 (t, J = 8.0 Hz, 12H), 0.42 (q, J = 7.9 Hz, 8H). ^{13}C{^{1}H}NMR (101 MHz, Benzene-d_6) δ 142.4, 129.1, 127.1, 126.5, 125.7, 121.8, 120.8, 119.7, 82.8, 44.8, 24.6, 7.4, 2.9.

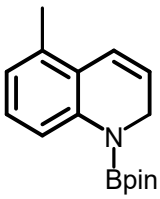

4h

5-methyl-1-(4,4,5,5-tetramethyl-1,3,2-dioxaborolan-2-yl)-1,2-dihydroquinoline (4h). ^{1}H NMR (400 MHz, Benzene-d_6) δ 7.59 (d, J = 8.2 Hz, 1H), 6.96 (t, J = 7.8 Hz, 1H), 6.60 (dt, J = 7.6, 1.0 Hz, 1H), 6.43 (dq, J = 9.8, 1.4 Hz, 1H), 5.63 (dt, J = 9.7, 4.3 Hz, 1H), 4.03 (dd, J = 4.4, 1.7 Hz, 2H), 2.02 (s, 3H), 1.00 (s, 12H), 0.88 (t, J = 8.0 Hz, 12H), 0.43 (q, J = 8.0 Hz, 8H). ^{13}C{^{1}H}NMR (101 MHz,

Benzene-d_6) δ 142.1, 133.2, 127.3, 125.4, 124.1, 123.5, 123.4, 119.3, 82.6, 42.6, 24.4, 18.8, 7.4, 3.0.

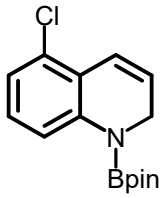

4i

5-chloro-1-(4,4,5,5-tetramethyl-1,3,2-dioxaborolan-2-yl)-1,2-dihydroquinoline (4i)[7]**.** ^{1}H NMR (400 MHz, Benzene-d_6) δ 7.51 (d, J = 8.0 Hz, 1H), 6.84 – 6.69 (m, 3H), 5.59 – 5.50 (m, 1H), 3.92 (d, J = 4.3 Hz, 2H), 0.97 (s, 12H), 0.88 (t, J = 8.0 Hz, 12H), 0.43 (q, J = 8.0 Hz, 8H). ^{13}C{^{1}H}NMR (101 MHz, Benzene-d_6) δ 143.6, 131.3, 128.8, 125.8, 124.7, 122.8, 122.3, 119.6, 82.8, 42.7, 24.3, 7.4, 3.0.

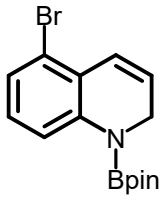

4j

5-bromo-1-(4,4,5,5-tetramethyl-1,3,2-dioxaborolan-2-yl)-1,2-dihydroquinoline (4j). ^{1}H NMR (400 MHz, Benzene-d_6) δ 7.54 (d, J = 8.1 Hz, 1H), 6.98 (dd, J = 8.0, 1.1 Hz, 1H), 6.78 (d, J = 9.8 Hz, 1H), 6.65 (t, J = 8.1 Hz, 1H), 5.53 (dt, J = 9.8, 4.4 Hz, 1H), 3.89 (dd, J = 4.3, 1.8 Hz, 2H), 0.97 (s, 12H), 0.88 (t, J = 8.0 Hz, 11H), 0.43 (q, J = 8.0 Hz, 8H). ^{13}C{^{1}H}NMR (101 MHz, Benzene-d_6) δ 143.7, 129.2, 128.3, 126.1, 125.6, 125.4, 121.9, 120.3, 82.8, 42.7, 24.3, 7.4, 3.0.

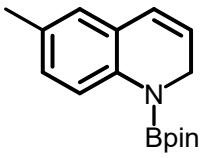

4k

6-methyl-1-(4,4,5,5-tetramethyl-1,3,2-dioxaborolan-2-yl)-1,2-dihydroquinoline (4k)[8]**.** ^{1}H NMR (400 MHz, Benzene-d_6) δ 7.69 (d, J = 8.2 Hz, 1H), 6.91 (d, J = 10.3 Hz, 1H), 6.66 (s, 1H), 6.27 (d, J = 9.4 Hz, 1H), 5.62 (dt, J = 8.8, 4.0 Hz, 1H), 4.15 (dd, J = 4.1, 1.8 Hz, 2H), 2.09 (s, 3H), 1.05 (s, 12H), 0.94 (t, J = 8.0 Hz,

12H), 0.49 (q, J = 7.9 Hz, 8H). $^{13}C\{^{1}H\}$NMR (101 MHz, Benzene-d_6) δ 139.4, 130.3, 128.4, 127.2, 126.7, 126.6, 124.3, 120.8, 82.6, 43.4, 24.3, 20.4, 7.4, 3.0.

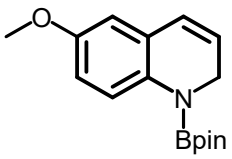

4l

6-methoxy-1-(4,4,5,5-tetramethyl-1,3,2-dioxaborolan-2-yl)-1,2-dihydroquinoline (4l)[1]**.** ^{1}H NMR (400 MHz, Benzene-d_6) δ 7.61 (d, J = 8.8 Hz, 1H), 6.64 (dd, J = 8.8, 2.9 Hz, 1H), 6.48 (d, J = 3.0 Hz, 1H), 6.17 (d, J = 9.6 Hz, 1H), 5.60 – 5.54 (m, 1H), 4.07 (d, J = 6.0 Hz, 2H), 3.28 (s, 3H), 1.00 (s, 12H), 0.88 (t, J = 8.0 Hz, 14H), 0.43 (q, J = 8.0 Hz, 9H). $^{13}C\{^{1}H\}$NMR (101 MHz, Benzene-d_6) δ 154.9, 135.1, 126.6, 125.3, 121.8, 113.3, 111.8, 82.6, 54.7, 43.4, 24.4, 7.4, 3.0.

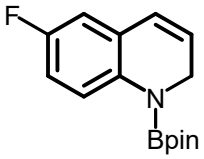

4m

6-fluoro-1-(4,4,5,5-tetramethyl-1,3,2-dioxaborolan-2-yl)-1,2-dihydroquinoline (4m)[9]**.** ^{1}H NMR (400 MHz, Benzene-d_6) δ 7.51 (dd, J = 8.9, 5.1 Hz, 1H), 6.68 (td, J = 8.7, 3.0 Hz, 1H), 6.47 (dd, J = 8.8, 3.0 Hz, 1H), 5.97 (d, J = 9.5 Hz, 1H), 5.53 – 5.45 (m, 1H), 3.98 (dd, J = 4.2, 1.8 Hz, 2H), 0.98 (s, 12H), 0.88 (t, J = 8.0 Hz, 11H), 0.43 (q, J = 8.0 Hz, 7H). $^{13}C\{^{1}H\}$NMR (101 MHz, Benzene-d_6) δ 159.4, 157.0, 137.7, 125.9, 121.9, 113.9, 113.7, 112.7, 82.6, 43.2, 24.3, 7.4, 3.0.

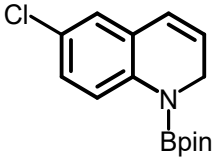

4n

6-chloro-1-(4,4,5,5-tetramethyl-1,3,2-dioxaborolan-2-yl)-1,2-dihydroquinoline (4n)[7]**.** ^{1}H NMR (400 MHz, Benzene-d_6) δ 7.50 (d, J = 8.7 Hz, 1H), 6.96 (d, J = 8.7 Hz, 1H), 6.73 (d, J = 2.6 Hz, 1H), 5.93 (d, J = 9.6 Hz, 1H), 5.43 (d, J = 9.6 Hz, 1H), 3.97 (dd, J = 4.2, 1.8 Hz, 2H), 0.97 (s, 12H), 0.88 (t, J = 8.0 Hz, 12H),

0.43 (q, J = 8.0 Hz, 8H). $^{13}C\{^{1}H\}$NMR (101 MHz, Benzene-d_6) δ 141.6, 140.4, 129.1, 126.4, 126.2, 125.6, 125.5, 122.0, 82.6, 43.2, 24.4, 7.4, 3.0.

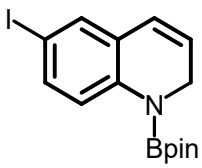

4o

6-iodo-1-(4,4,5,5-tetramethyl-1,3,2-dioxaborolan-2-yl)-1,2-dihydroquinoline (4o). ^{1}H NMR (400 MHz, Benzene-d_6) δ 7.29 (d, J = 8.6 Hz, 1H), 7.23 (d, J = 8.6 Hz, 1H), 7.04 (d, J = 2.2 Hz, 1H), 5.89 (d, J = 9.6 Hz, 1H), 5.41 (dt, J = 9.6, 4.2 Hz, 1H), 3.95 (d, J = 6.0 Hz, 2H), 0.96 (s, 12H), 0.87 (t, J = 8.0 Hz, 12H), 0.42 (q, J = 8.0 Hz, 8H). $^{13}C\{^{1}H\}$NMR (101 MHz, Benzene-d_6) δ 141.6, 138.0, 136.4, 134.9, 128.9, 125.3, 125.2, 122.8, 82.6, 43.2, 24.3, 7.4, 3.0.

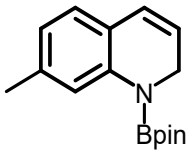

4p

7-methyl-1-(4,4,5,5-tetramethyl-1,3,2-dioxaborolan-2-yl)-1,2-dihydroquinoline (4p)[4]**.** ^{1}H NMR (400 MHz, Benzene-d_6) δ 7.52 (d, J = 1.7 Hz, 1H), 6.73 (d, J = 7.6 Hz, 1H), 6.58 (dt, J = 7.6, 2.3 Hz, 1H), 6.23 (dd, J = 9.5, 1.9 Hz, 1H), 5.51 (dt, J = 9.5, 4.2 Hz, 1H), 4.09 (dd, J = 4.2, 1.7 Hz, 2H), 2.11 (s, 3H), 0.99 (s, 12H), 0.88 (t, J = 8.0 Hz, 14H), 0.43 (q, J = 8.0 Hz, 10H). $^{13}C\{^{1}H\}$NMR (101 MHz, Benzene-d_6) δ 141.9, 137.3, 126.57, 124.3, 123.25, 122.42, 121.60, 120.29, 82.59, 43.35, 24.31, 7.38, 2.96.

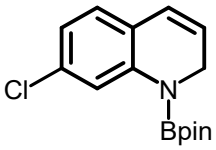

4q

7-chloro-1-(4,4,5,5-tetramethyl-1,3,2-dioxaborolan-2-yl)-1,2-dihydroquinoline (4q)[4]**.** ^{1}H NMR (400 MHz, Benzene-d_6) δ 7.84 (s, 1H), 6.76 (d, J = 10.2 Hz, 1H), 6.53 (d, J = 8.0 Hz, 1H), 6.08 (d, J = 9.6 Hz, 1H), 5.51 – 5.45 (m, 1H), 4.04 (d, J = 6.0 Hz, 2H), 1.01 (s, 12H), 0.94 (t, J = 8.0 Hz, 12H), 0.49 (q, J = 8.0 Hz,

8H). $^{13}C\{^{1}H\}$NMR (101 MHz, Benzene-d_6) δ 143.2, 133.0, 125.6, 125.4, 124.9, 124.2, 121.4, 120.7, 82.6, 43.2, 24.3, 7.4, 3.0.

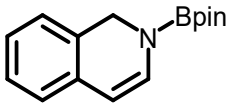

4r

2-(4,4,5,5-tetramethyl-1,3,2-dioxaborolan-2-yl)-1,2-dihydroisoquinoline (4r)[8]. ^{1}H NMR (400 MHz, Benzene-d_6) δ 6.94 – 6.90 (m, 1H), 6.82 (t, J = 6.8 Hz, 1H), 6.76 – 6.69 (m, 2H), 6.66 (d, J = 7.4 Hz, 1H), 5.54 (d, J = 7.5 Hz, 1H), 4.52 (s, 2H), 0.98 (s, 12H), 0.88 (t, J = 8.0 Hz, 11H), 0.43 (q, J = 8.0 Hz, 7H). $^{13}C\{^{1}H\}$NMR (101 MHz, Benzene-d_6) δ 133.2, 132.5, 128.6, 127.2, 125.8, 125.1, 123.4, 105.8, 83.0, 45.9, 24.4, 7.4, 3.0.

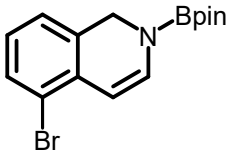

4s

5-bromo-2-(4,4,5,5-tetramethyl-1,3,2-dioxaborolan-2-yl)-1,2-dihydroisoquinoline (4s)[8]. ^{1}H NMR (400 MHz, Benzene-d_6) δ 7.15 (d, J = 7.7 Hz, 1H), 6.73 (d, J = 7.7 Hz, 1H), 6.44 (d, J = 13.3 Hz, 2H), 6.06 (d, J = 7.7 Hz, 1H), 4.36 (s, 2H), 0.97 (s, 12H), 0.87 (t, J = 8.0 Hz, 12H), 0.42 (q, J = 8.0 Hz, 8H). $^{13}C\{^{1}H\}$NMR (101 MHz, Benzene-d_6) δ 134.73, 132.75, 131.3, 130.3, 126.59, 124.21, 119.13, 104.35, 83.27, 46.00, 24.37, 7.38, 2.97.

6. NMR Spectra (▲ stand for internal standard tetraethylsilane**)**

6.1 NMR Spectra for pyridines

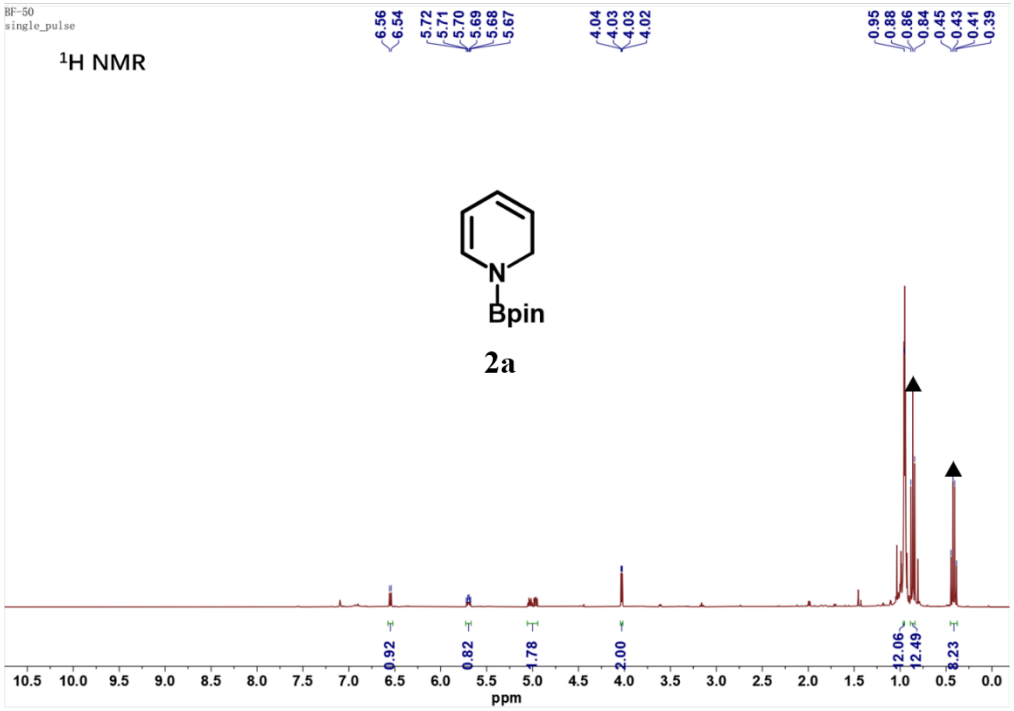

Figure S21. ^{1}H NMR spectrum of **2a** (400 MHz, Benzene-d_6).

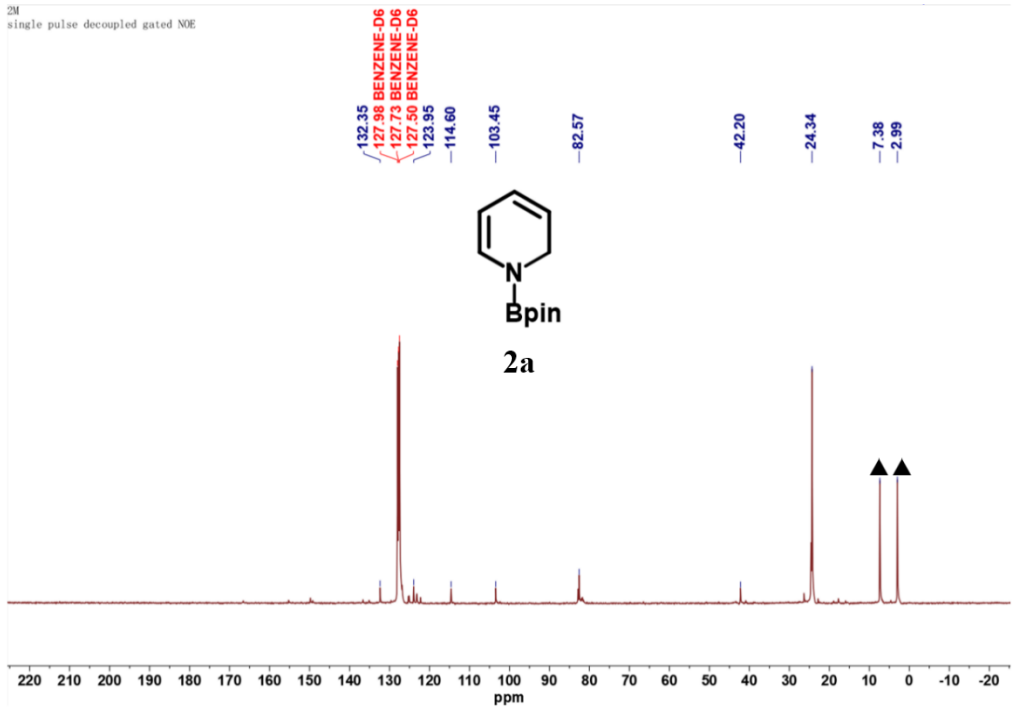

Figure S22. ^{13}C NMR spectrum of **2a** (101 MHz, Benzene-d_6).

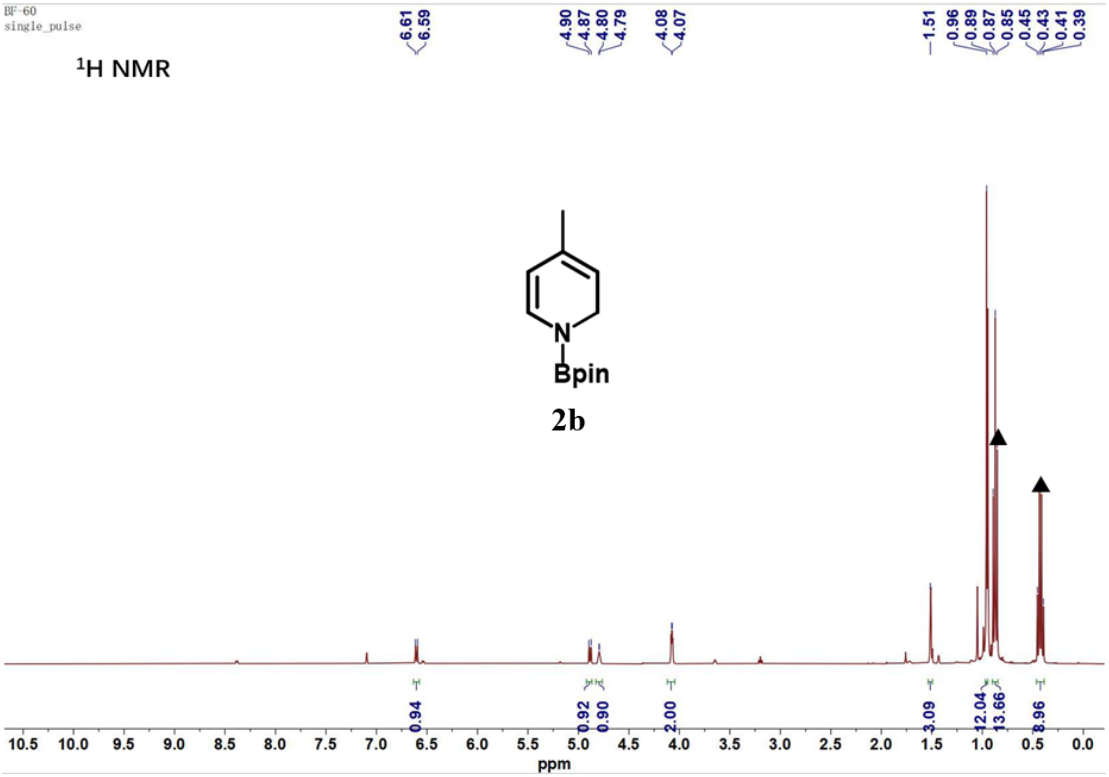

Figure S23. ^{1}H NMR spectrum of **2b** (400 MHz, Benzene-d_6).

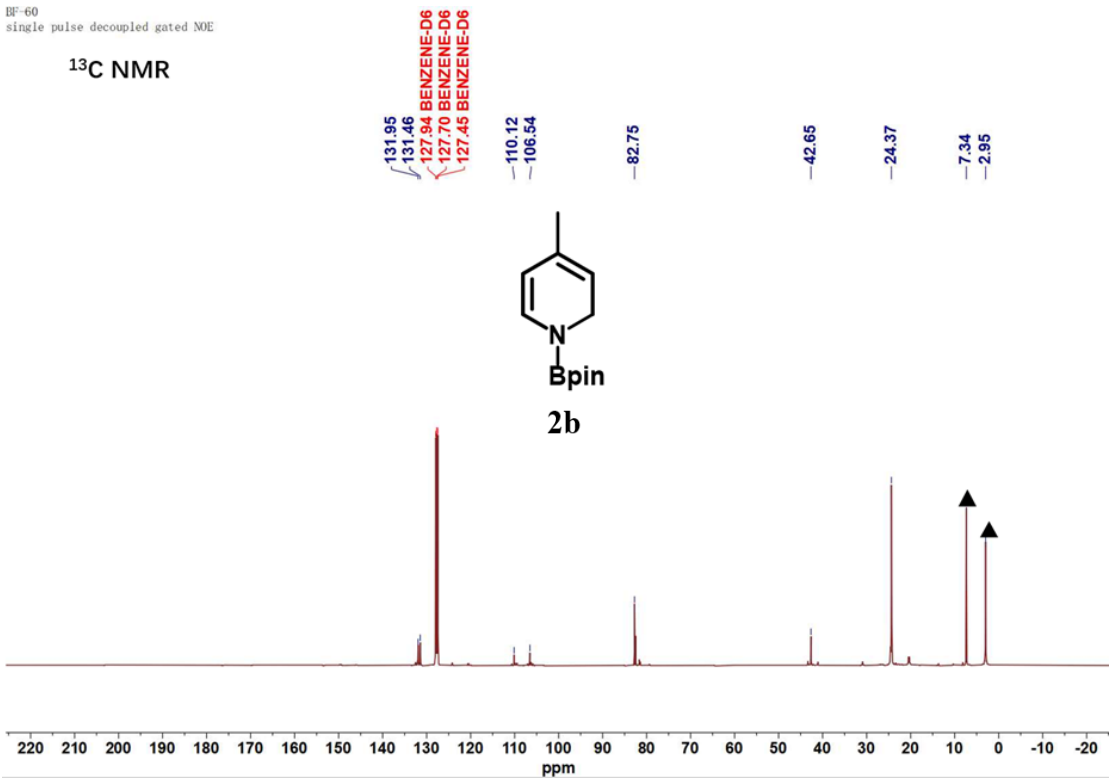

Figure S24. ^{13}C NMR spectrum of **2b** (101 MHz, Benzene-d_6).

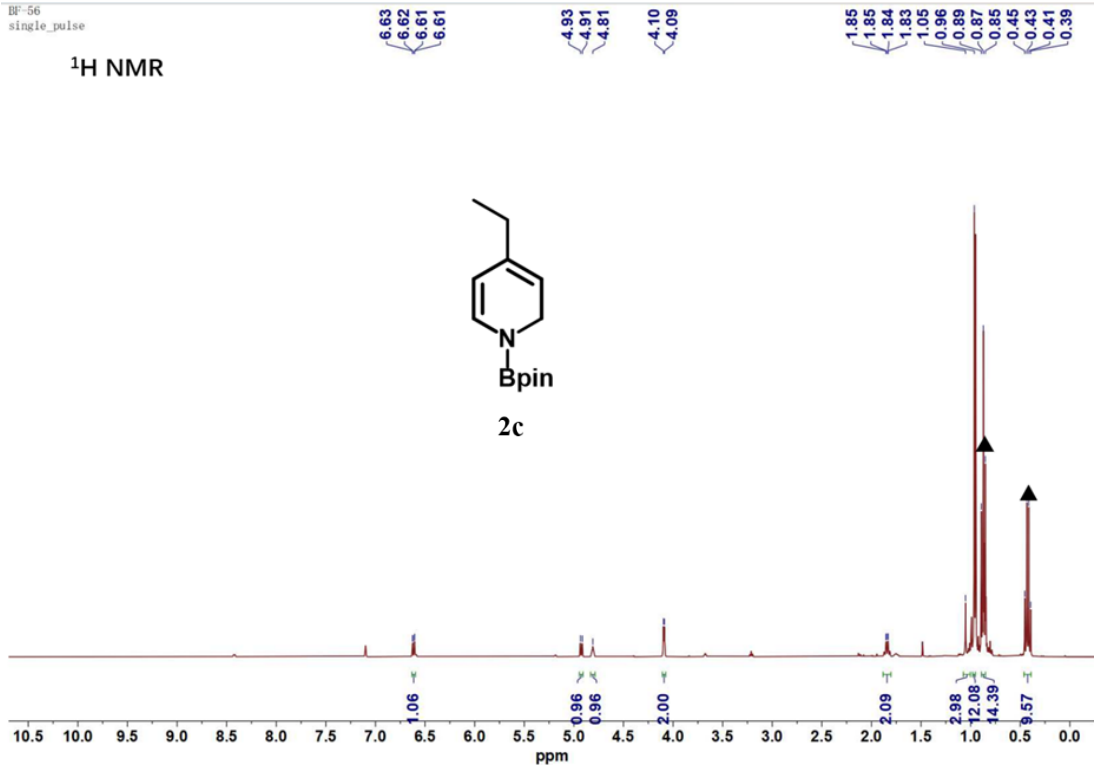

Figure S25. ^{1}H NMR spectrum of **2c** (400 MHz, Benzene-d_6).

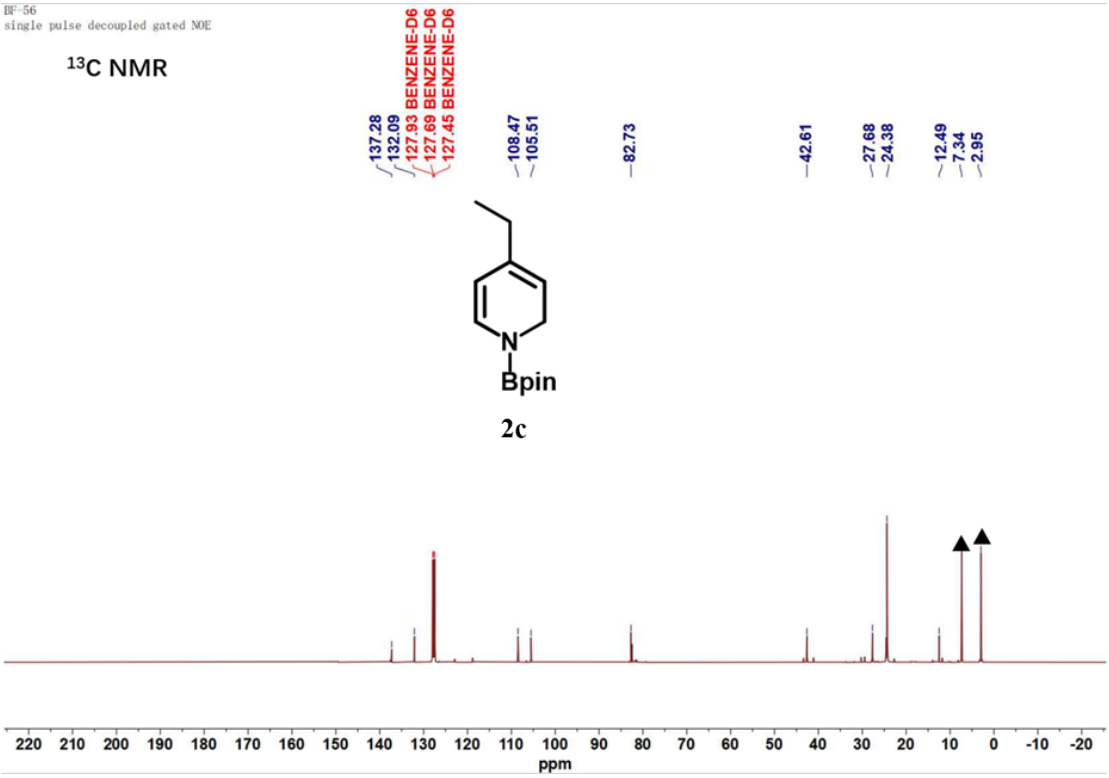

Figure S26. ^{13}C NMR spectrum of **2c** (101 MHz, Benzene-d_6).

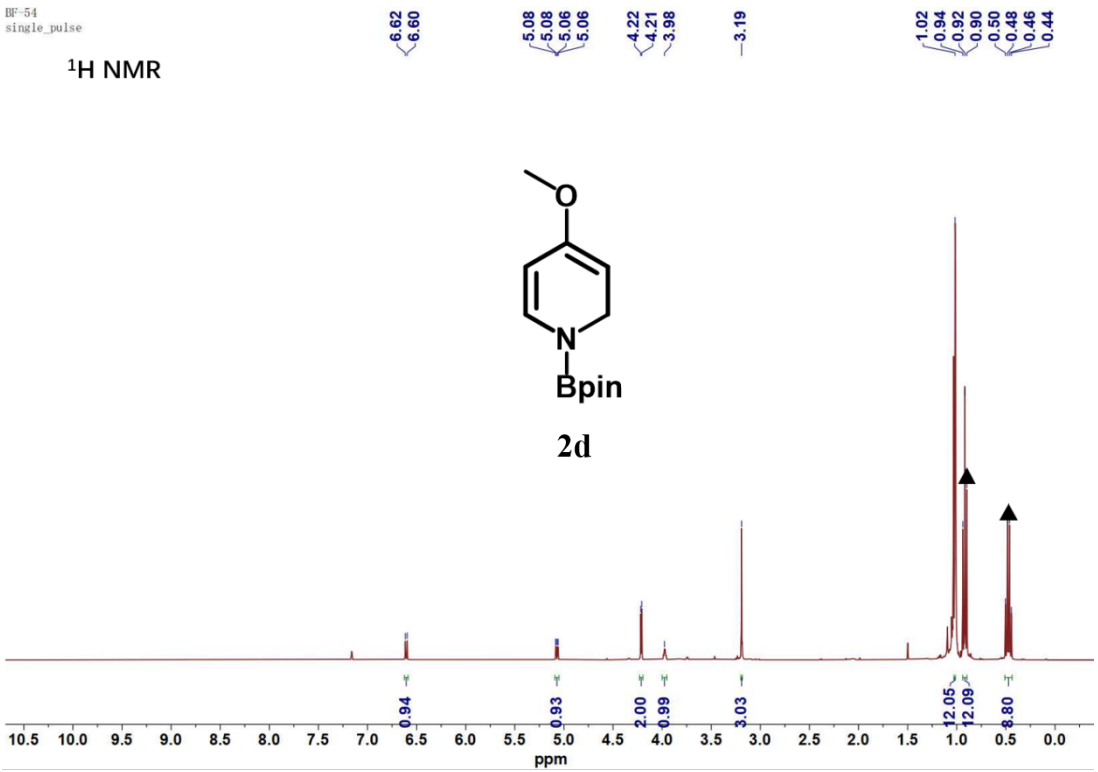

Figure S27. ^{1}H NMR spectrum of **2d** (400 MHz, Benzene-d_6).

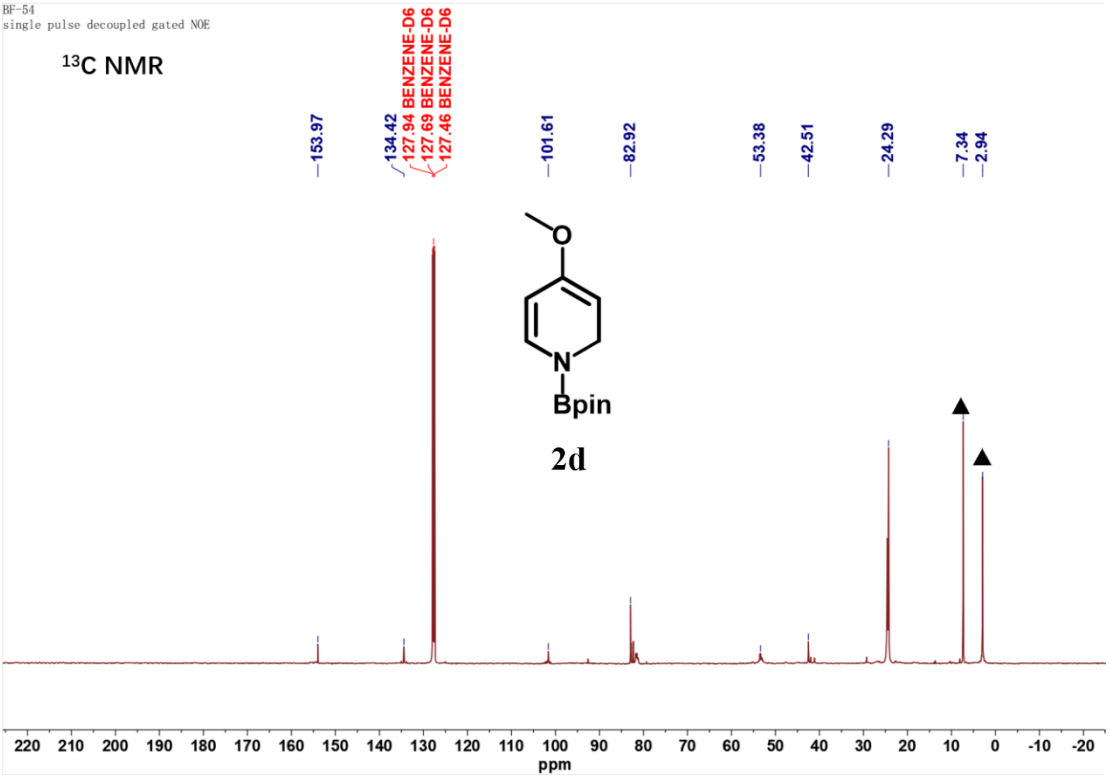

Figure S28. ^{13}C NMR spectrum of **2d** (101 MHz, Benzene-d_6).

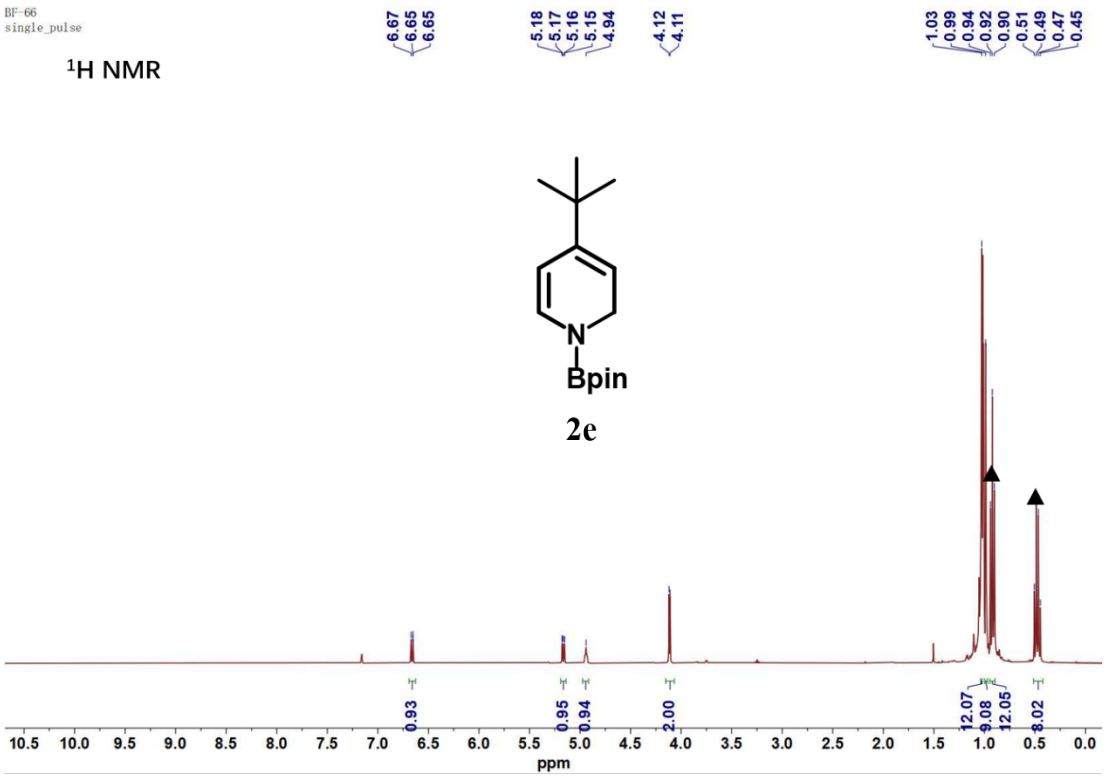

Figure S29. ^{1}H NMR spectrum of **2e** (400 MHz, Benzene-d_6).

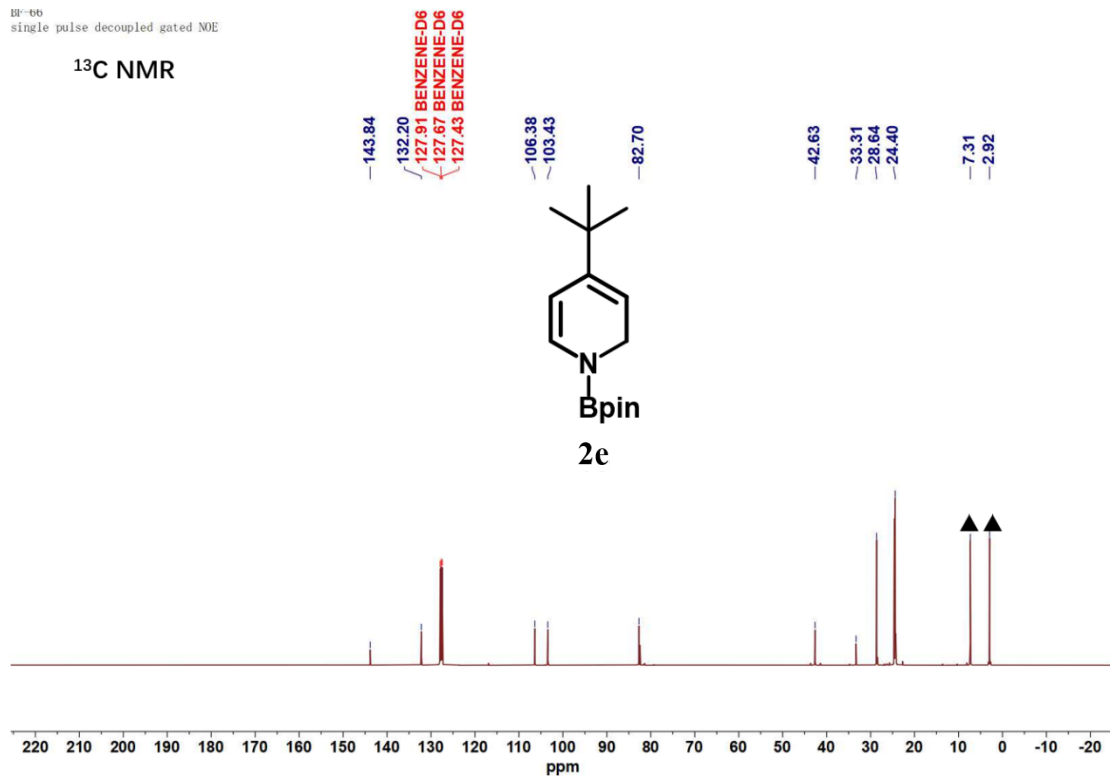

Figure S30. ^{13}C NMR spectrum of **2e** (101 MHz, Benzene-d_6).

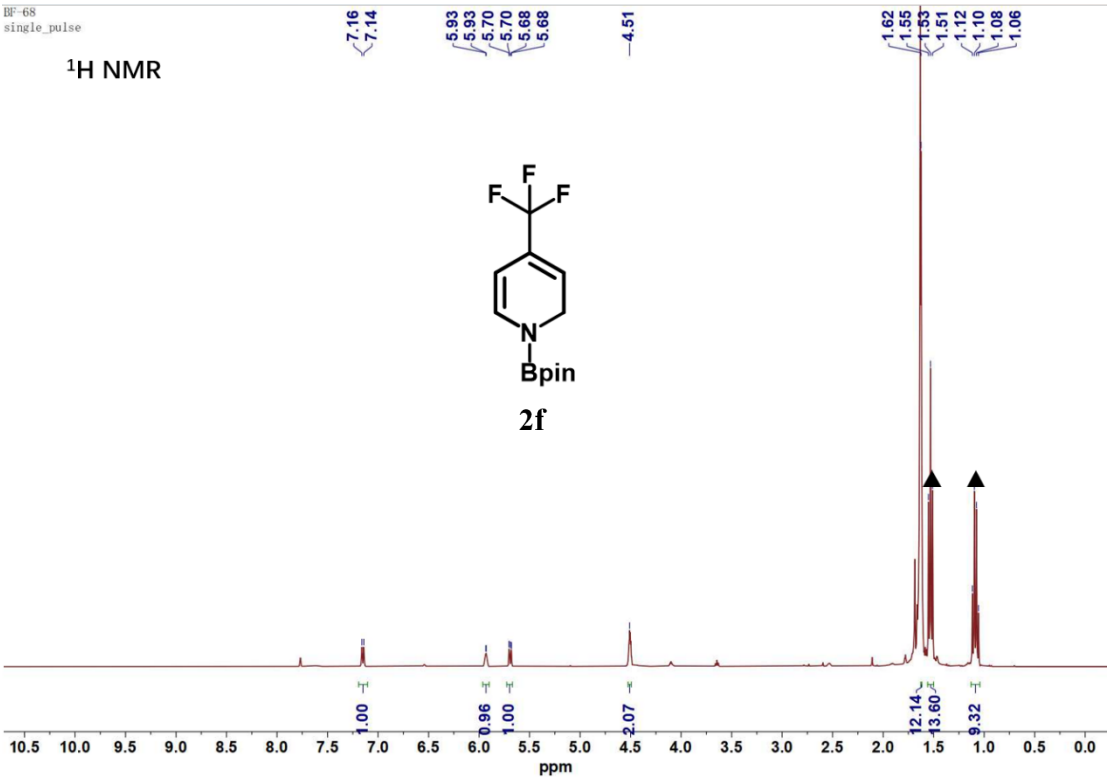

Figure S31. ^{1}H NMR spectrum of **2f** (400 MHz, Benzene-d_6).

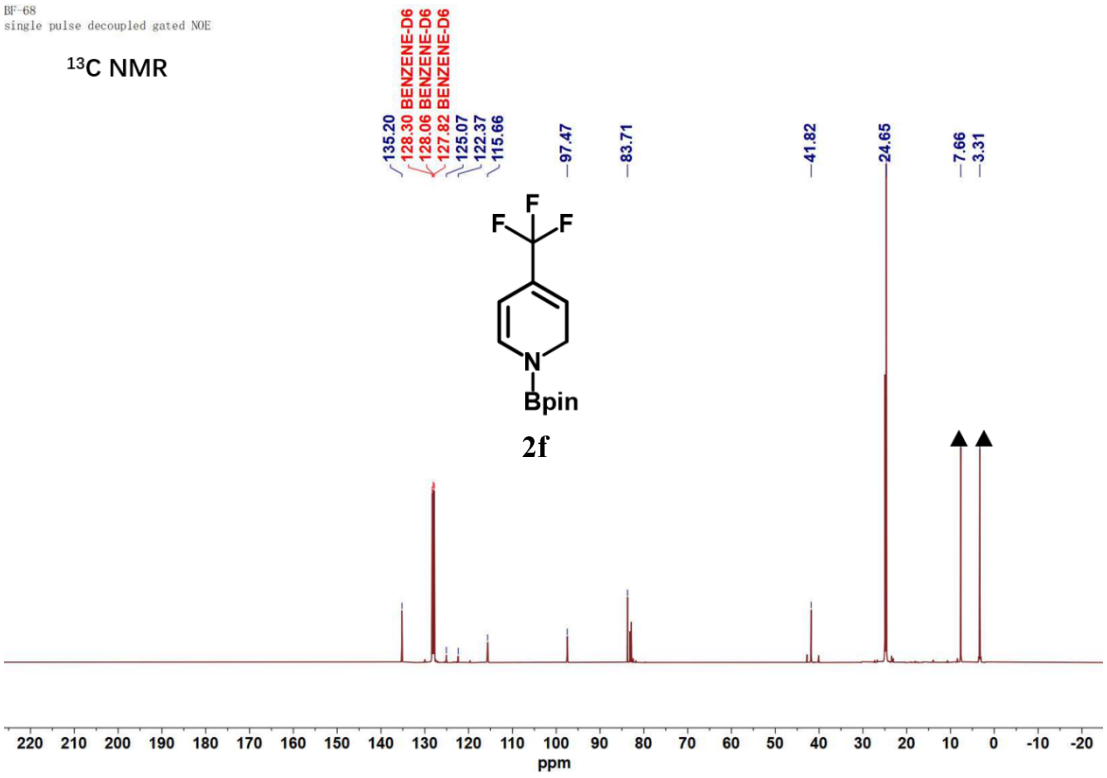

Figure S32. ^{13}C NMR spectrum of **2f** (101 MHz, Benzene-d_6).

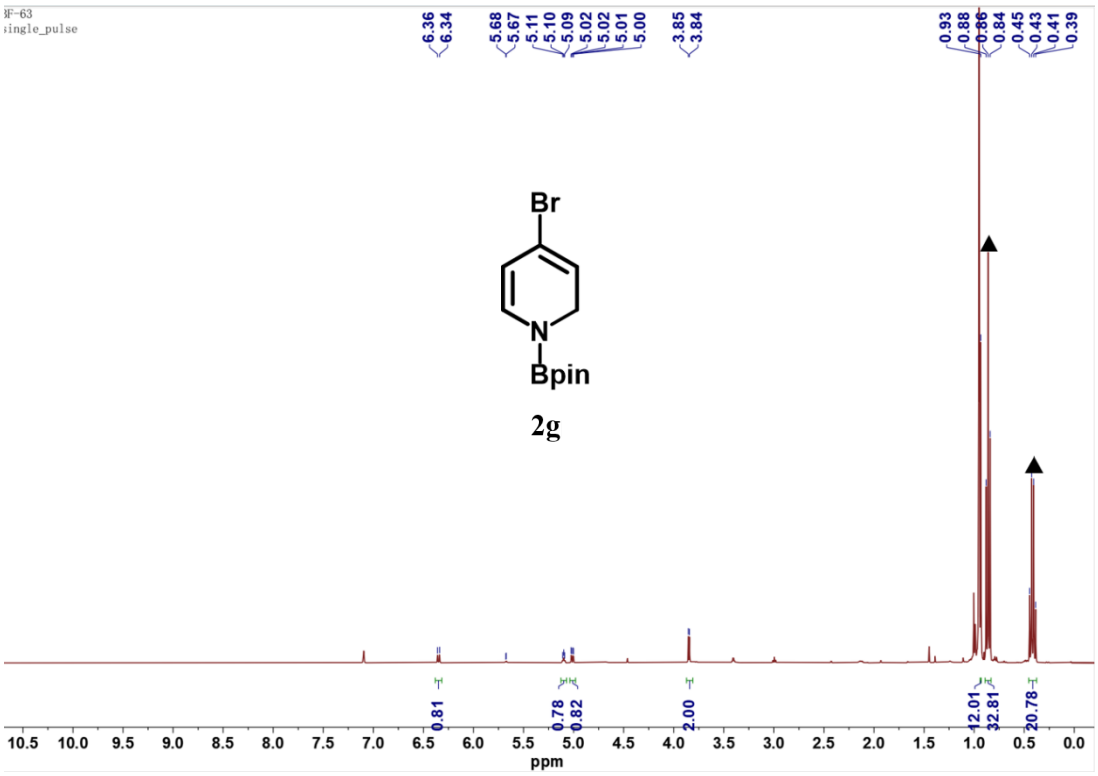

Figure S33. ^{1}H NMR spectrum of **2g** (400 MHz, Benzene-d_6).

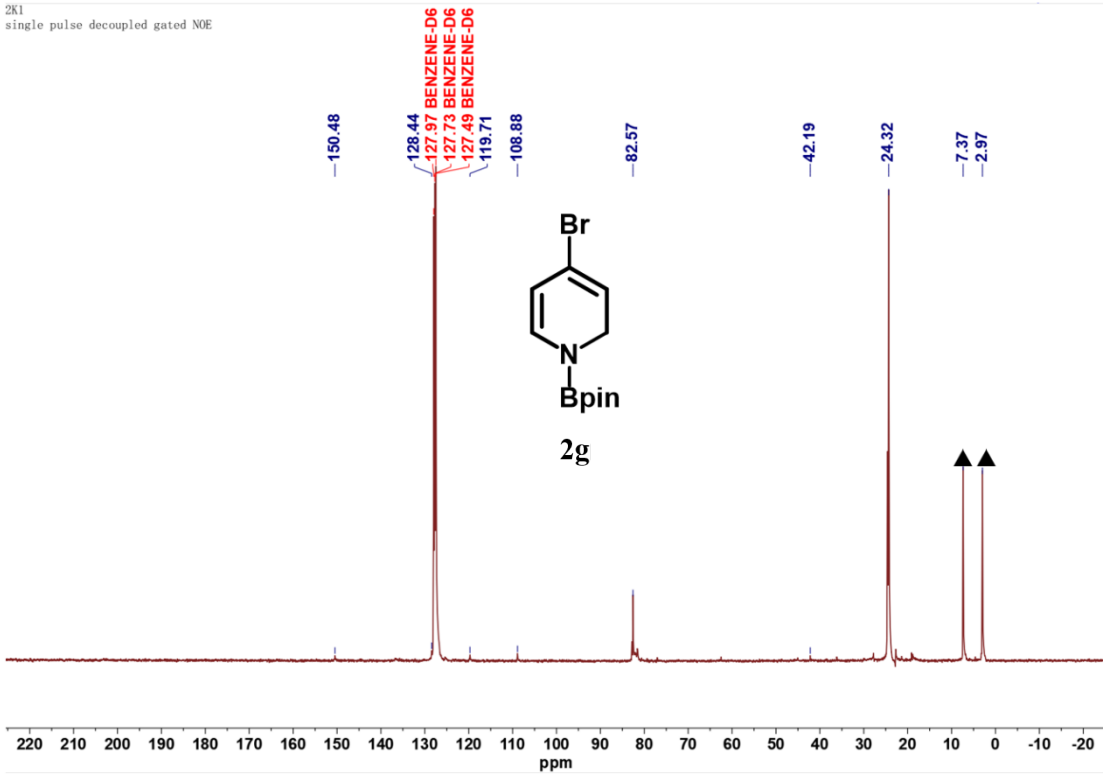

Figure S34. ^{13}C NMR spectrum of **2g** (101 MHz, Benzene-d_6).

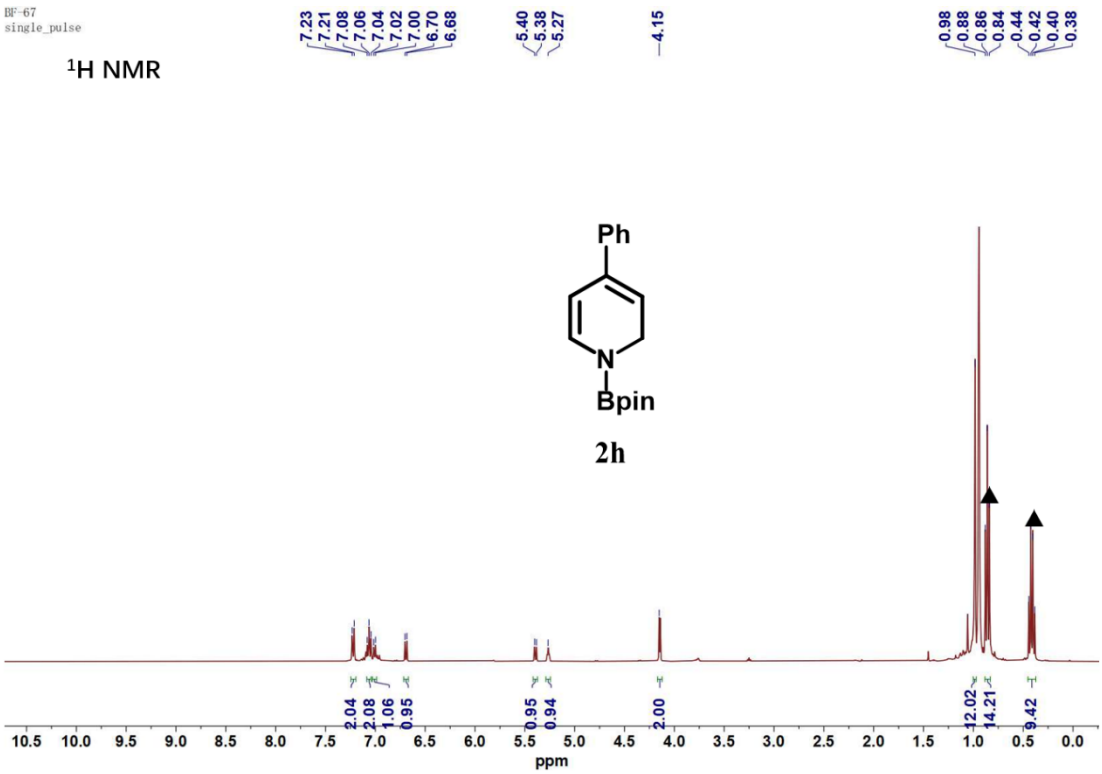

Figure S35. ^{1}H NMR spectrum of **2h** (400 MHz, Benzene-d_6).

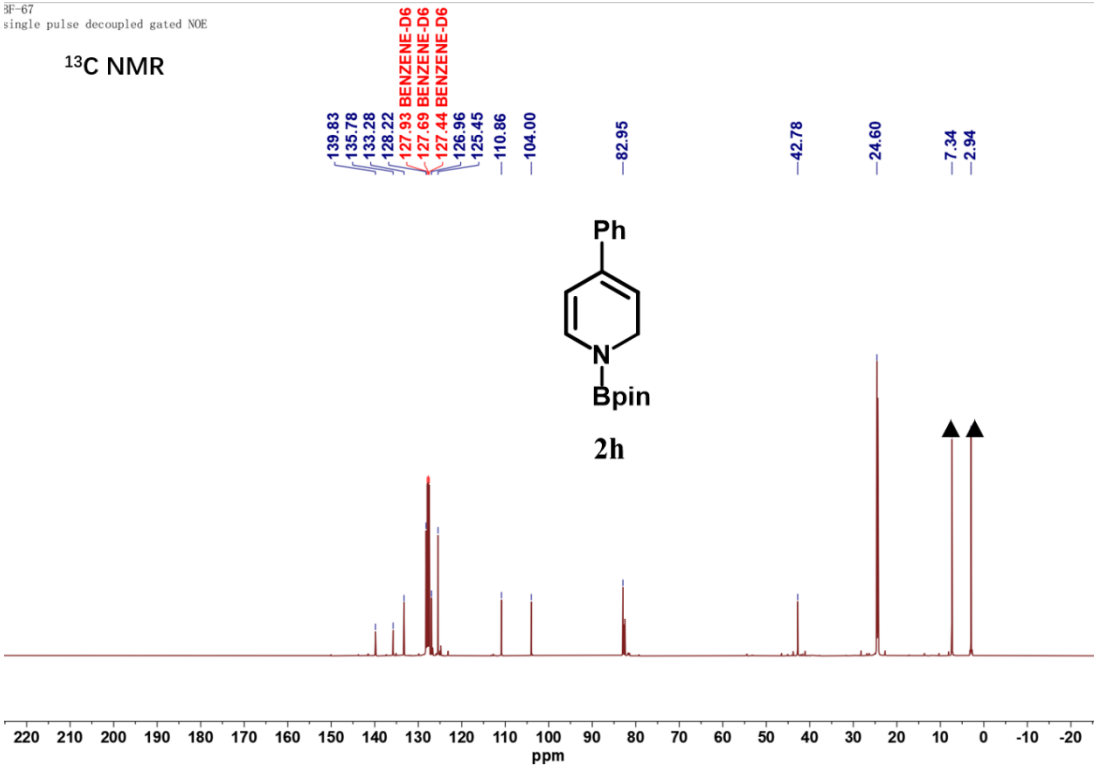

Figure S36. ^{13}C NMR spectrum of **2h** (101 MHz, Benzene-d_6).

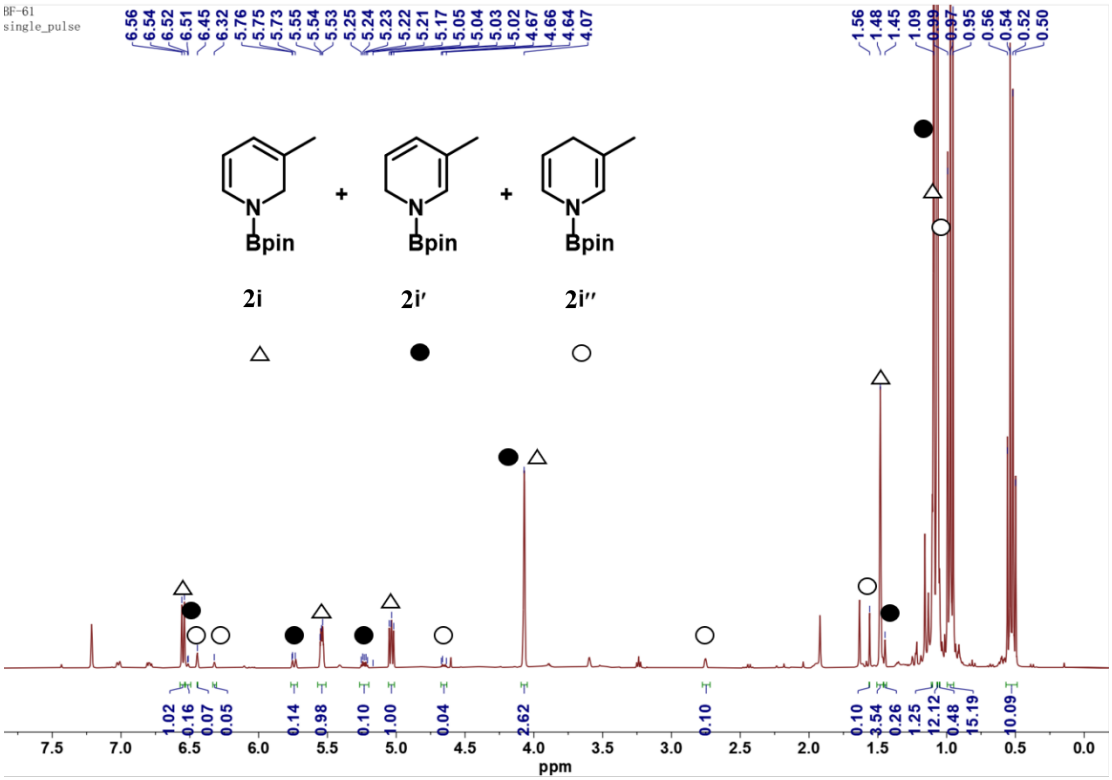

Figure S37. ^{1}H NMR spectrum of **2i'** (400 MHz, Benzene-d_6).

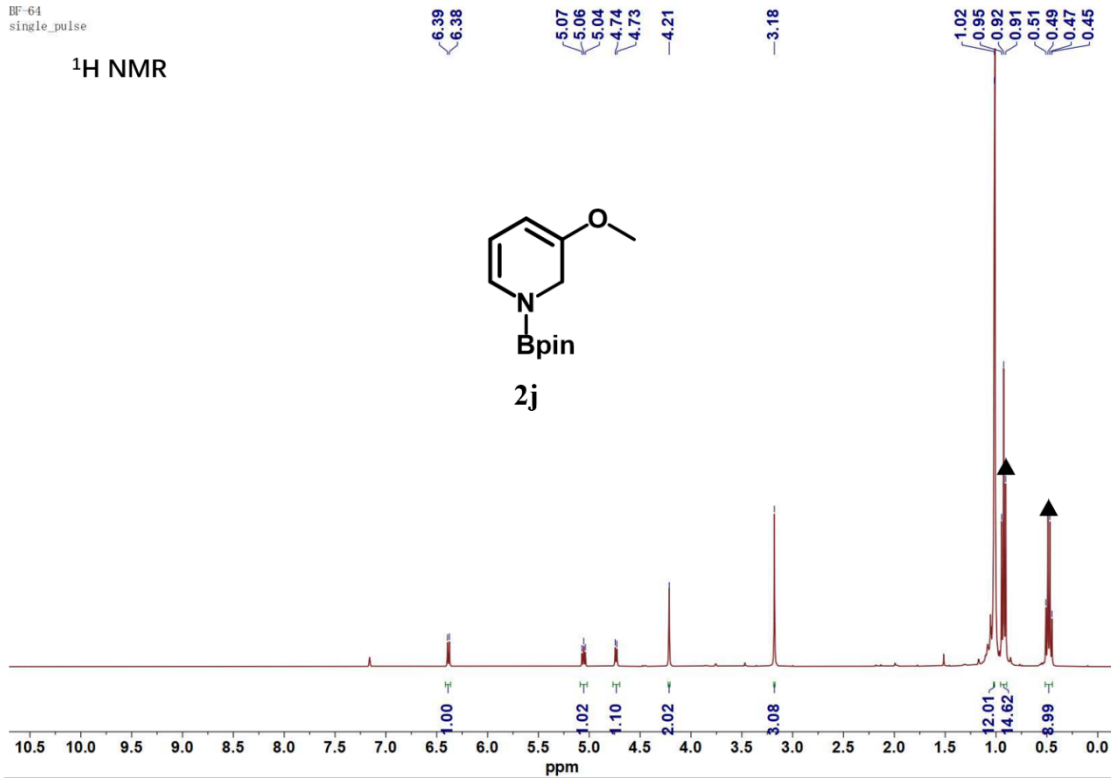

Figure S38. ^{1}H NMR spectrum of **2j** (400 MHz, Benzene-d_6).

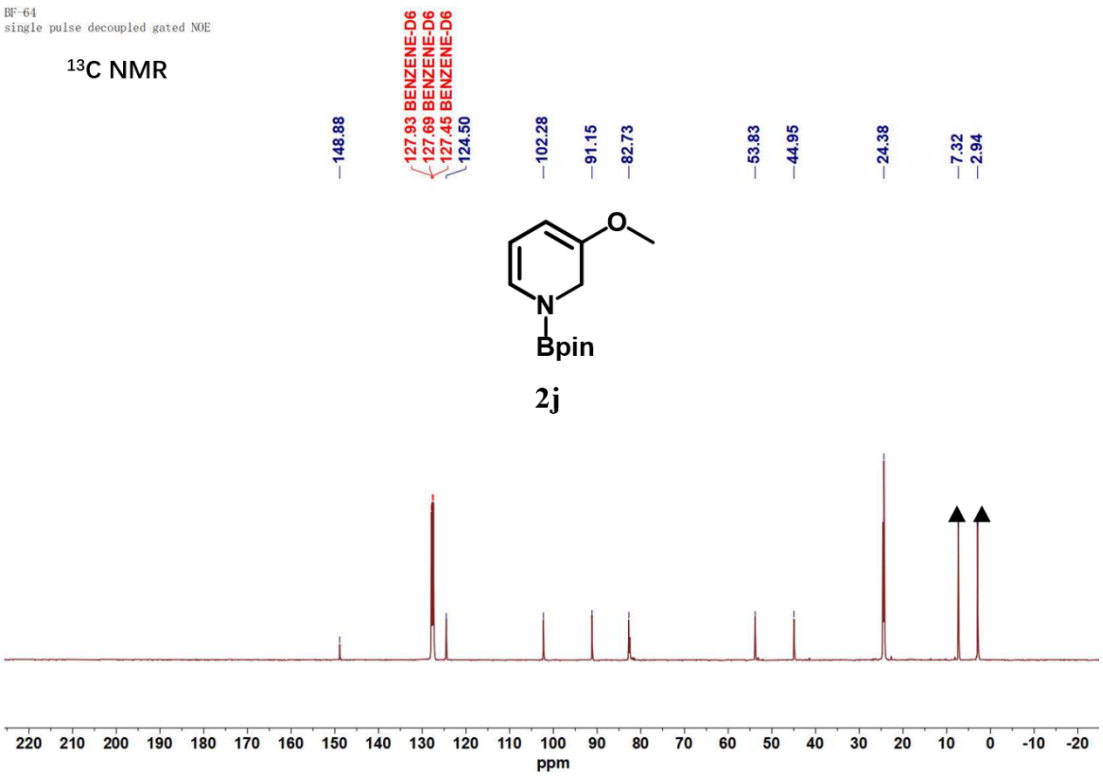

Figure S39. ^{13}C NMR spectrum of **2j** (101 MHz, Benzene-d_6).

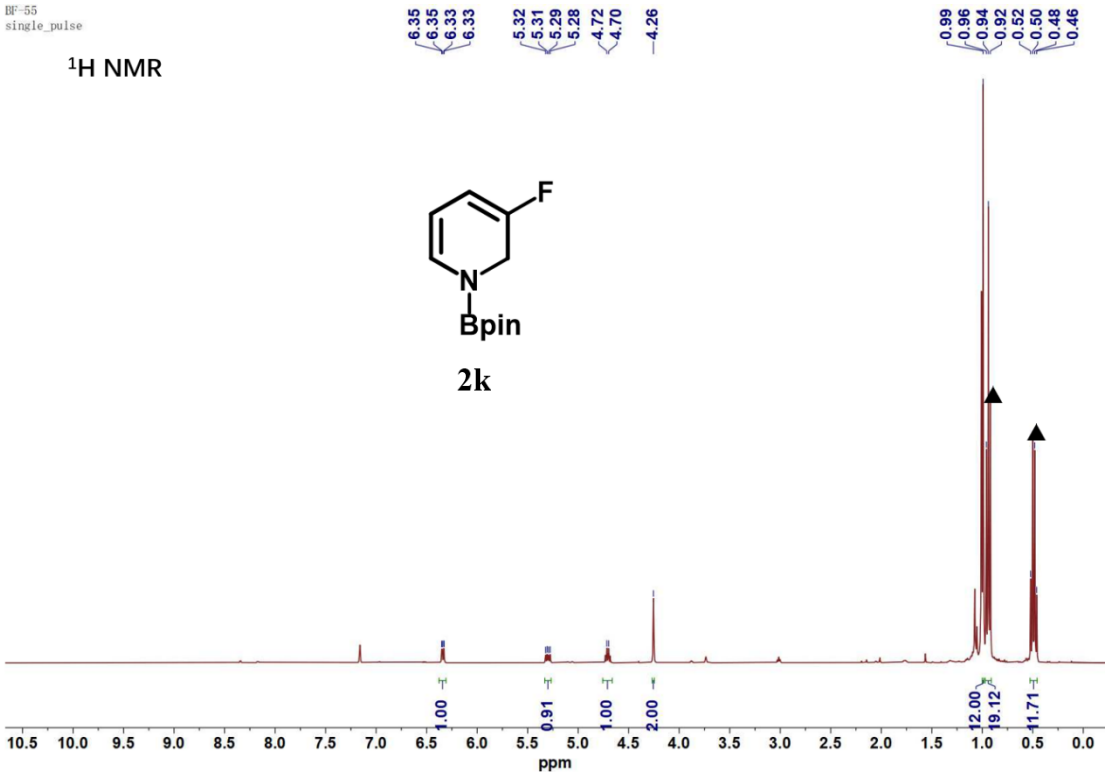

Figure S40. ^{1}H NMR spectrum of **2k** (400 MHz, Benzene-d_6).

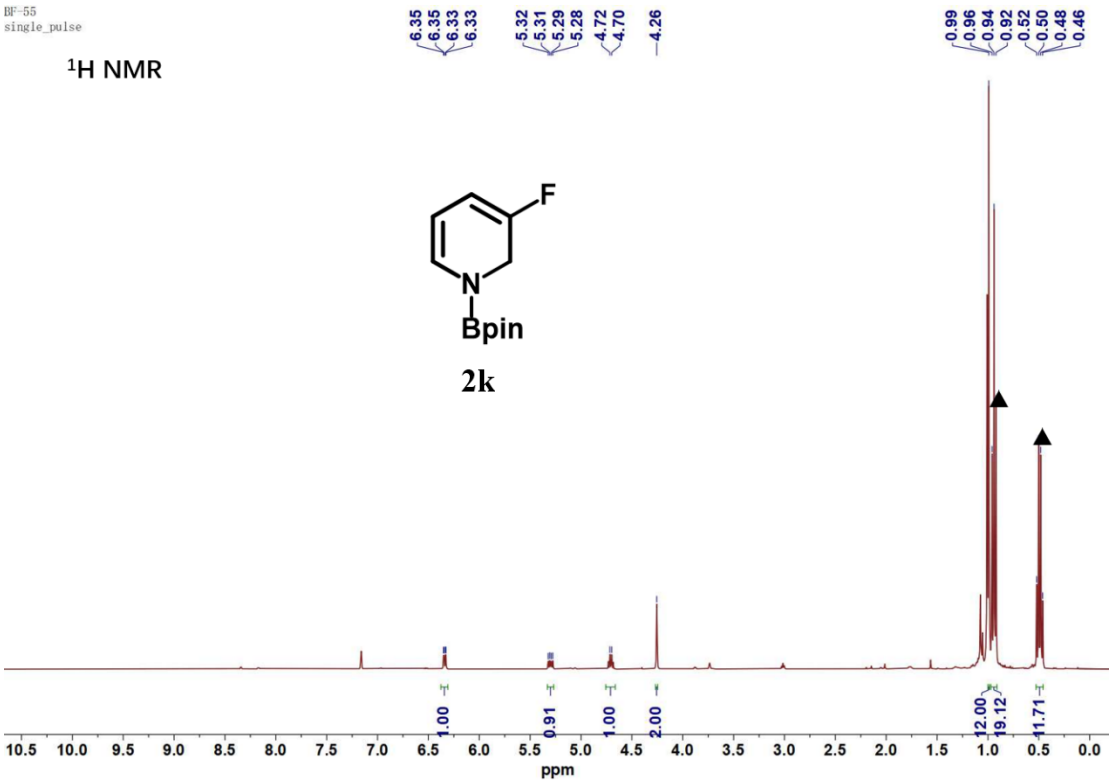

Figure S41. ^{13}C NMR spectrum of **2k** (101 MHz, Benzene-d_6).

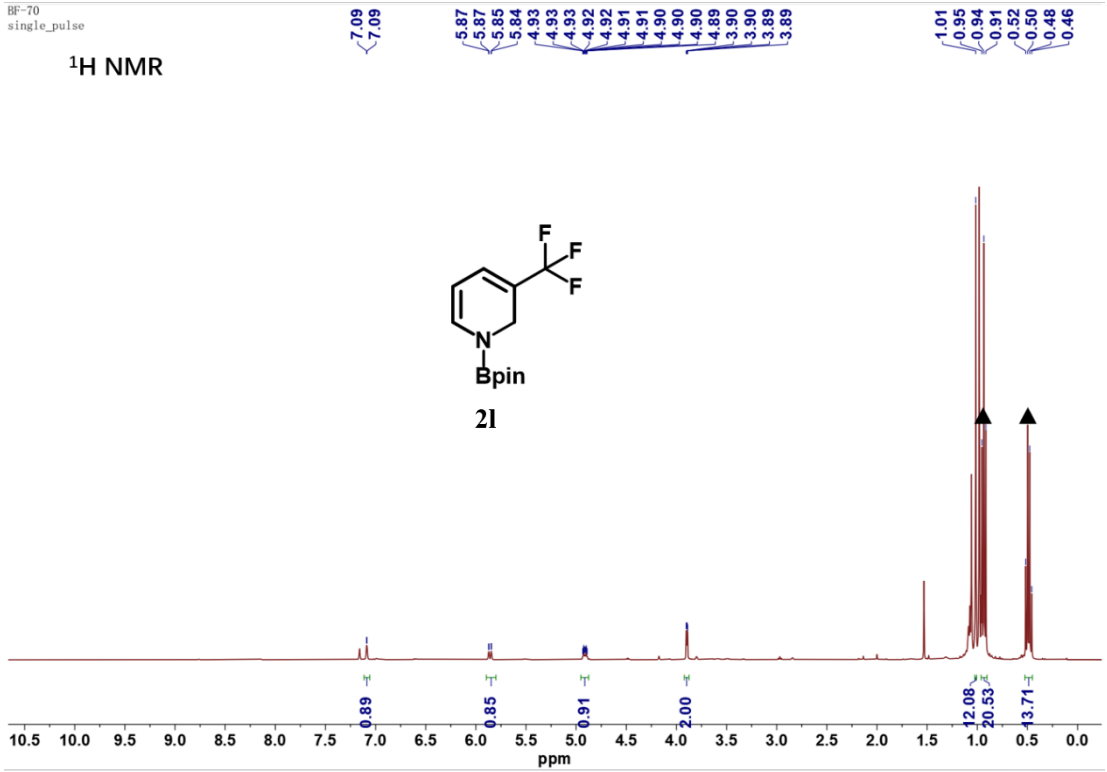

Figure S42. ^{1}H NMR spectrum of **2l** (400 MHz, Benzene-d_6).

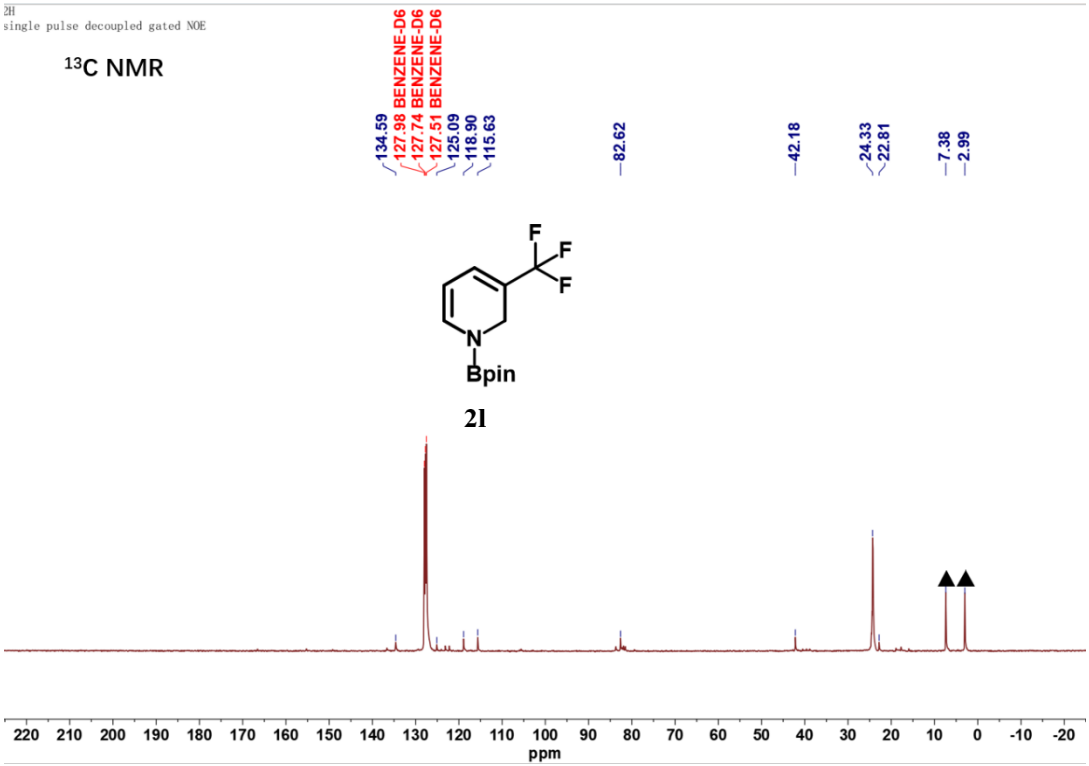

Figure S43. ^{13}C NMR spectrum of **2l** (101 MHz, Benzene-d_6).

6.2. NMR Spectra for quinolines

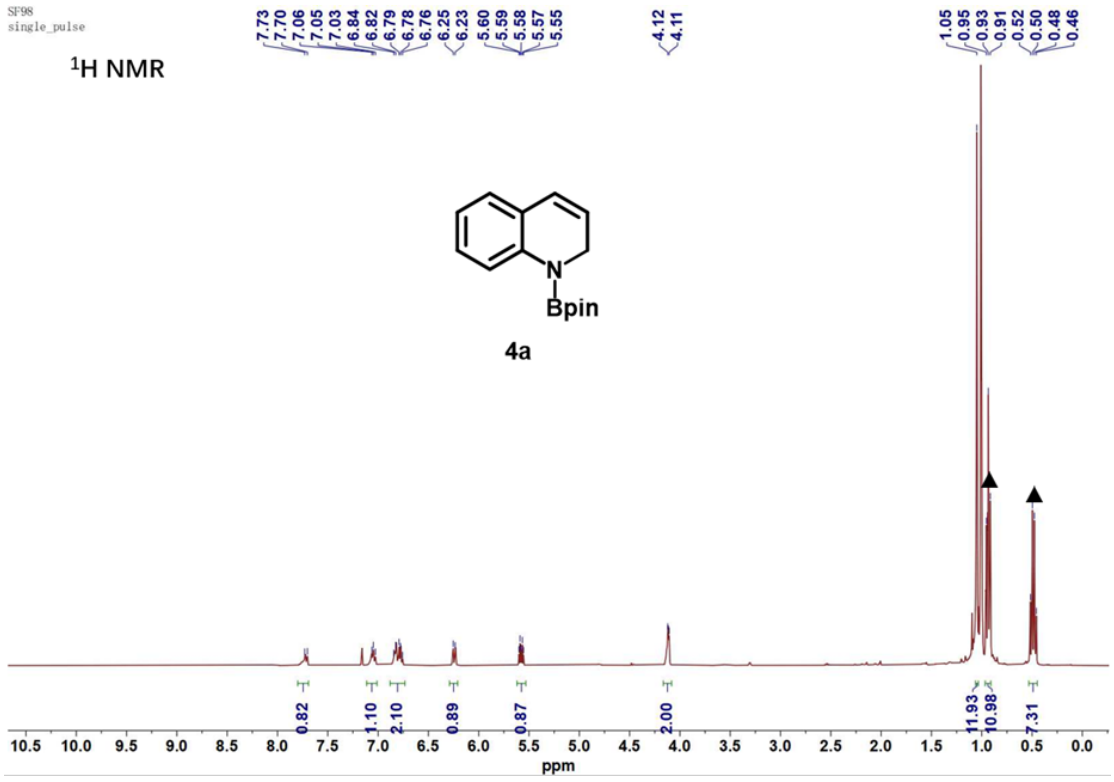

Figure S44. ^{1}H NMR spectrum of **4a** (400 MHz, Benzene-d_6).

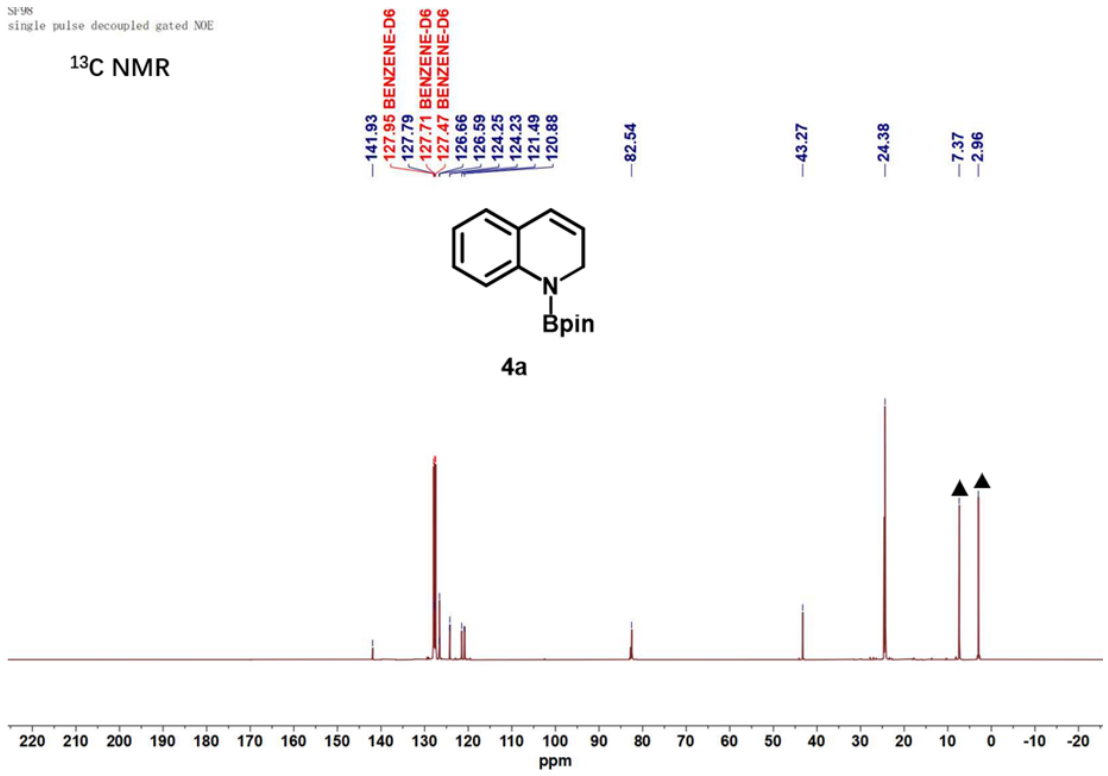

Figure S45. ^{13}C NMR spectrum of **4a** (101 MHz, Benzene-d_6).

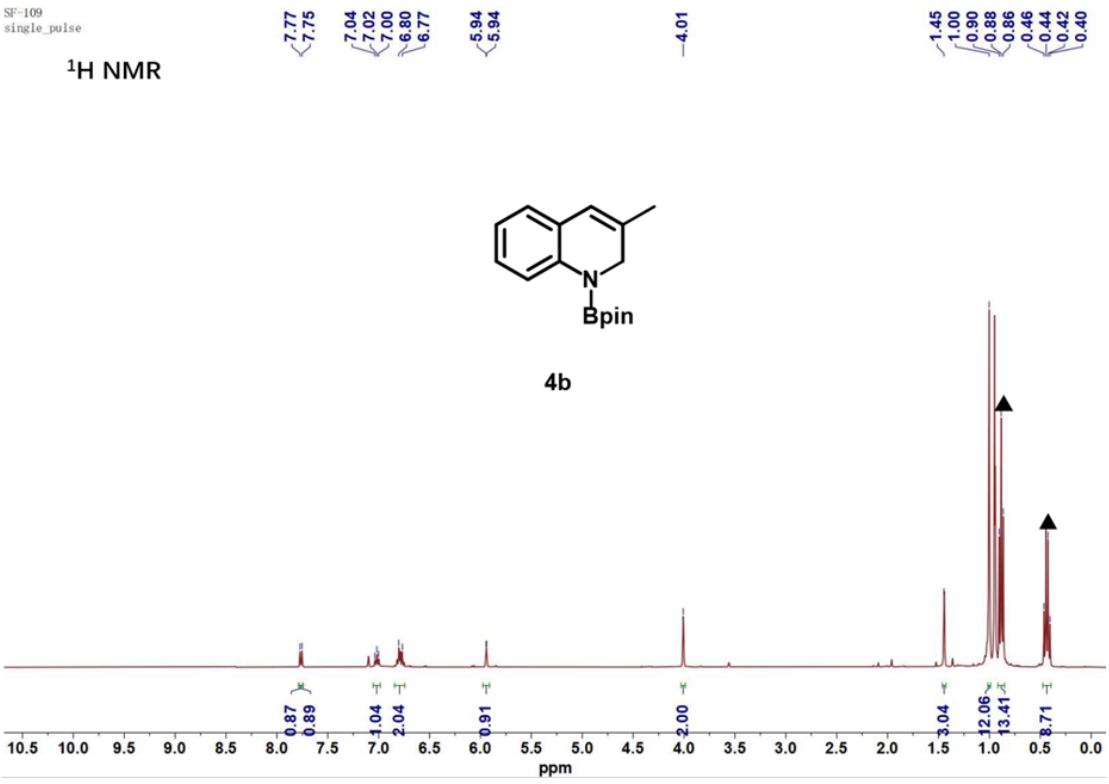

Figure S46. ^{1}H NMR spectrum of **4b** (400 MHz, Benzene-d_6).

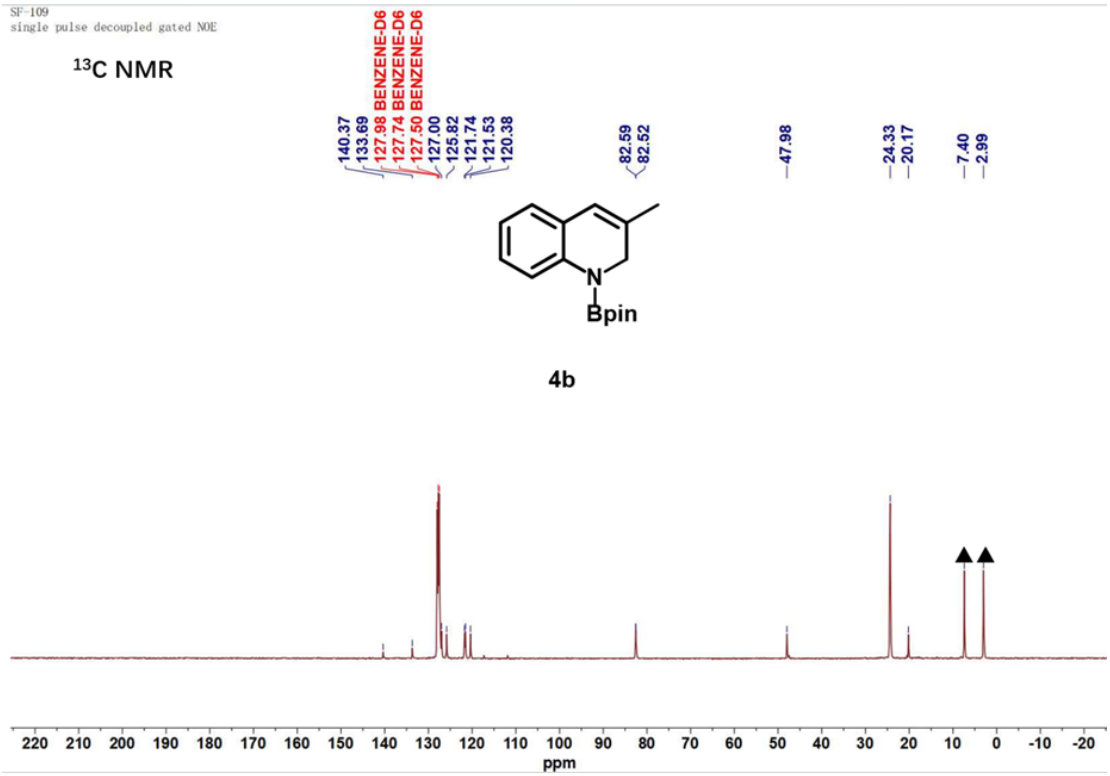

Figure S47. ^{13}C NMR spectrum of **4b** (101 MHz, Benzene-d_6).

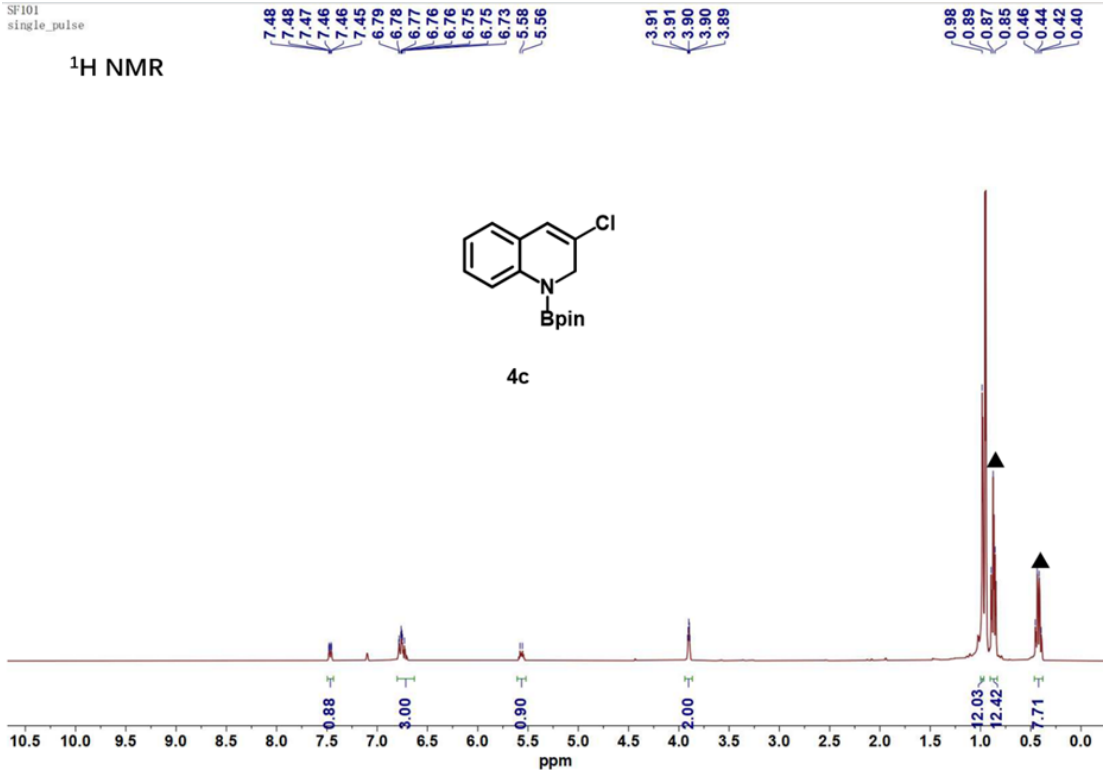

Figure S48. ^{1}H NMR spectrum of **4c** (400 MHz, Benzene-d_6).

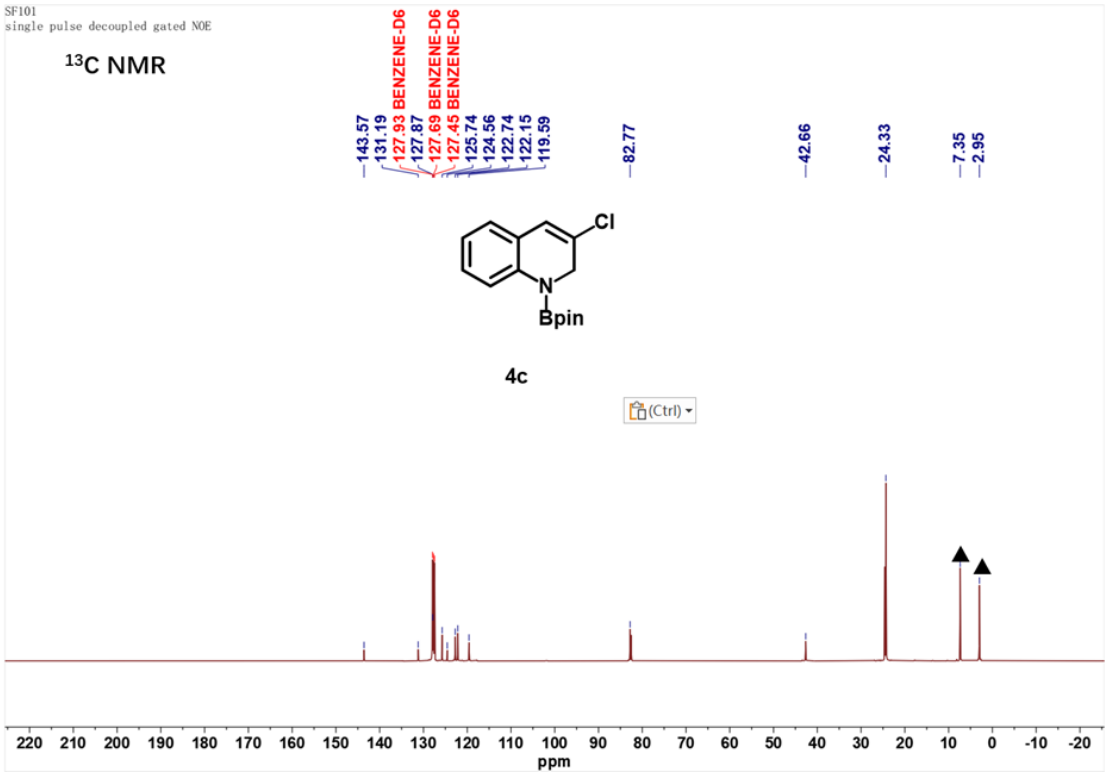

Figure S49. ^{13}C NMR spectrum of **4c** (101 MHz, Benzene-d_6).

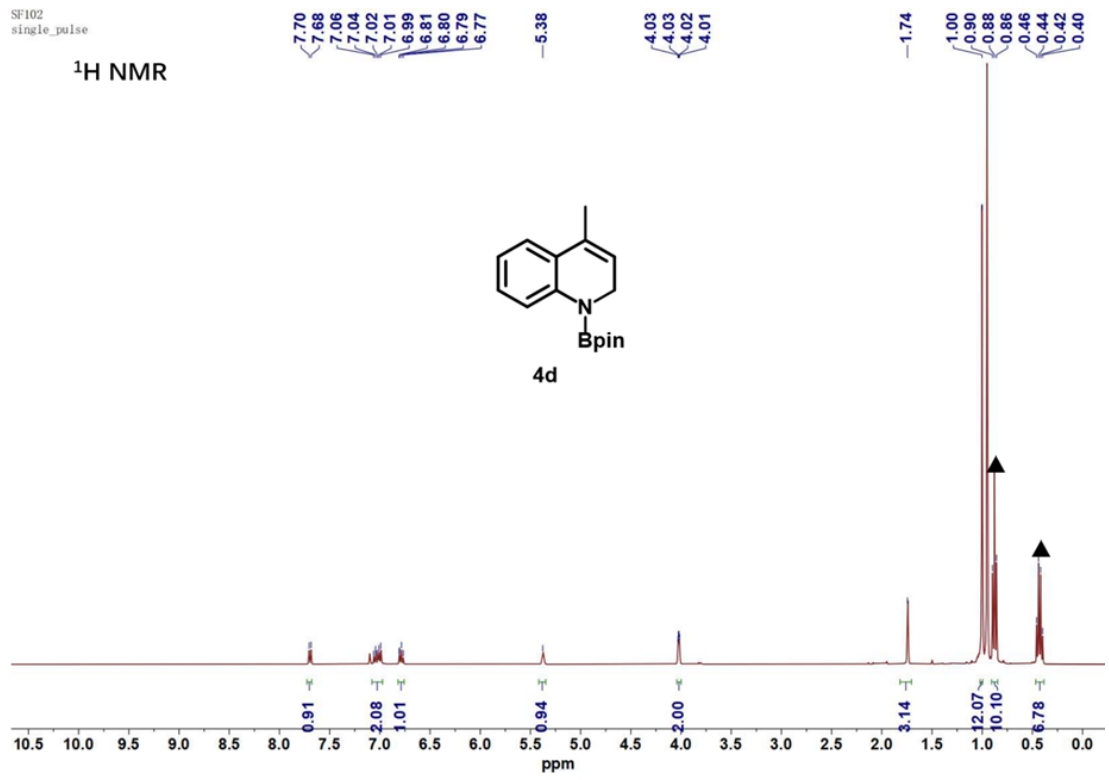

Figure S50. ^{1}H NMR spectrum of **4d** (400 MHz, Benzene-d_6).

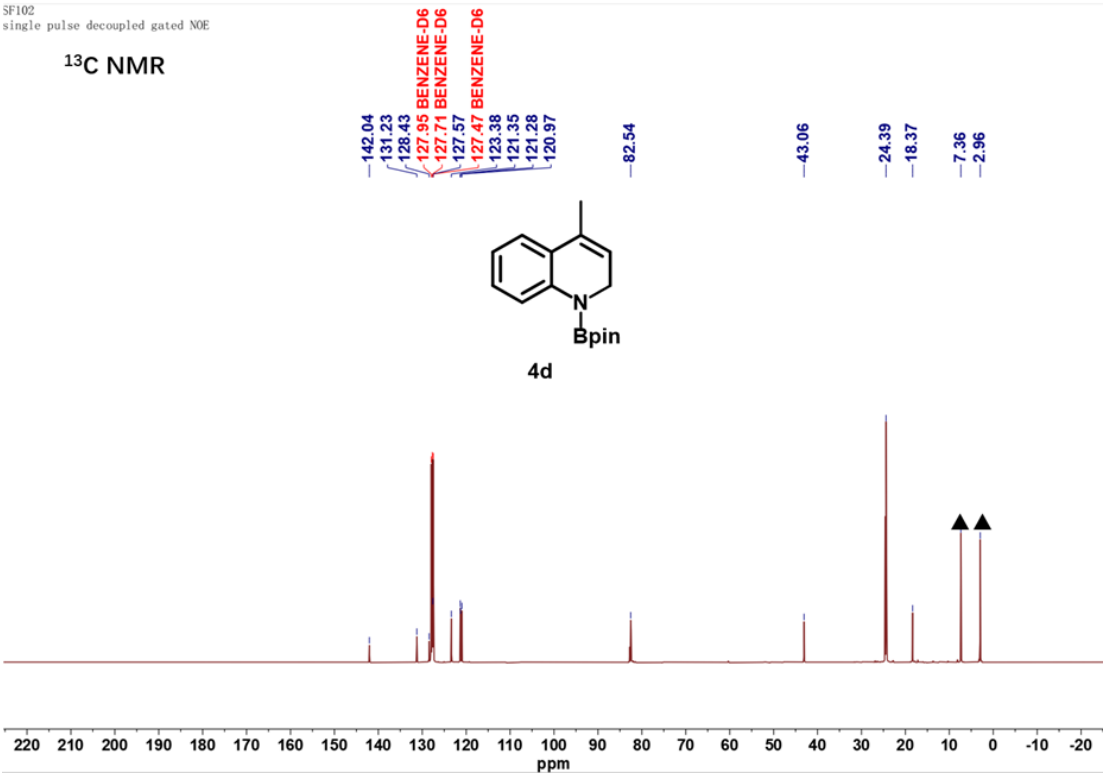

Figure S51. ^{13}C NMR spectrum of **4d** (101 MHz, Benzene-d_6).

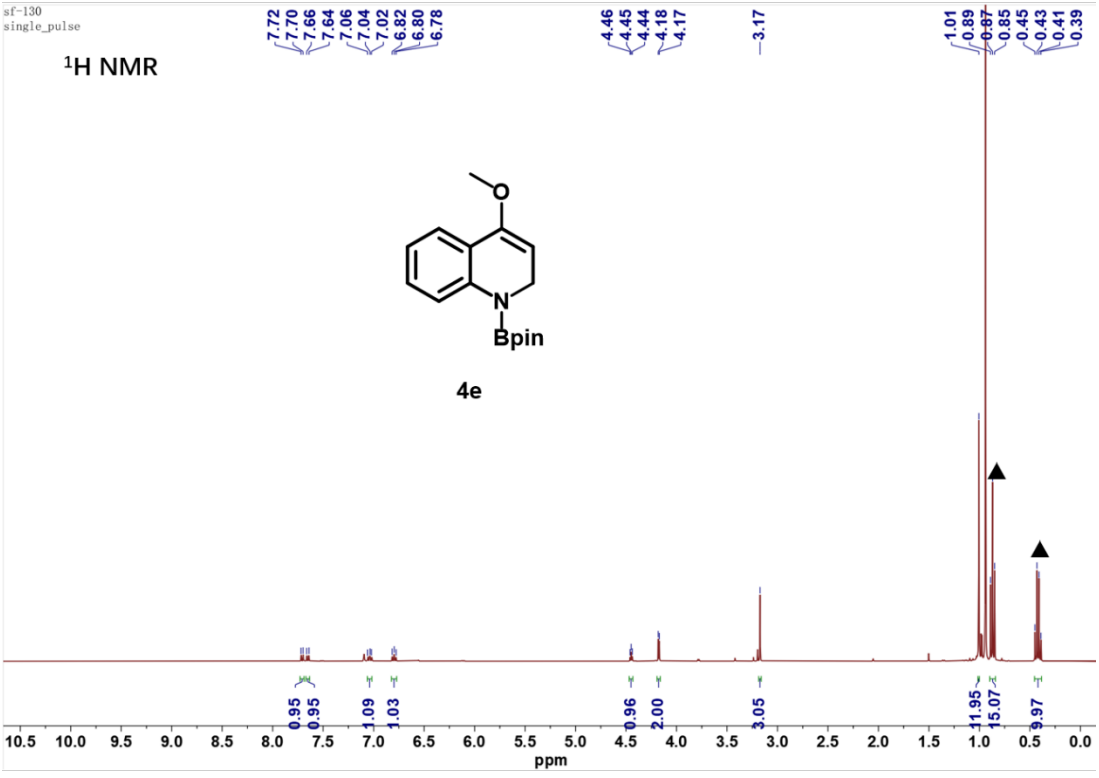

Figure S52. ^{1}H NMR spectrum of **4e** (400 MHz, Benzene-d_6).

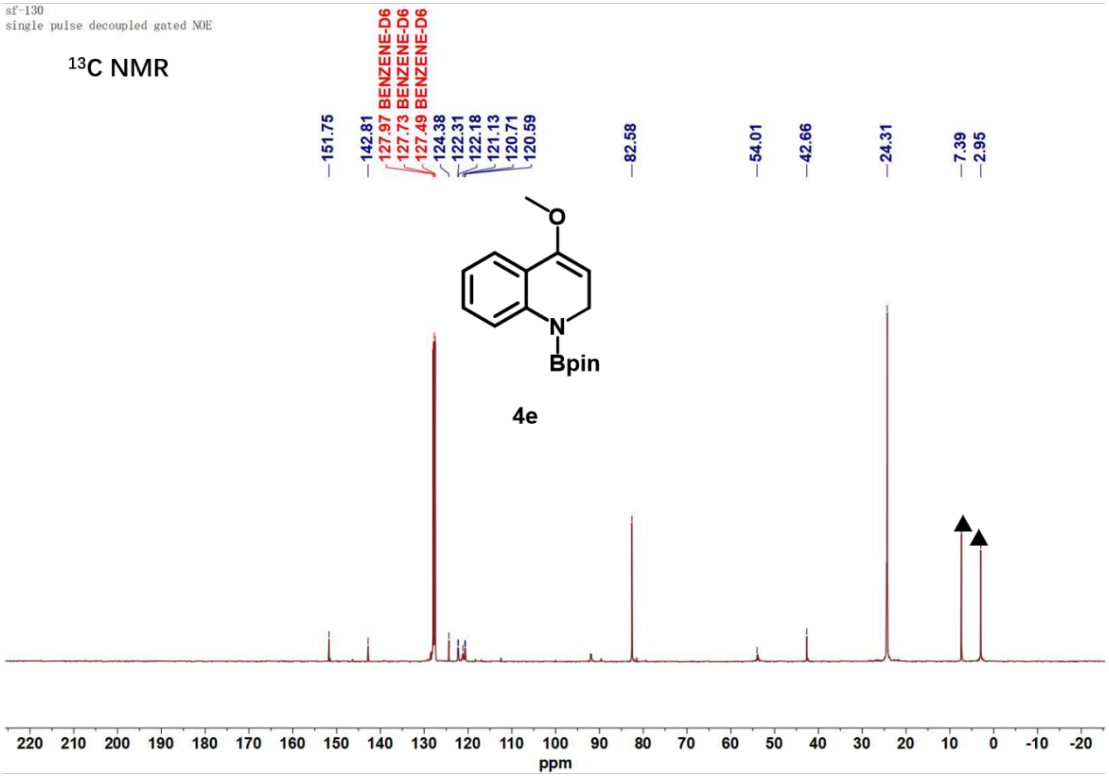

Figure S53. ^{13}C NMR spectrum of **4e** (101 MHz, Benzene-d_6).

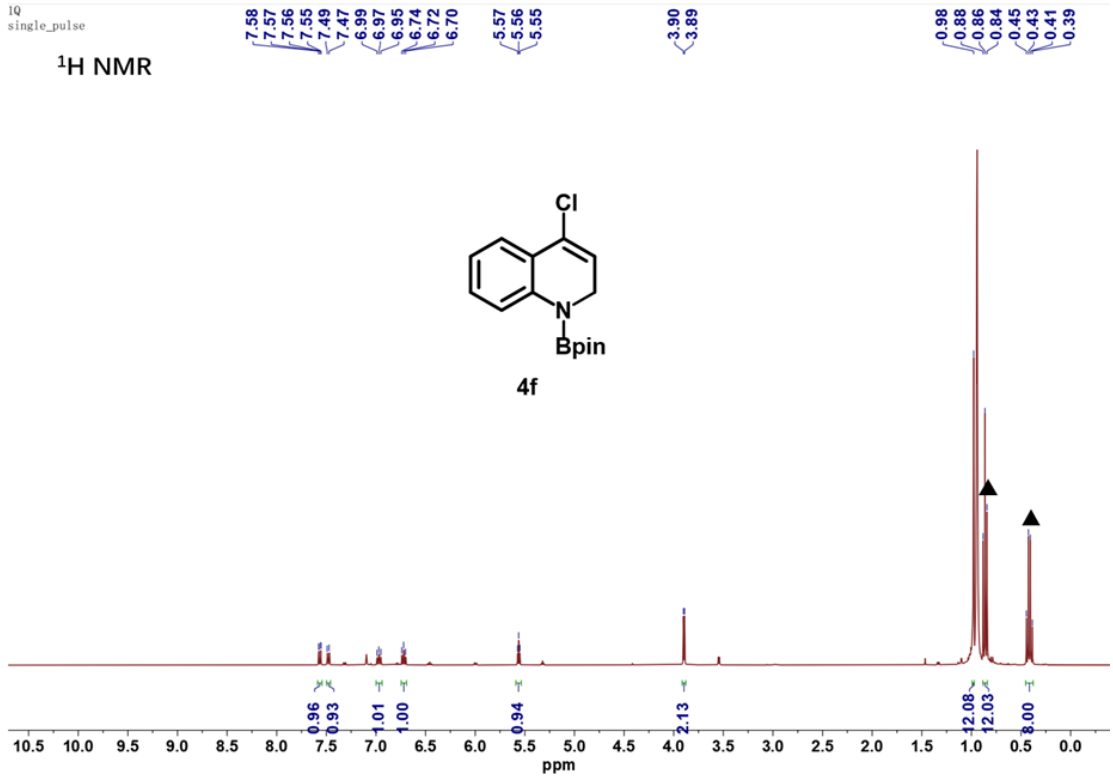

Figure S54. ^{1}H NMR spectrum of **4f** (400 MHz, Benzene-d_6).

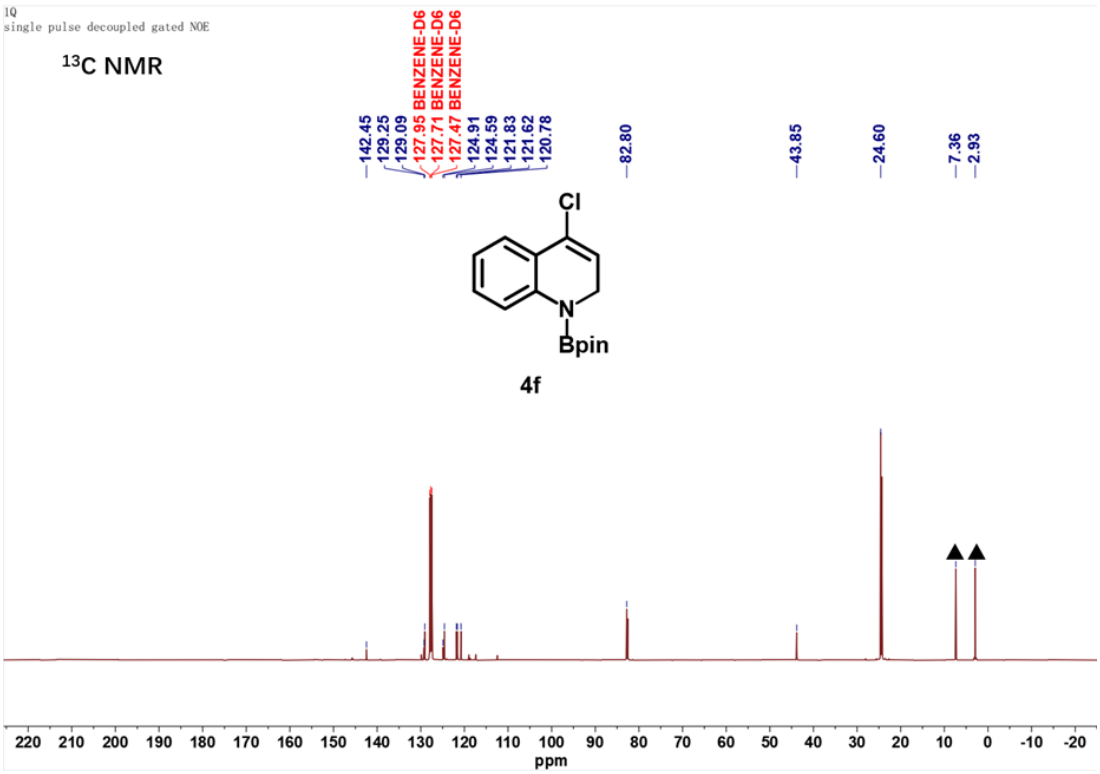

Figure S55. ^{13}C NMR spectrum of **4f** (101 MHz, Benzene-d_6).

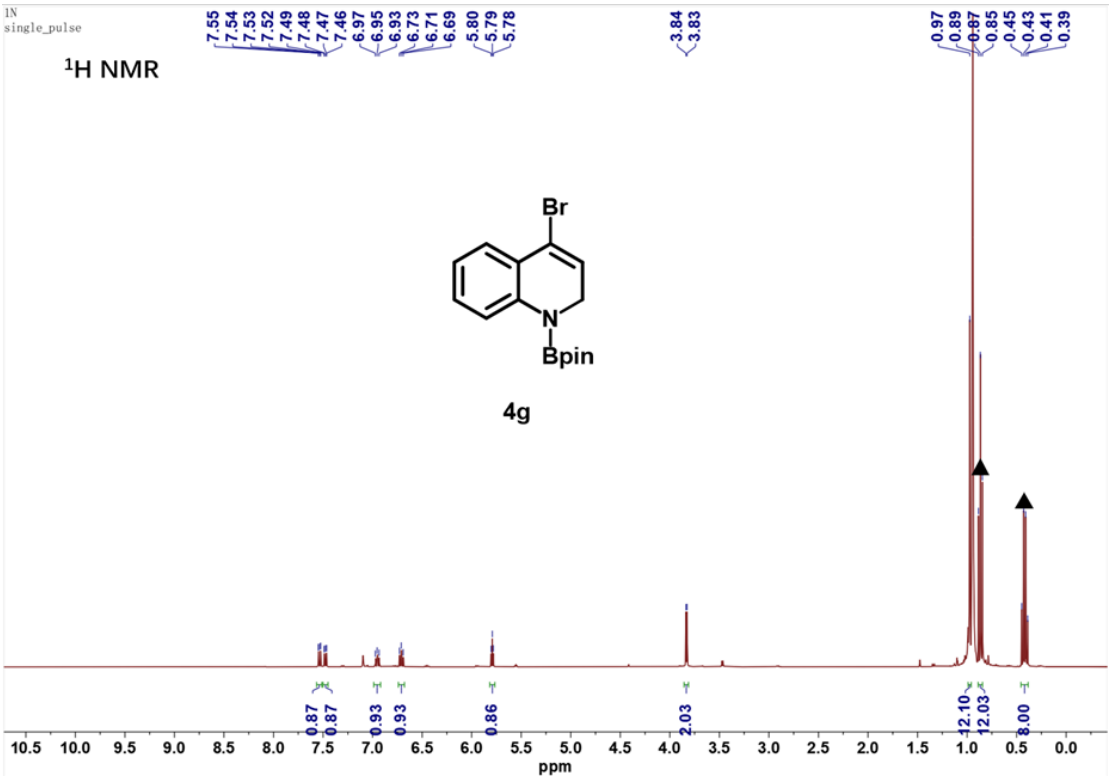

Figure S56. ^{1}H NMR spectrum of **4g** (400 MHz, Benzene-d_6).

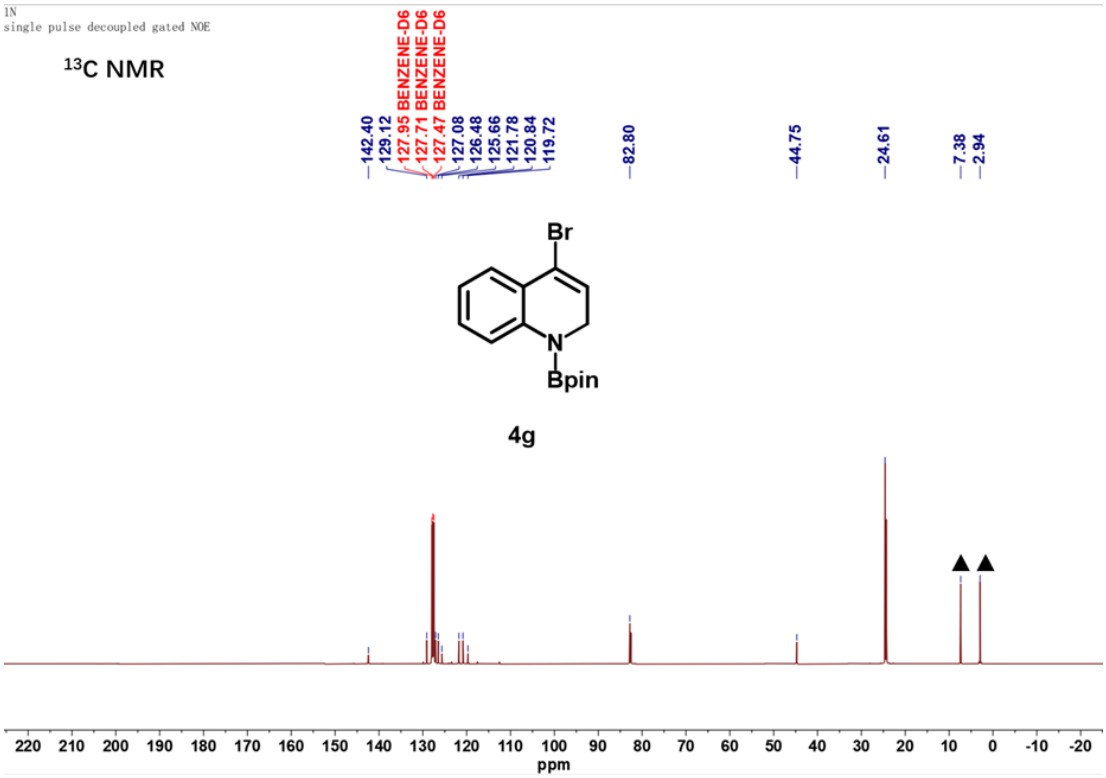

Figure S57. ^{13}C NMR spectrum of **4g** (101 MHz, Benzene-d_6).

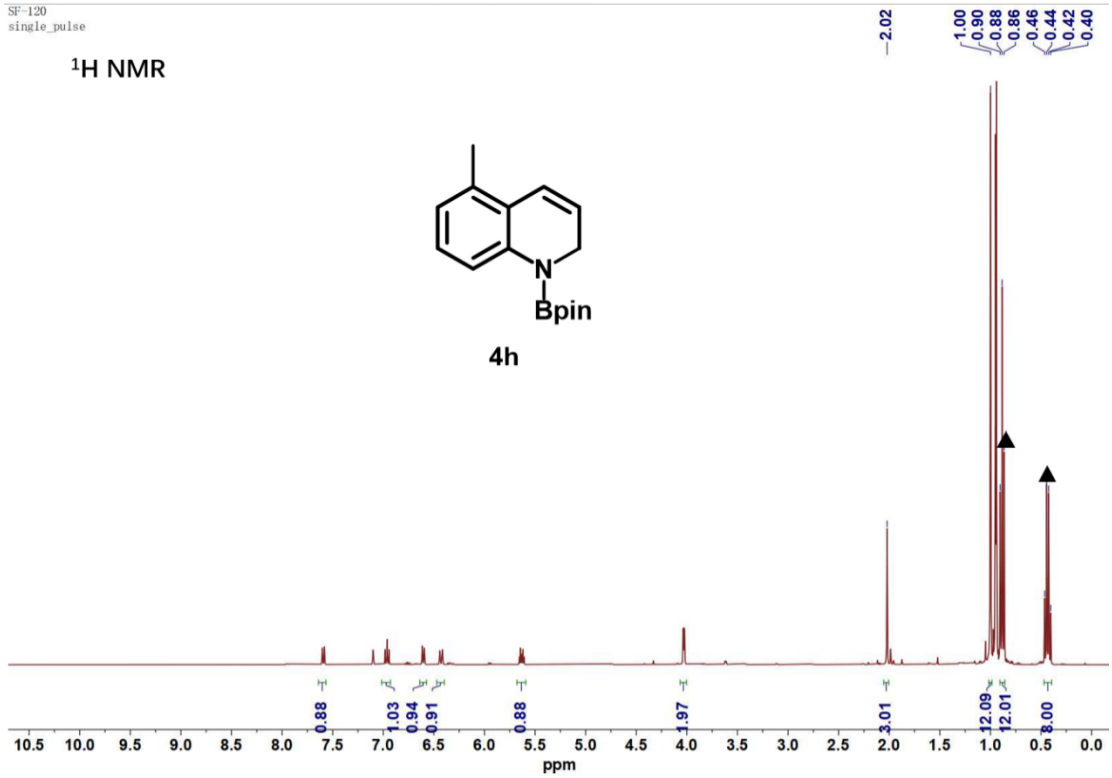

Figure S58. ^{1}H NMR spectrum of **4h** (400 MHz, Benzene-d_6).

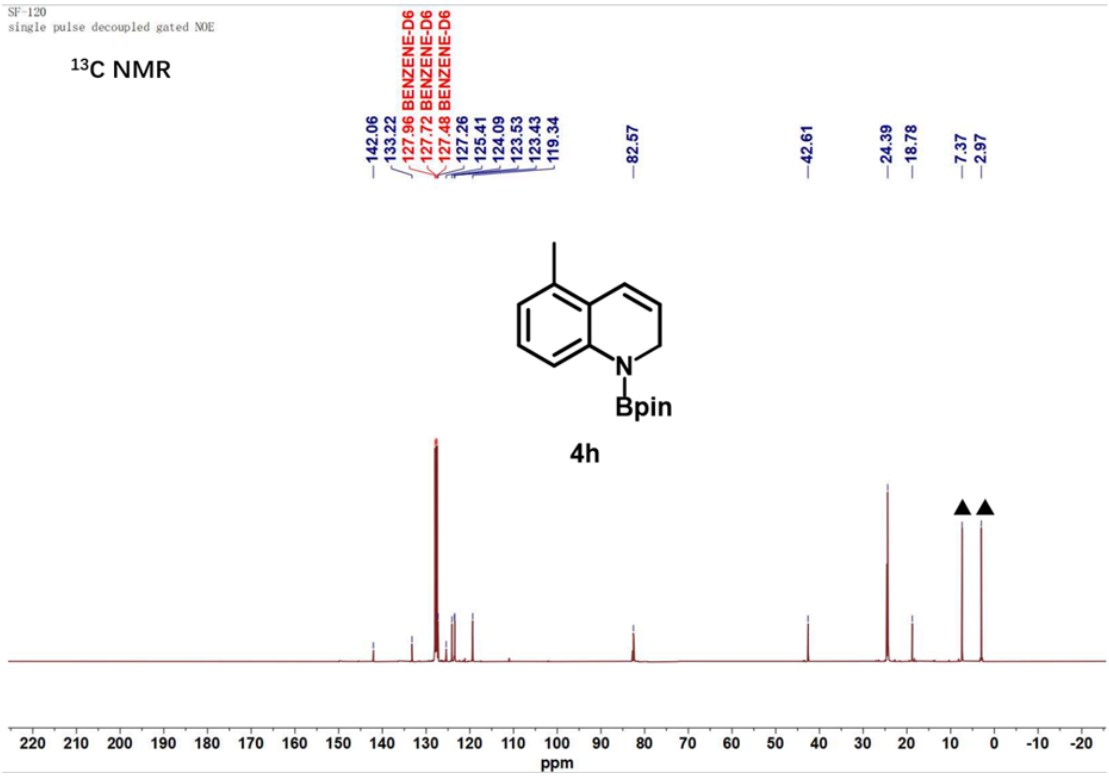

Figure S59. ^{13}C NMR spectrum of **4h** (101 MHz, Benzene-d_6).

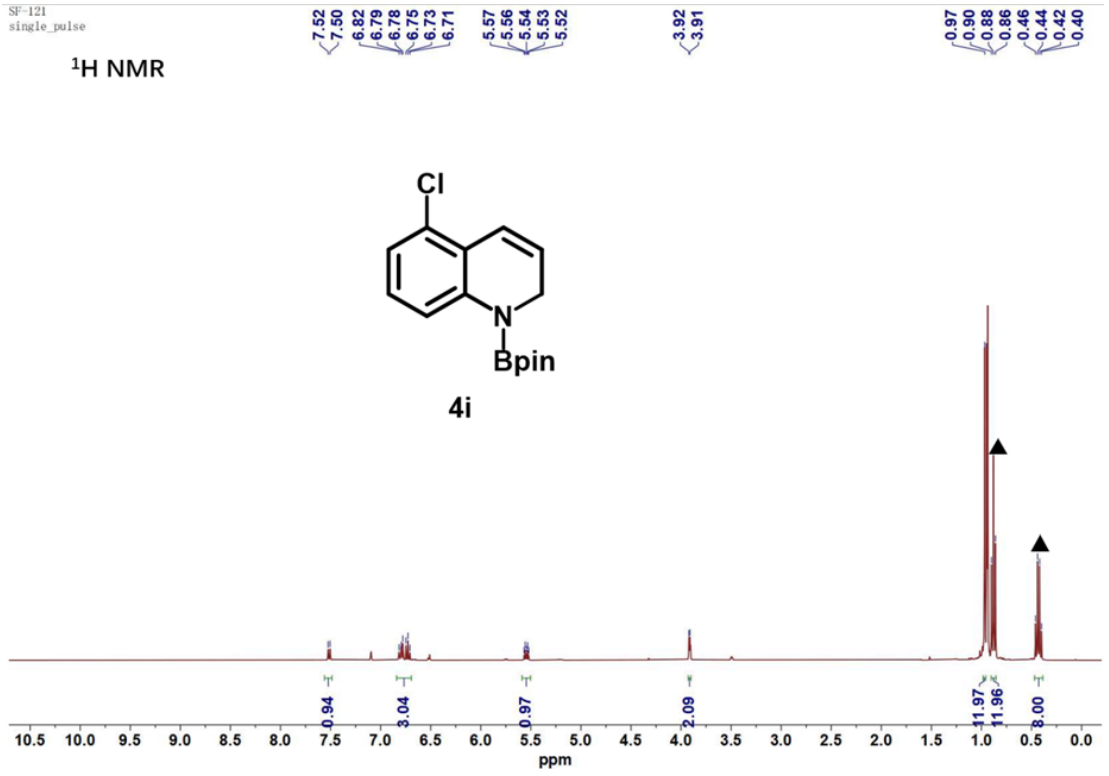

Figure S60. ^{1}H NMR spectrum of **4i** (400 MHz, Benzene-d_6).

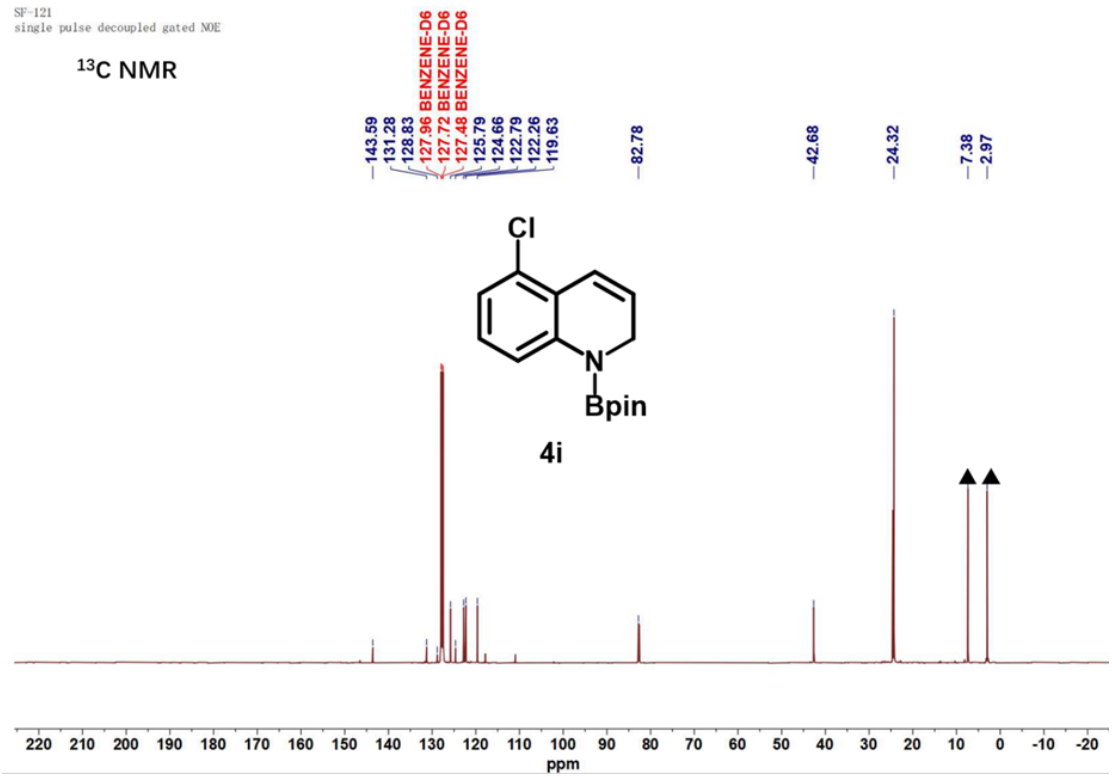

Figure S61. ^{13}C NMR spectrum of **4i** (101 MHz, Benzene-d_6).

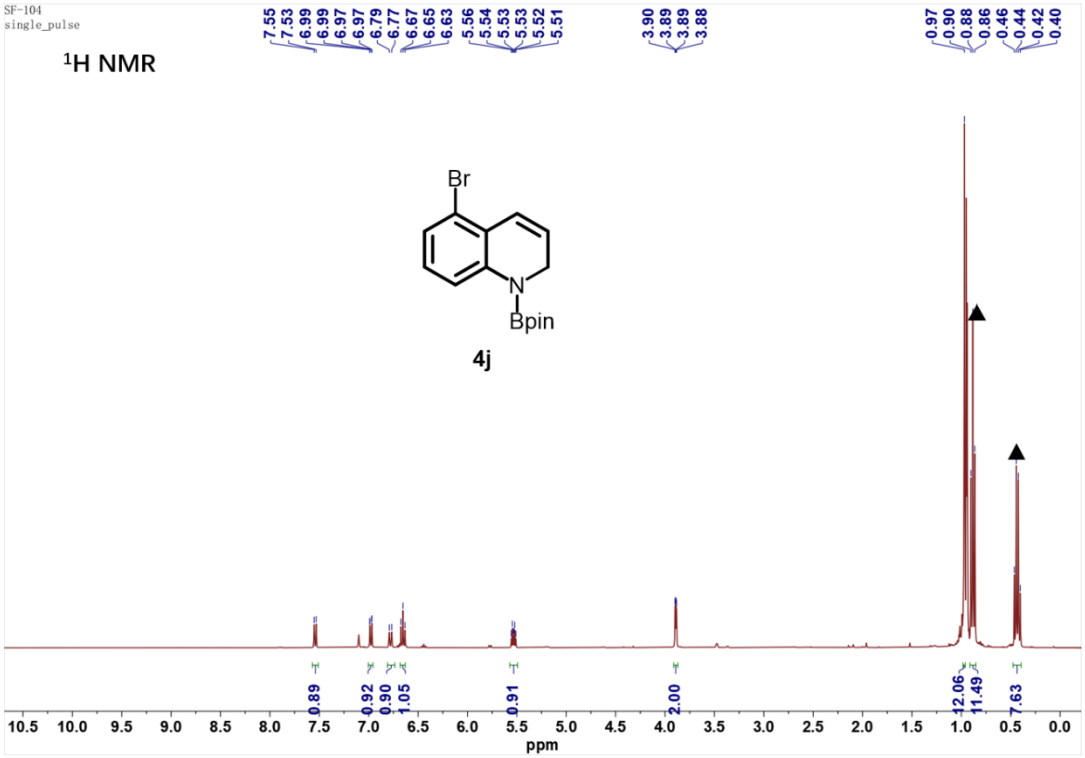

Figure S62. ^{1}H NMR spectrum of **4j** (400 MHz, Benzene-d_6).

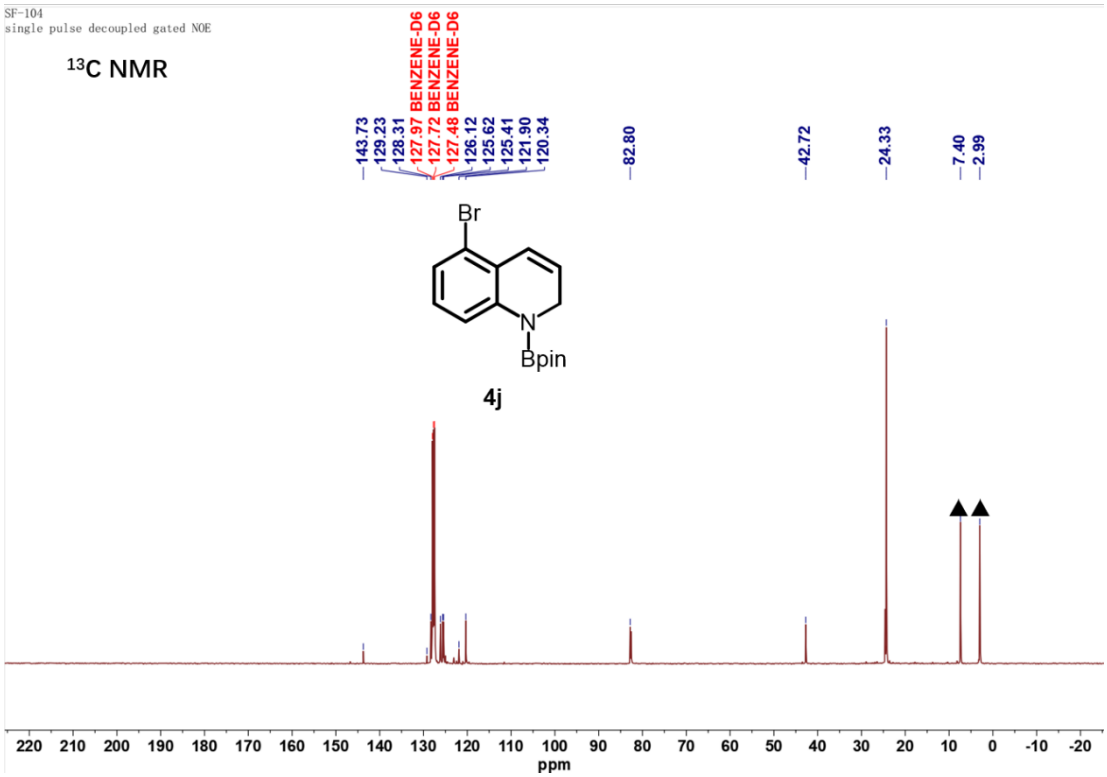

Figure S63. ^{13}C NMR spectrum of **4j** (101 MHz, Benzene-d_6).

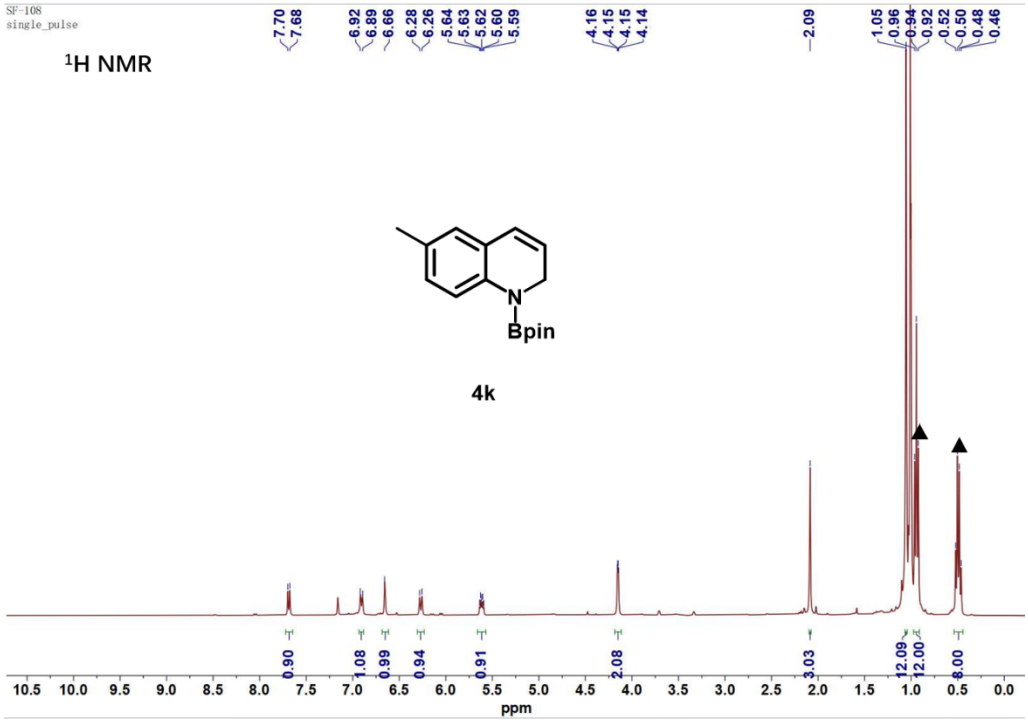

Figure S64. ^{1}H NMR spectrum of **4k** (400 MHz, Benzene-d_6).

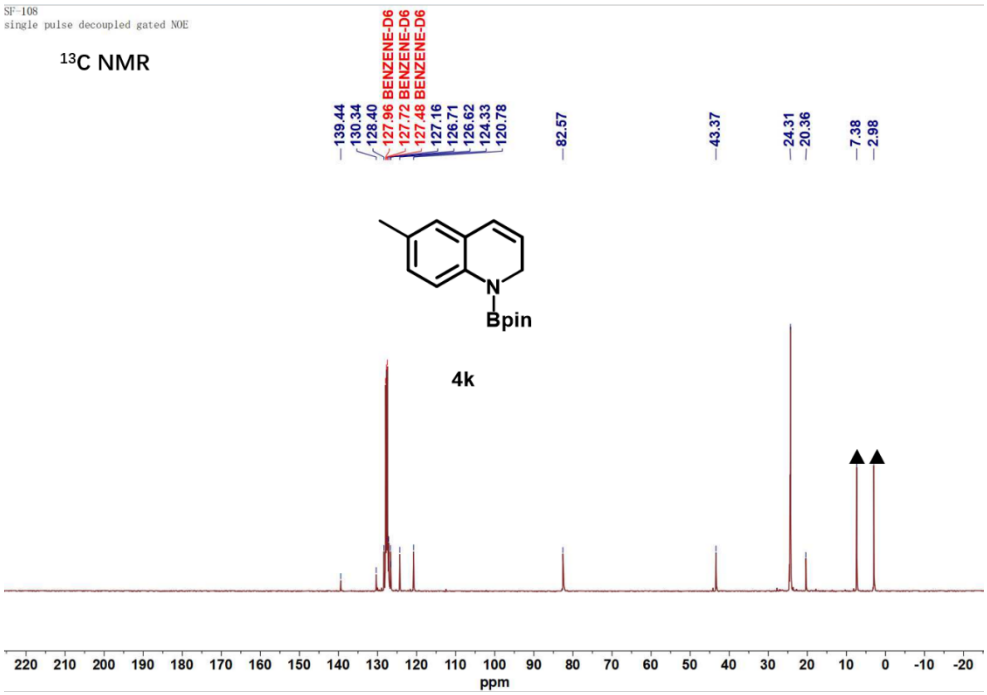

Figure S65. ^{13}C NMR spectrum of **4k** (101 MHz, Benzene-d_6).

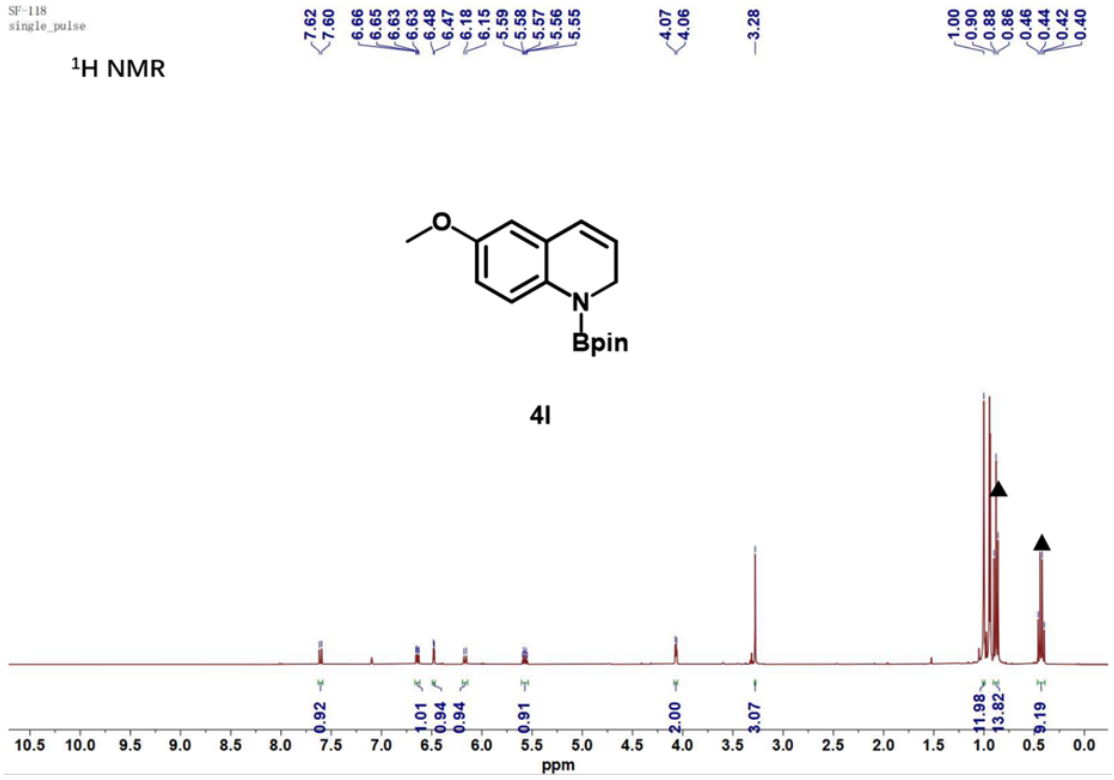

Figure S66. ^{1}H NMR spectrum of **4l** (400 MHz, Benzene-d_6).

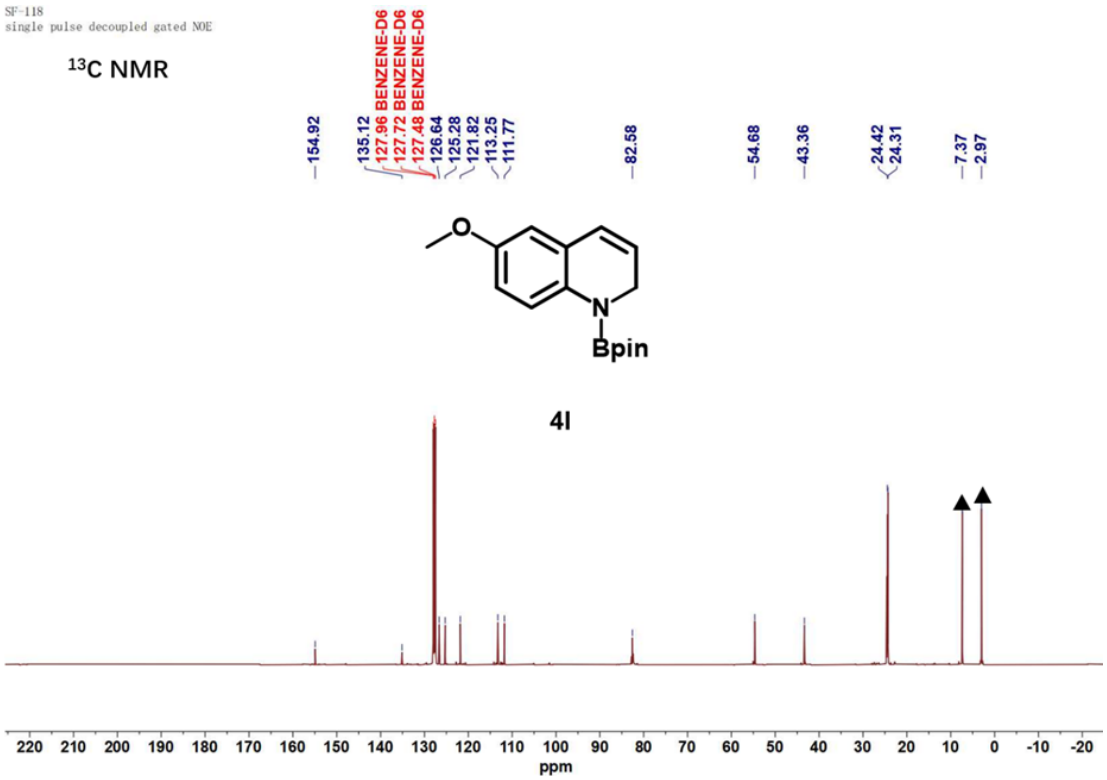

Figure S67. ^{13}C NMR spectrum of **4l** (101 MHz, Benzene-d_6).

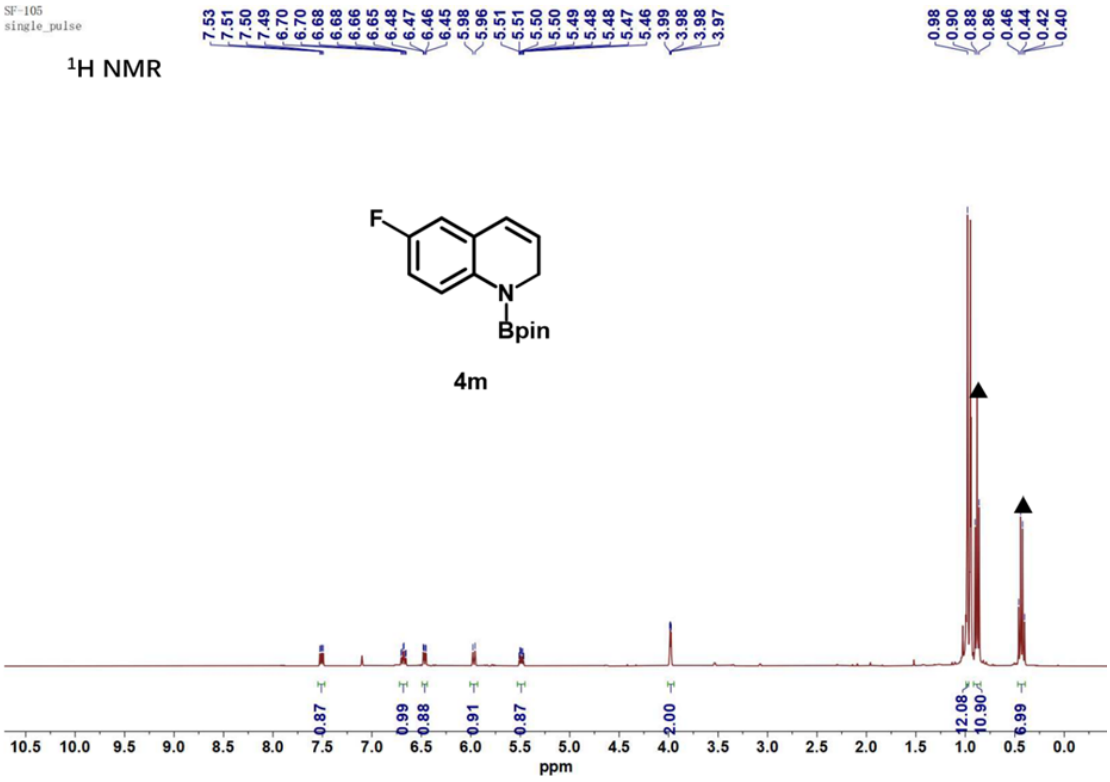

Figure S68. ^{1}H NMR spectrum of **4m** (400 MHz, Benzene-d_6).

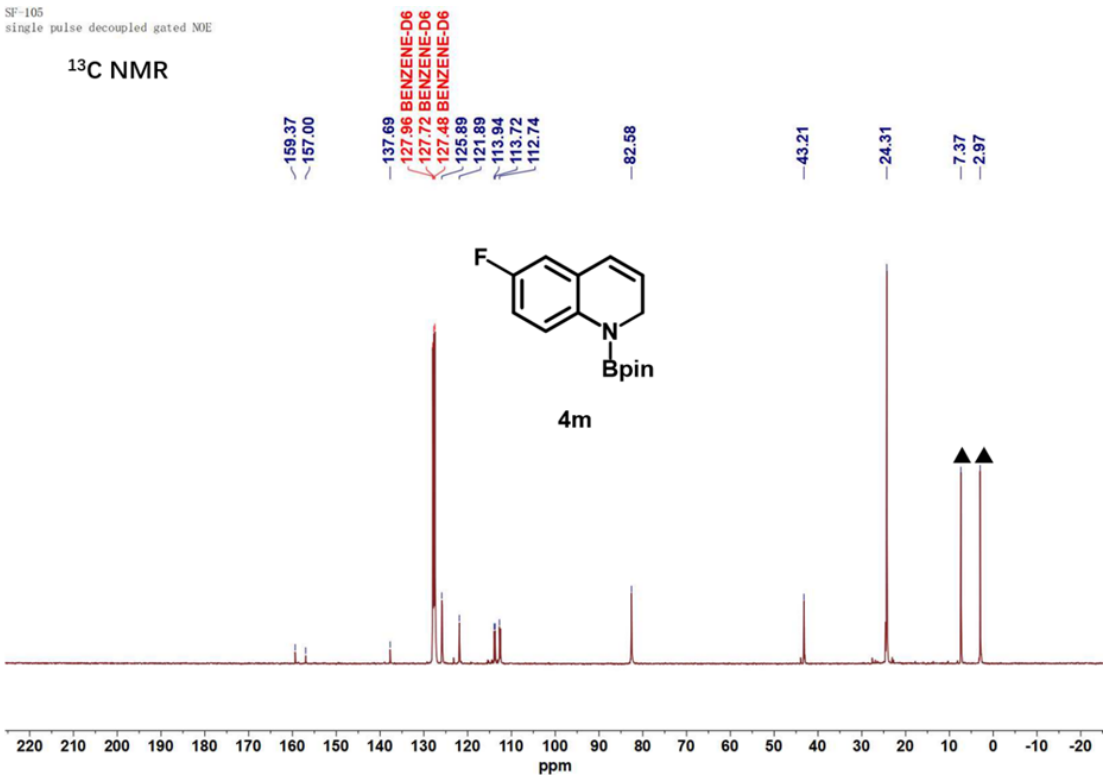

Figure S69. ^{13}C NMR spectrum of **4m** (101 MHz, Benzene-d_6).

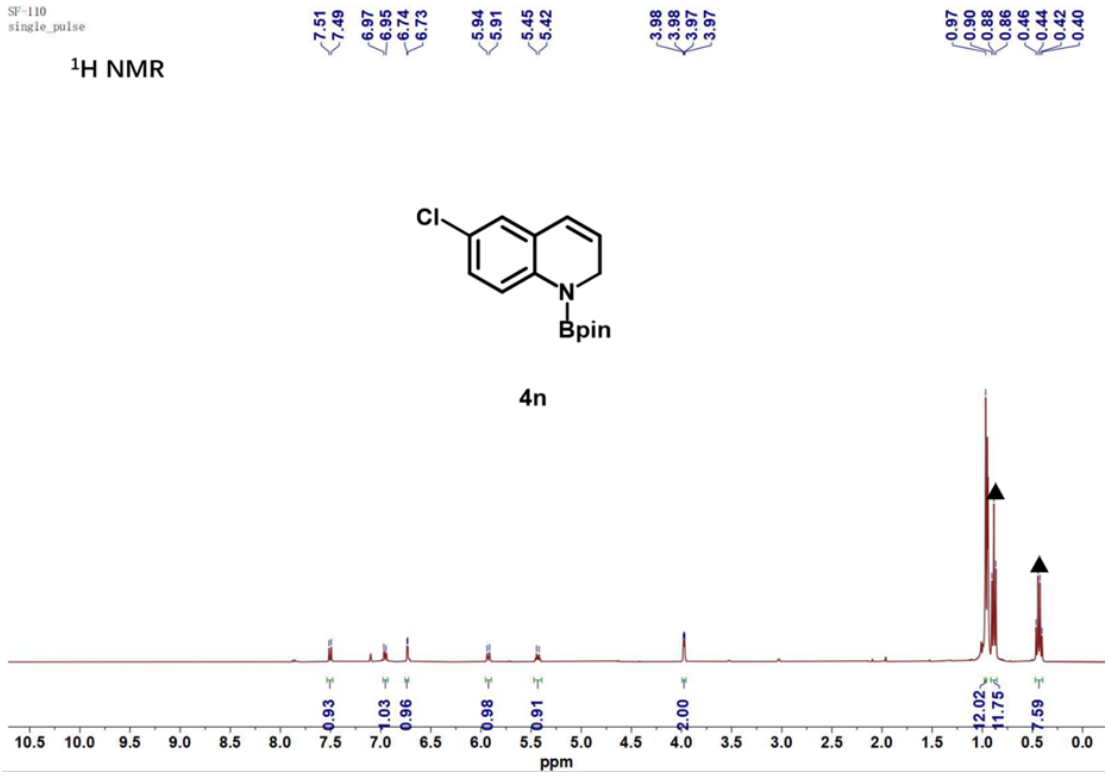

Figure S70. ^{1}H NMR spectrum of **4n** (400 MHz, Benzene-d_6).

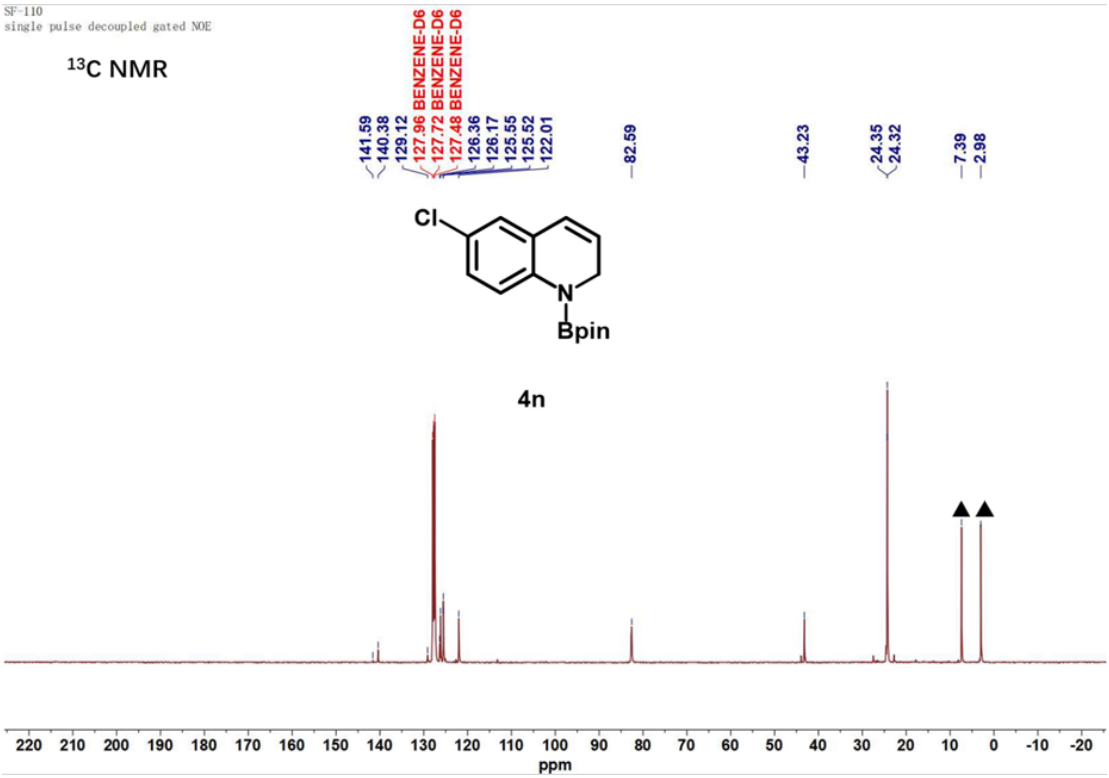

Figure S71. ^{13}C NMR spectrum of **4n** (101 MHz, Benzene-d_6).

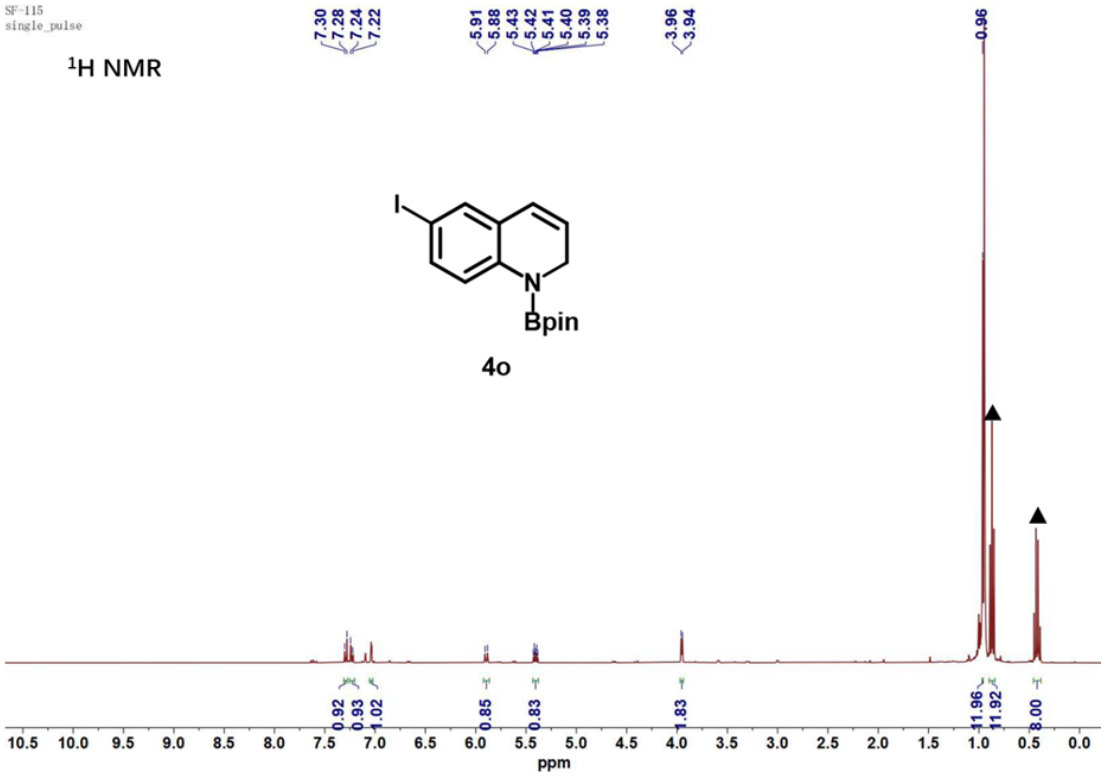

Figure S72. ^{1}H NMR spectrum of **4o** (400 MHz, Benzene-d_6).

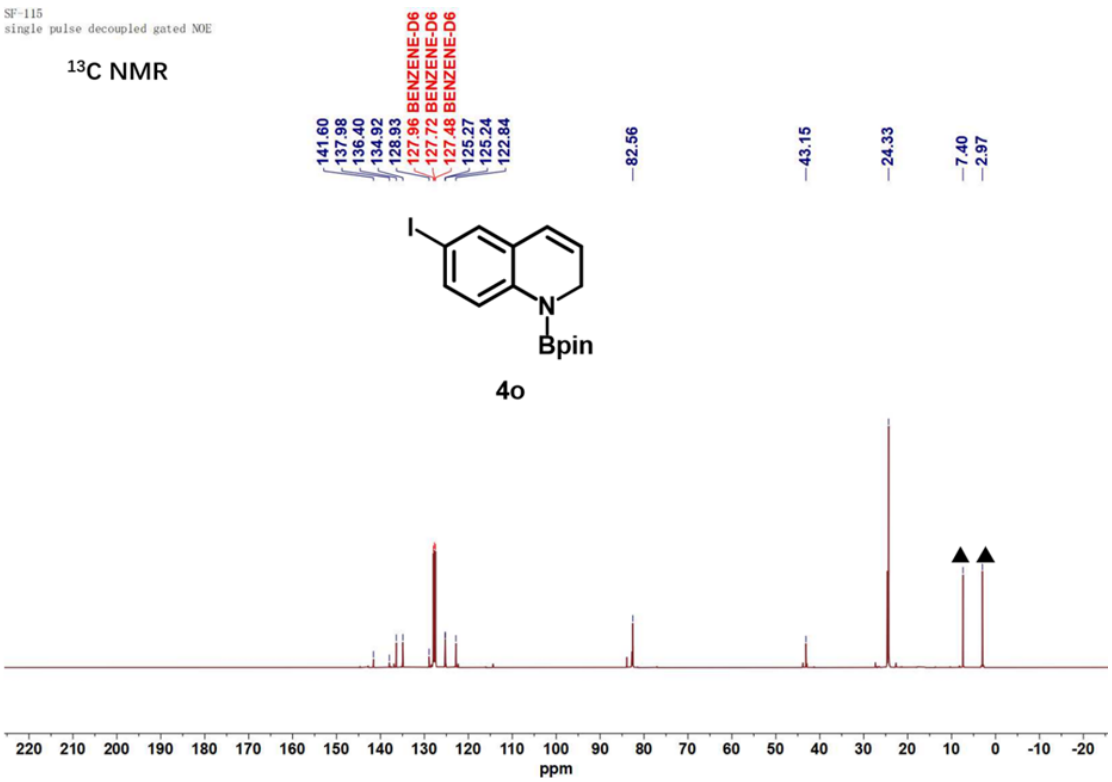

Figure S73. ^{13}C NMR spectrum of **4o** (101 MHz, Benzene-d_6).

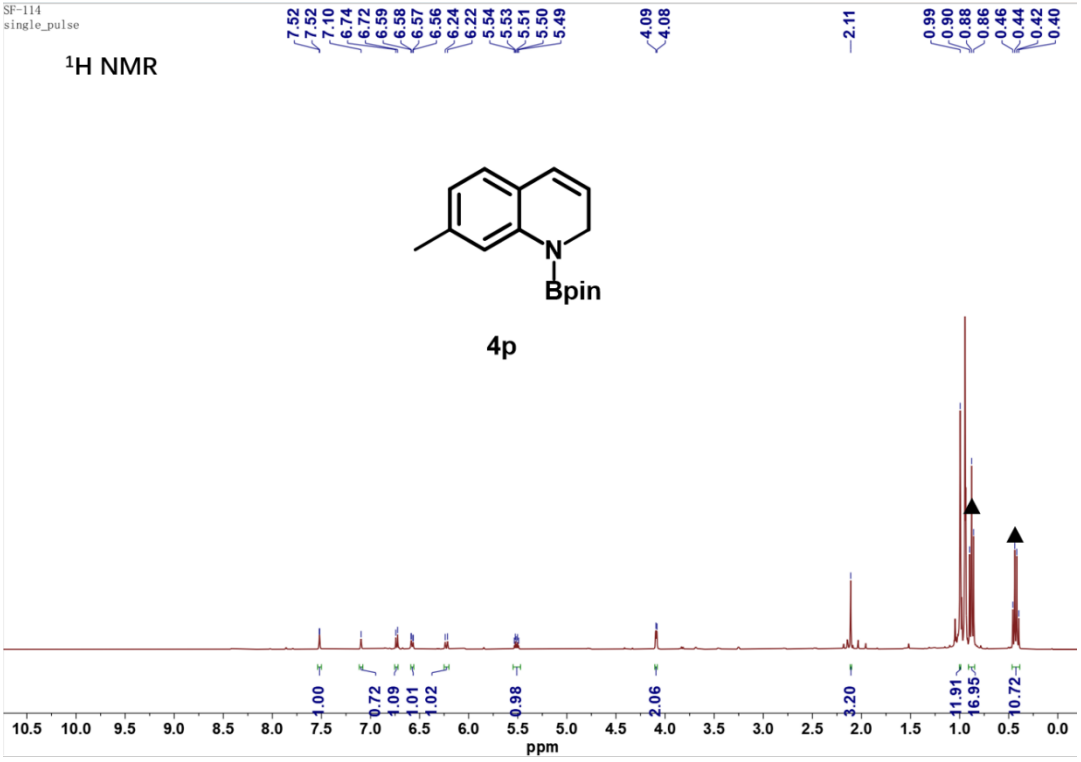

Figure S74. ^{1}H NMR spectrum of **4p** (400 MHz, Benzene-d_6).

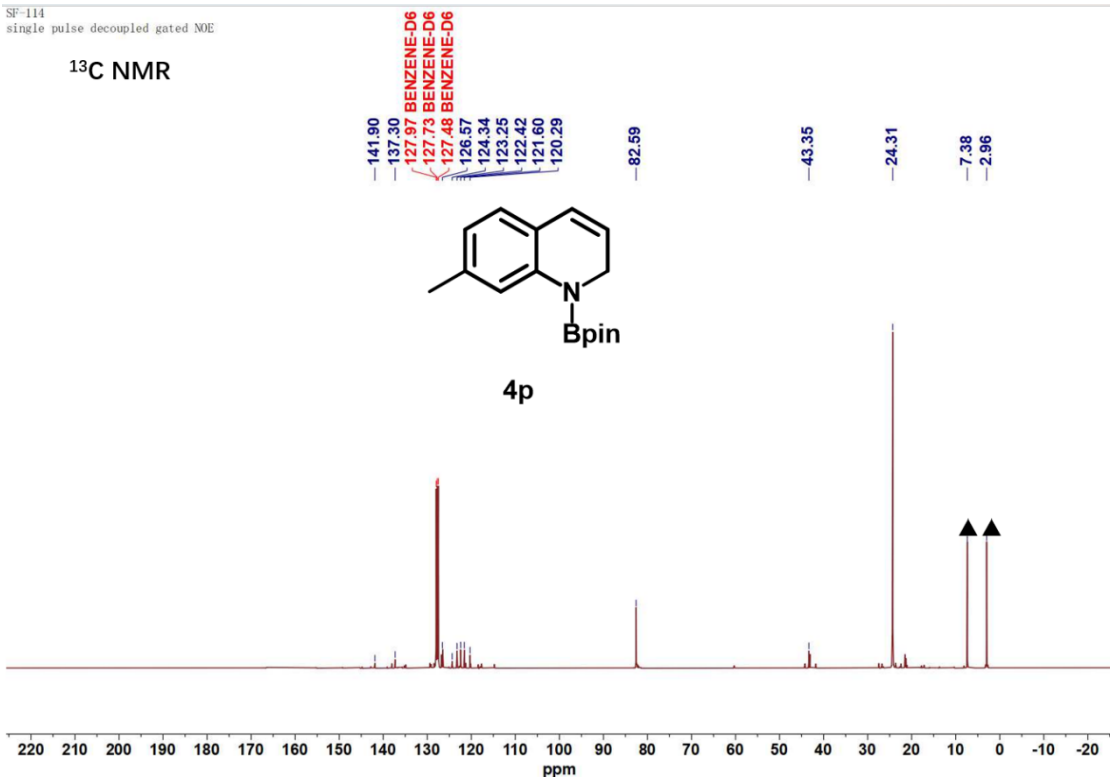

Figure S75. ^{13}C NMR spectrum of **4p** (101 MHz, Benzene-d_6).

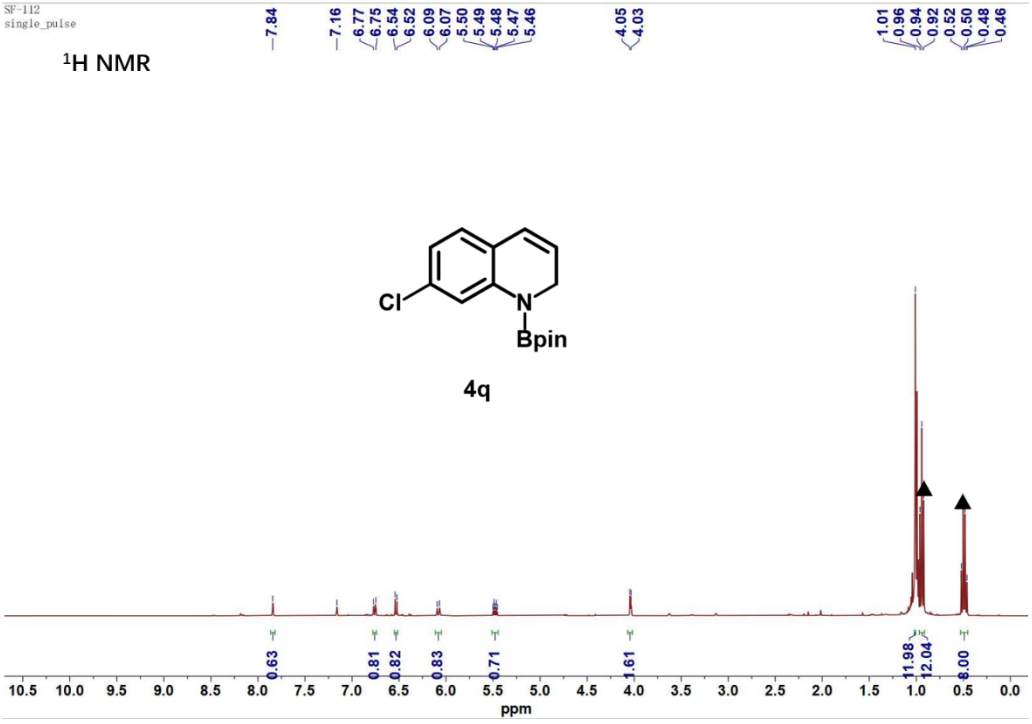

Figure S76. ^{1}H NMR spectrum of **4q** (400 MHz, Benzene-d_6).

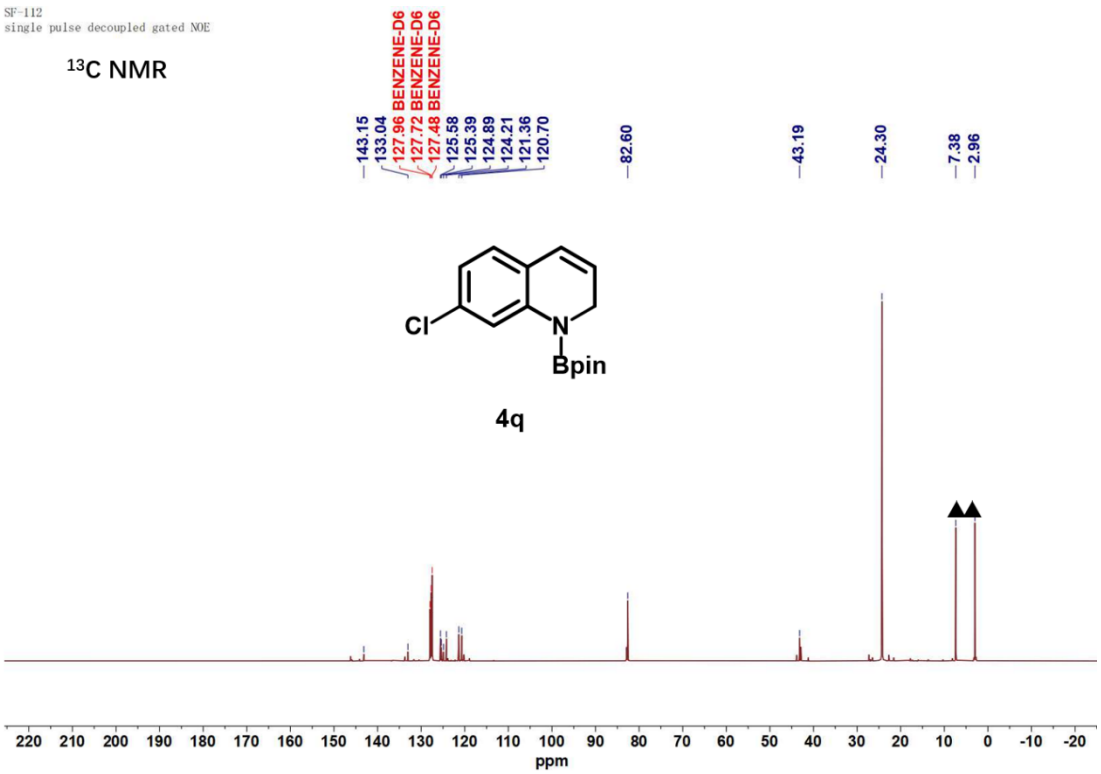

Figure S77. ^{13}C NMR spectrum of **4q** (101 MHz, Benzene-d_6).

7. Crystal Data and Structure Refinement Parameters

Table S5. Crystal Data and Structure Refinement Parameters for W-1

Table S5 Crystal data and structural parameters for **W-1**

	W-1
Empirical formula	$C_{22}H_{22}N_2O_4W$
Formula weight	562.26
Temperature (K)	300.00
Crystal system	orthorhombic
Space group	Pbca
a (Å)	15.0109(8)
b (Å)	15.0108(8)
c (Å)	19.9307(10)
α (°)	90
β (°)	90
γ (°)	90
Volume (Å^3)	4490.9(4)
Z	8
Density (calculated) (g/cm^3)	1.663
Absorption coefficient (mm^{-1})	5.172
F(000)	2192.0
Radiation	Mo-Kα (λ = 0.71073)
Crystal color, morphology	purplish red
θ range (°)	5.608 to 55.128
Absorption correction	Multi-scan
Index ranges	-18 ≤ h ≤ 18, -19 ≤ k ≤ 18, -25 ≤ l ≤ 23
GOF	1.024
Reflections collected	23229
Independent reflections	5087 [R_{int} = 0.0286, R_{sigma} = 0.0229]
Final R indexes [I>=2σ (I)]	R_1 = 0.0233, wR_2 = 0.0483
Final R indexes (all data)	R_1 = 0.0433, wR_2 = 0.0555
Largest diff. peak / hole (e.Å^{-3})	0.72/-0.53

Table S6. Crystal Data and Structure Refinement Parameters for W-2

Table S6 Crystal data and structural parameters for **W-2**

	W-2
Empirical formula	$C_{37}H_{43}N_3O_4W$
Formula weight	777.28
Temperature (K)	296.15
Crystal system	monoclinic
Space group	$P2_1/c$
a (Å)	14.1010(3)
b (Å)	10.3729(2)
c (Å)	28.2822(5)
α (°)	90
β (°)	95.9630(10)
γ (°)	90
Volume (Å^3)	4114.41(14)
Z	4
Density (calculated) (g/cm^3)	1.388
Absorption coefficient (mm^{-1})	4.930
F(000)	2.851
Radiation	Mo-Kα (λ = 0.71073)
Crystal color, morphology	red
θ range (°)	4.186 to 55.09
Absorption correction	Multi-scan
Index ranges	-18 ≤ h ≤ 17, -12 ≤ k ≤ 13, -36 ≤ l ≤ 36
GOF	1.211
Reflections collected	32151
Independent reflections	9437 [R_{int} = 0.0207, R_{sigma} = 0.0220]
Final R indexes [I>=2*σ* (I)]	R_1 = 0.0290, wR_2 = 0.0601
Final R indexes (all data)	R_1 = 0.0368, wR_2 = 0.0619
Largest diff. peak / hole (e.Å^{-3})	0.99/-1.74

Table S7. Crystal Data and Structure Refinement Parameters for W-3

Table S7 Crystal data and structural parameters for **W-3**

	W-3
Empirical formula	$C_{24}H_{24}N_2O_4W$
Formula weight	588.30
Temperature (K)	296.15
Crystal system	monoclinic
Space group	$P2_1/c$
a (Å)	12.344(4)
b (Å)	9.316(4)
c (Å)	21.158(9)
α (°)	90
β (°)	104.30(2)
γ (°)	90
Volume (Å^3)	2357.7(16)
Z	4
Density (calculated) (g/cm^3)	1.657
Absorption coefficient (mm^{-1})	4.930
F(000)	1152.0
Radiation	Mo-Kα (λ = 0.71073)
Crystal color, morphology	red
θ range (°)	3.404 to 52.736
Absorption correction	Multi-scan
Index ranges	-15 ≤ h ≤ 15, -11 ≤ k ≤ 6, -19 ≤ l ≤ 26
GOF	1.013
Reflections collected	11704
Independent reflections	4812 [R_{int} = 0.0683, R_{sigma} = 0.0993]
Final R indexes [I>=2*σ* (I)]	R_1 = 0.0462, wR_2 = 0.0775
Final R indexes (all data)	R_1 = 0.0981, wR_2 = 0.0914
Largest diff. peak / hole (e.Å^{-3})	0.76/-1.49

8. References

1. Sahoo, R. K.; Sarkar, N.; Nembenna, S. Intermediates, Isolation and Mechanistic Insights into Zinc Hydride-Catalyzed 1,2-Regioselective Hydrofunctionalization of *N*-Heteroarenes. *Inorg. Chem.* **2023**, *62*, 304-317.
2. Rodriguez, J.; Conley, M. P. A Heterogeneous Iridium Catalyst for the Hydroboration of Pyridines. *Org. Lett.* **2022**, *24*, 4680-4683.
3. Meher, N. K.; Verma, P. K.; Geetharani, K. Cobalt-Catalyzed Regioselective 1,2-Hydroboration of N-Heteroarenes. *Org. Lett.* **2023**, *25*, 87-92.
4. Wang, X.; Zhang, Y.; Yuan, D.; Yao, Y. Regioselective Hydroboration and Hydrosilylation of N-Heteroarenes Catalyzed by a Zinc Alkyl Complex. *Org. Lett.* **2020**, *22*, 5695-5700.
5. harma, A.; Tiwari, V.; Yadav, R.; Das, B.; Majumder, C.; Das, A.; Karmakar, T.; Kundu, S. Synthesis of Cyclic (Alkyl)(amino)carbene-Stabilized Copper–Iron Heterobimetallic Complexes and Their Application in Pyridine Hydroboration. *Organometallics.* **2024**, *43*, 3054-3061.
6. Chacón-Terán, M. A.; Landaeta, V. R.; Wolf, R.; Rodríguez-Lugo, R. E. Regioselective Rhodium-Catalyzed 1,2-Hydroboration of Pyridines and Quinolines Enabled by the Tris(8-quinolinyl) phosphite Ligand. *Eur. J. Inorg. Chem.* **2023**, *26*, e202300267.
7. Jeong, E.; Heo, J.; Park, S.; Chang, S. Alkoxide-Promoted Selective Hydroboration of N-Heteroarenes: Pivotal Roles of in situ Generated BH3 in the Dearomatization Process. *Chem. Eur. J.* **2019**, *25*, 6320-6325.
8. Zhang, Z.; Huang, S.; Huang, L.; Xu, X.; Zhao, H.; Yan, X. Synthesis of Mesoionic N-Heterocyclic Olefins and Catalytic Application for Hydroboration Reactions. *J. Org. Chem.* **2020**, *85*, 12036-12043.
9. Liu, J.; Chen, J.-Y.; Jia, M.; Ming, B.; Jia, J.; Liao, R.-Z.; Tung, C.-H.; Wang, W. Ni–O Cooperation versus Nickel (II) Hydride in Catalytic Hydroboration of *N*-Heteroarenes. *ACS Catal.* **2019**, *9*, 3849-3857.